CARBON DEPOSITION IN A BOSCH PROCESS USING A COBALT AND NICKEL CATALYST

by

James Edwin Garmirian

B.A., Hope College (1976)

SUBMITTED IN PARTIAL FULFILLMENT OF THE REQUIREMENTS FOR THE DEGREE OF DOCTOR OF PHILOSOPHY

at the

MASSACHUSETTS INSTITUTE OF TECHNOLOGY

March 1980

Signature of Author: _____
Department of Chemical Engineering

Certified by: _____
Thesis Supervisor

Certified by: _____
Thesis Supervisor

Accepted by: _____
Chairman, Departmental Committee on Graduate Theses

Abstract

NASA has been active in developing processes to recover oxygen from metabolic carbon dioxide. Their ultimate objective has been to construct a life support system capable of supplying oxygen in a cyclic process. The cycle of interest here begins by reducing the carbon dioxide with hydrogen to form solid carbon and is known as the Bosch process. An iron catalyst is normally used.

$$CO_2 + 2H_2 \xrightarrow{\text{Catalyst}} C + 2H_2O$$
$$2H_2O \xrightarrow{\text{Electroylsis}} 2H_2 + O_2$$
$$\overline{CO_2 \longrightarrow C + O_2}$$

The water is then electrolyzed to oxygen and hydrogen. The overall process results in the conversion of carbon dioxide to carbon and oxygen.

Previous studies have shown that water concentrations over an iron catalyst are limited to a maximum of 16% (915K) due to the formation of non-catalytic iron oxides. It has been found in this thesis that through the use of cobalt and nickel catalysts, water concentrations of 32% (800K) and 25% (825K), respectively, may be obtained. The assumption that the gas phase is in equilibrium with graphite leads to predictions that even higher water concentrations could be obtained at lower temperatures. However, it is shown that the equilibrium state cannot be achieved. A mechanism has been proposed which suggests that carbon formation occurs via a carbide intermediate. The difference in Gibbs energy between carbide and graphite reactions correlates with the decrease of water concentrations at low operating temperatures.

DEDICATION

This thesis is dedicated to my parents,

Edwin and Rachael Garmirian,
for all their love, guidance, and
support which they have given
me throughout my life.

Acknowledgements

This project was supported by a research grant from the National Aeronautics and Space Administration. The assistance of Dr. Philip D. Quattrone is gratefully acknowledged.

To Hope College, I give great thanks for providing me with more than just a college education, most of all, to Professors Sheldon Wettack, and William Mungall, and the rest of the Chemistry department for their encouragement and leadership. I thank Professors Richard Brockmeirer, James Van Puttan, and James Toevs of the Physics department for their guidance and education. To Lise Hager, thanks for everything, Stratford, school, and just fooling around.

Bill Doerr and James Christowski made life in the basement interesting and were always very supportive, thanks. The friendship of Ted Bush, John Ninniger, Ken Hellyar, Tom Irwin, Patty Rich, Gina Shuck, Mike Klein and of course David Stern made graduate life both in and out of the lab enjoyable and entertaining. The friendship, discussions, and technical advice of Charles Foshey are greatly appreciated. Harold Duffett was a good friend, thanks.

I must thank (Father) Frank Bates, Peter Levy (Goodwrench), and Sue Harrison for their friendship and my Armenian wife.

Without the help and friendship of both Sally Kreuz and Stan Mitchell this thesis would have never been bound. Jeffrey Wingard's participation in collecting the experimental data is also appreciated.

I would like to thank Professor Williams for sincerely and patiently answering the somewhat obscure questions of a wondering graduate student. I appreciate the time Professors Meissner and Satterfield spent discussing this thesis with me.

Albert Sacco was the one who inspired my initial interest in the Bosch process, to him I give many thanks.

I would like to thank Professor Robert Reid for the guidance and inspiration he has given me throughout my years here at M.I.T. Without Professor Michael Manning's daily discussions and technical advice, I still might have finished this thesis, but without his inspiration, dedication, and genuine concern for my development both as an engineer and a human being, I would have drifted by the wayside.

I would like to thank my brothers and sisters Bobby, Calvin, Paul, Bob, Dawn, Pat, Mary, Peter, Cutts, Billy, Mag, Jim, Joanne, and of course Patty for all their love and support.

For a beautiful family, Sunday dinners, all the love in the world, and their daughter, I thank Marty and Helen (Granny) Mehron.

And of course, who can forget Barbara. The two years I have known her have been the happiest years of my life. Without her unfailing love and support I might have ended up an automechanic.

Department of Chemical Engineering
Massachusetts Institute of Technology
Cambridge, Massachusetts 02139

Professor Jack P. Ruina
Secretary of the Faculty
Massachusetts Institute of Technology
Cambridge, Massachusetts 02139

Dear Professor Ruina:

In accordance with the regulations of the Faculty, I herewith submit a thesis entitled, "Carbon Deposition in a Bosch Process Using a Cobalt and Nickel Catalyst", in partial fulfillment of the requirements for the degree of Doctor of Philosophy In Chemical Engineering at the Massachusetts Institute of Technology.

Respectively submitted,

James E. Garmirian

Table of Contents

Table of Figures

Table of Tables

1.0 Summary

The Bosch process had been investigated by NASA as a means of recovering oxygen from metabolic carbon dioxide. The ultimate objective has been to construct a life support system capable of supplying oxygen in a cyclic process.

$$CO_2 + 2H_2 \rightarrow C + 2H_2O$$

An iron catalyst is normally used. The water formation reaction is followed by electrolysis to yield hydrogen and oxygen,

$$2H_2O \rightarrow 2H_2 + O_2$$

The overall process results in the reduction of metabolic carbon dioxide to carbon which accumulates on the iron catalyst, and oxygen which is returned to the spacecraft.

In the past, NASA scientists have run Bosch reactors using a steel wool catalyst and recycling unreacted gases to obtain complete reaction (Holmes et al., 1970). One problem which they encountered was that the maximum water concentration obtained in the reactor was significantly less than the thermodynamically predicted equilibrium water concentration. Investigators at MIT were able to show that the phenomena which occurred resulted from oxide inhibition rather than slow reaction rates. That is, in addition to the reactions which occurred between carbon monoxide, carbon dioxide, methane, hydrogen, water and carbon, oxidation of the iron catalyst also occurred. Above 860K the reaction

$$Fe + H_2O \rightleftarrows FeO + H_2$$

occurred, and below 860K,

$$3Fe + 4H_2O \rightleftarrows Fe_3O_4 + 4H_2$$

These reactions, coupled with the discovery that iron oxide does not catalyze carbon deposition reactions, led to an explanation for the low water concentrations present in the NASA reactors. Manning's (1976) and Sacco's (1977) experimental data on the Bosch system were in good agreement with iron-iron-oxide-gas equilibrium calculations based on tabulated Gibbs energy data.

Preliminary theoretical calculations have revealed that water production limitations associated with the iron catalyzed Bosch process may not be encountered when the iron is replaced by nickel or cobalt. This suggests that a study of the nickel and cobalt catalyzed Bosch process may lead to a more efficient reactor.

1.1 Experimental Apparatus

The experimental apparatus is shown schematically in Figure 3-1. It is composed of the feed-gas delivery system, a thermogravimetric reactor, and a gas-sampling system. In the feed-gas delivery system, chemically pure gases were individually metered and mixed to synthesize desired gas compositions which could be reacted over a given catalyst. Water was added to the mixture as steam. The steam feed was produced by metering liquid water and then vaporizing it.

The quartz reactor is shown in Figure 3-4. The catalyst assembly shown in Figure 3-5 rests on the lower ground-glass joint which is located in the lower reactor support tube. The feed gases were preheated and then directed vertically through the catalyst assembly. Within the catalyst assembly, the catalyst was held between plugs of quartz wool. Weight measurements were taken periodically by suspending the catalyst carrier from an analytical balance by the suspension "T". Weight changes within ±1 mg could be detected.

Three catalysts were employed in the study. The first was a Ni/Al_2O_3 catalyst powder supplied by the Alfa division of Ventron Corp. It had a BET surface area of 200 m^2/g. It was reported to be 60-65 wt% Ni. A second catalyst, cobalt powder, was supplied by Bram Metallurgical Co. The powder was formed from 1-5μm spheres fused to form approximately 40μm aggregates. The purity was reported to be 99.9% and had a BET surface area of 0.7 m^2/g. A third catalyst used was prepared by drying a 5 wt% sulution of cobalt nitrate (Fischer Scientific Company) on 1g of quartz wool, at 423K over a copper screen. This was then calcined in air and reduced in hydrogen at 700K to form metallic cobalt.

A gas sampling system, which consisted of a vacuum system, heated gas-sample valve, and gas chromatograph, allowed the determination of inlet and outlet compositions.

1.2 Approach

In the Bosch process carbon dioxide is reacted with hydrogen to form water and solid carbon. In the process carbon monoxide and methane are also formed. For a given temperature, pressure, and gas phase O/H ratio, if any three independent reactions are chosen, such as

$$H_2 + CO_2 \rightleftarrows CO + H_2 \qquad (A)$$

$$CH_4 + H_2O \rightleftarrows 3H_2 + CO \qquad (B)$$

$$2CO \rightleftarrows C + CO_2 \qquad (C)$$

then the equilibrium mole fractions of each component can be calculated.

Typically, a solid carbon phase of pure β-graphite is assumed in making the calculations. However, results of Dent (1945) and Rostrup-Nielsen (1972) indicate that such a simplification can lead to erroneous results. The equilib-

rium constant for reaction (C) and (D) were measured by both Dent and Rostrup-Nielsen.

$$CH_4 \rightleftarrows 2H_2 + C \qquad (D)$$

They found that only at temperatures of about 1000K would the assumption of a solid phase of β-graphite be justified. At temperatures below that, it was found that the Gibbs energy change for their reactions was apparently greater than that for the corresponding reaction with a solid phase of graphite. This difference was about 1.5 and 3.0 kcal/mole at 800 and 700K, respectively. Table 4-1 shows the equilibrium gas composition at various temperatures, 1 atmosphere and an O/H ratio of 0.5, assuming a solid phase of either graphite or one which deviated from graphite by the amount reported by Dent. As can be seen the results are quite different depending upon the form of carbon chosen for the calculation. The water concentration changes from 18 to 13%, 32 to 17%, and 45 to 11%, at temperatures of 900, 800, and 700K, respectively, for solid phases of graphite versus "Dent" carbon, respectively. These calculations demonstrate the magnitude effect that the Gibbs energy differences can have on equilibrium water concentrations obtainable in a Bosch process and emphasize the importance of experimentally determining the carbon-gas equilibrium.

In the calculations of graphite-gas equilibrium discussed previously three independent reactions, (A), (B) and (C), were chosen for the computations. The only reaction which included graphite was (C). Since it has been shown that the Gibbs energy change of reactions involving carbon could not be calculated as that for a reaction with graphite, the parameter, ΔG_c, was defined to account for this Gibbs energy difference, so that

$$\Delta G_c = -RT \ln K_{p_{observed}} + RT \ln K_{p_{graphite}}$$

where K_p may be written as

$$K_p = \frac{P_{CO_2}}{P_{CO}^2} \qquad (C)$$

By allowing the equilibrium constant of reaction (C) to vary as

$$K_{p_{(C)}} = K_{p_{(C)graphite}} \exp(-\Delta G_C/RT)$$

equilibrium gas calculations can be made for a given temperature, pressure, O/H ratio, and Gibbs energy of the experimental carbon.

Equilibrium gas compositions were then calculated for values of the parameter ΔG_c, from -5.0 kcal/mole to +5.0 kcal/mole. To determine the carbon deposition boundary, gas mixtures corresponding to these ΔG_c's were passed over a nickel or cobalt catalyst to determine whether carbon deposition, carbon removal, or neither occurred. The calculations and associated gas compositions extended beyond literature values of ΔG_c which were reported by Dent (1945), Rostrup-Nielsen (1972), and Schenck (1927) to insure that the gas compositions employed experimentally would enclose the equilibrium point.

1.3 Experimental Results

The experiments were run at temperatures of 700, 750, 800 and 900K and a pressure of 1.0 atm. Measurements were made for the binary-gas systems of CO-CO_2 and CH_4-H_2 over carbon and catalyst. Multicomponent experiments with H_2, CO,CH_4, CO_2, H_2O, and C were also carried out at gas phase O/H ratios of 0.17 0.5 and 1.5. Preceeding every equilibrium run where fresh catalyst was put into the reactor and reduced, carbon was deposited from a 1:1 mixture of hydrogen and carbon monoxide. This was done at the reaction temperature of the equilibrium run. In each case about 0.2 g C/g catalyst was deposited.

The life of the catalyst (g carbon/g catalyst) used in the Bosch process is critical. Certainly, no benefit from the Bosch process is obtained if one must transport a larger mass of catalyst than the mass of oxygen which it eventually regenerates. To determine the catalyst life, an experiment similar to the preliminary carbon deposition described in the last paragraph was run at 800K. Figure 4-4 shows the results. As can be seen, the rate of carbon deposition remains constant up to 100 gC/g cobalt.

Figure 4-5 shows the results from an experiment to determine the carbon deposition boundary at 900K, 1.0 atm, and an O/H ratio of 0.5 over cobalt. In the figure, the experimentally obtained rates of carbon deposition (mg/min) are plotted as a function of the parameter ΔG_c (kcal/mole), which is characteristic of the corresponding gas phase composition. Simultaneously drawn are curves which represent the gas compositions which yielded the experimental data at the various values of ΔG_c. These compositions were calculated to be in equilibrium with a carbon of the corresponding ΔG_c. As can be seen the equilibrium point is indicated where the rate of carbon deposition and removal go to zero. This occurs when the parameter ΔG_c is zero. Hence the equilibrium gas composition is that which one would expect to be in equilibrium with graphite.

In other experiments, the equilibrium point was not so clearly defined. For example, in Figure 4-7 a region of zero rate of carbon deposition exists between the point at which carbon deposition stopped ($\Delta G_c \approx 1.5$ kcal/mole), and carbon removal began ($\Delta G_c \approx -1.0$ kcal/mole). The results of over 30 experiments similar to the one portrayed in Figure 4-7 are summarized for cobalt in Figure 4-27 and nickel in Figure 4-39. In these figures, the limits of the region of no carbon deposition or removal are plotted. That is, for a given experiment, the point at which carbon deposition stops or carbon removal begins is plotted as a function of temperature. As can be seen in

the two figures, the carbon deposition boundary is seen to deviate more from the graphite equilibrium at low temperature. Carbon removal, for the most part, is observed to occur for ΔG_c less than zero. For the experiments at 700K, over nickel and cobalt, carbon removal is typically not observed.

1.4 Discussion of the Equilibrium Results

In the iron-catalyzed Bosch process studied by both Manning (1976) and Sacco (1977), the iron-iron oxide-gas equilibrium curve was shown to correspond with the carbon deposition boundary and hence determines the concentration in that system. The inacitivity of the iron oxide as a catalyst for carbon deposition prevented the attainment of the higher water-concentrations expected at the graphite-gas equilibrium. In other words, if iron oxide was active for the various carbon deposition reactions, the graphite-gas equilibrium would be reached.

The experimental results presented clearly show that the high water concentration predicted by the graphite-gas equilibrium at both 700 and 750K is also not attainable over either a nickel or cobalt catalyst. For example, as shown in Figure 4-7, the mole fraction of water expected to be in equilibrium with graphite ($\Delta G_c = 0$) is about 38% at 750K. However, carbon deposition and hence the overall process stops ($\Delta G_c = 1.5$ kcal/mole) at a water mole fraction of about 24%. This effect is important when considering the optimization of the Bosch process.

The results at low temperatures may be due to a carbide intermediate. That is, one may have a reversible reaction to form carbide from metal and methane such as

$$CH_4 + nMe \rightleftarrows Me_nC + 2H_2$$

where Me can be either nickel (where n=3) or cobalt (where n=2 or 3). The formation of carbide can also occur from other reactions, such as

$$H_2 + CO + nMe \rightleftarrows Me_nC + H_2O$$

and

$$2CO + nMe \rightleftarrows Me_nC + CO_2$$

The carbide can also decompose to free metal and carbon

$$Me_nC \rightarrow C + nMe$$

It is suggested that the formation of carbon occurs by this reaction series. Quite specifically, the carbon is formed via an intermediate carbide. The net results, using the methane-hydrogen-carbon reaction as one example, is

$$CH_4 \rightarrow C + 2H_2$$

In our experimental results, the observed weight increases are much greater than could be accounted for by the formation of a carbide. Thus, if a carbide formed, it must have continuously decomposed to account for the mass increases observed in the experiments.

Carbides have, in fact, been shown to exhibit a metastable behavior. Hofer et al. (1949, 1950) have shown that both nickel and cobalt carbides decompose readily at temperatures of 630K; the time required was less than one hour. Nagakura (1957, 1961) reported that in a temperature programmed study, decomposition of nickel carbide did not occur until 704K. He also indicated that the maximum rate of carbide formation (formation less decomposition) occurred at 623K. For the cobalt system, the decomposition of Co_2C occurred at 723K and at 750K for Co_3C. The maximum rate of formation (formation - decomposition) of both carbides occurred at temperatures between 723 and 773K. It should also be noted that Renshaw et al. (1971) observed Ni_3C at temperatures

as high as 823K. In Nagakura's study, only free metal and carbon were observed at temperatures above 773K for Ni and 823K for Co. Thus, the available experimental evidence indicates that the existence of both nickel and cobalt carbide at temperatures between 700 and 800K is highly likely.

Browning and Emmett (1952) also studied the equilibrium of nickel carbide with both nickel and a gas phase of methane and hydrogen. Little scatter was observed in them in the nickel data. Also, the stability of the carbide was shown to be greater than that of cobalt carbide. With X-ray analysis, the hexagonal close-packed sturcture of Ni_3C was observed confirming that measurements of the carbide equilibrium were in fact being made. Upon comparison of this low temperature study with the high temperature results of both Dent (1945) and Rostrup-Nielsen (1972), it is seen that the data fall on a line which results from a plot of ΔG_c versus temperature (Figure 4-39). Since thermodynamics would predict a straight line for a given process, when ΔH and ΔS are constant, ($\Delta G = \Delta H - T\Delta S$), it is believed that the solid species in equilibrium with the gas phase, at high temperature (above 700K), is the carbide and metal phase.

The results obtained over nickel and cobalt have several interesting similarities. First, the point at which carbon deposition ceases deviates more from graphite at lower temperatures. This would be expected if the carbon deposition boundary corresponded not with the graphite-gas equilibrium, but with an equilibrium with a different solid phase, such as a carbide. Most important is the agreement between the experimental results over nickel of Figure 4-39 and the nickel-nickel carbide methane-hydrogen equilibrium line as shown in Figure 4-40. Secondly, although for the experiments over cobalt at temperatures of 800 and 900K carbon deposition and removal were observed close to the point where the rate of weight change equaled zero, for

most of the other cases this was not so.

There either existed a region of no weight change or, as for the temperature of 700K, no carbon removal was observed. This indicates that either the method of weight detection was not sufficiently sensitive, or below the point at which carbon deposition ceased the catalyst was converted to a less active form. In almost all cases carbon removal occurred only if ΔG_c of the gas mixture was less than 0.0 kcal/mole. This would also be expected for a system where graphite was present. In Figure 4-41 the positions of the graphite-gas and nickel-nickel carbide-gas equilibrium lines are shown at 700 and 800K. The diagram for cobalt is similar. As temperature is increased the graphite and carbide lines are seen to move closer together. The carbide phase line indicates the points at which the gas phase is in equilibrium with both metal and metal carbide. Above the line, the free metal will react to form carbide; below the line, the carbide will react to form free metal. The graphite equilibrium is different since there is only one solid phase which is considered along with the gas phase. Gas mixtures, which are represented by a point above the line, deposit carbon, while ones which are below the line remove carbon.

In the experiments studied in this work, carbon deposition was observed in the region of the phase diagram above the metal-metal carbide equilibrium curve. This was a given distance from the graphite-gas equilibrium curve. Since the upper boundary is in fact a carbide phase line, in the region above the line ("X"), metal carbide is present. For most of the experiments there existed a region of no weight change. Although carbon removal was not always observed below the graphite phase line (ΔG_c = 0.0 kcal/mole), very rarely was it observed above. In the region below the carbide phase line ("Y" and "Z"), no carbide would be expected to be present. If carbon formation only occurred through a carbide intermediate, no carbon deposition would be expected below

the carbide equilibrium curve ("Y"). The reaction

$$Me_nC + 2H_2 \rightarrow nMe + CH_4$$

is not observed in that region either because the carbide decomposes to carbon quickly, or the amount present is a relatively small fraction of the total mass of metal plus carbon.

Carbon removal was in fact observed under some conditions. This must have occurred via the reaction

$$C + 2H_2 \rightarrow CH_4$$

which will only occur for gas mixtures where ΔG_c is less than 0.0 kcal/mole. For the most part, Figures 4-27 and 4-39 support this thermodynamic argument

In this analysis, the carbon deposition could have been considered to result from a carbon with a different Gibbs energy. The Gibbs energy difference could have been accounted for by structural differences such as those described in the analysis by Rostrup-Nielsen (1972). However, if this were the case, carbon removal would have been expected in the region just below the carbon equilibrium curve for the hypothesized non-graphitic carbon. Also the agreement (Figure 4-40) between the experimental data over nickel presented in Figure 2-13a and the nickel carbide equilibrium data of other authors gives strong evidence that the carbon deposition boundary coincides with the metal-metal carbide-gas equilibrium curve.

In summary, carbon deposition occurred via a metal carbide intermediate, upon reaching the metal-metal carbide-gas equilibrium carbon deposition ceased. In the region between the carbide and graphite equilibrium curves ("Y"), where no carbide was present, no carbon deposition or removal was detected. Below the graphite phase line, carbon removal was observed. The rate, however,

was slow and became negligible as the temperature of the experiments was lowered.

1.5 Application of Results

To date, iron nickel, and cobalt have been examined as possible catalysts for the Bosch process. The maximum water concentration obtainable in the iron system was shown by both Manning (1976) and Sacco (1977) to be determined by the iron-iron oxide-gas equilibrium at low temperature and by the graphite-gas equilibrium at high temperature. The present results, however, with nickel and cobalt catalysts, indicate that the maximum water concentration is determined by the corresponding carbide equilibrium at low temperature and by the graphite-gas equilibrium at high temperature.

The equilibrium water concentrations obtainable in the graphite, cobalt, nickel, and iron system are shown in Figure 5-1. For the iron system, the maximum water concentration obtainable occurs at 915K, the temperature at which the iron-iron oxide-gas equilibrium and the graphite equilibrium intersect at an O/H ratio of 0.5 For the cobalt system, it occurs at 800K, the point at which the carbide-gas equilibrium begins to have an effect. In the experiments run over nickel, the graphite-gas equilibrium was not reached even at 900K. The maximum water concentration here occurred at 825K. The water concentrations were 16, 32, and 25% for iron, cobalt, and nickel, respectively. In a simple recycle reactor, the recycle ratio is calculated as

$$r = 2\left(\frac{1}{\chi_{H_2O,Eq.}} - 1\right)\frac{\text{moles gas recycled}}{\text{mole } CO_2 \text{ fed}}$$

For the iron, cobalt, and nickel systems, the minimum recycle ratio is 10.5, 4.3, and 6.0, respectively. For an equilibrium reactor, cobalt yields the lowest recycle ratio. The recycle ratios for the various catalysts are plotted

versus temperature in Figure 5-3.

2. Literature Survey

The Bosch process has been investigated by NASA as a means of recovering oxygen from metabolic carbon dioxide. The ultimate objective has been to construct a life support system capable of supplying oxygen in a cyclic process. The cycle begins by reducing the carbon dioxide with hydrogen to form solid carbon in what is known as the Bosch process. An iron catalyst is normally used. The water formation reaction is followed by electrolysis to yield hydrogen and oxygen,

$$CO_2 + 2H_2 \rightarrow C + 2H_2O$$

$$2H_2O \rightarrow 2H_2 + O_2.$$

The overall process results in the accumulation of carbon on the iron catalyst with no net change in carbon dioxide, oxygen, or hydrogen mass.

In the past, NASA scientists have run Bosch reactors using a steel wool catalyst and recycling unreacted gases to obtain complete reaction (Holmes et al., 1970). One problem which they encountered was that the maximum water concentration obtained in the reactor was significantly less than the thermodynamically predicted equilibrium water concentration. Investigators at MIT were able to show that the phenomena which occurred resulted from oxide inhibition rather than slow reaction rates. That is, in addition to the reactions which occurred between carbon monoxide, carbon dioxide, methane, hydrogen, water and carbon, oxidation of the iron catalyst also occurred. Above 860K the reaction

$$Fe + H_2O \rightleftarrows FeO + H_2$$

occurred, and below 860K,

$$3Fe + 4H_2O \rightleftharpoons Fe_3O_4 + 4H_2$$

These reactions, coupled with the discovery that iron oxide does not catalyze carbon deposition reactions, were given as an explanation for the low water concentrations present in the NASA reactors. Sacco's (1977) and Manning's (1976) experimental data on the Bosch system were in good agreement with iron-oxide-gas equilibrium calculations based on tabulated Gibbs energy data.

Preliminary theoretical calculations have revealed that water production limitations associated with the iron catalyzed Bosch process may not be encountered when the iron is replaced by nickel or cobalt. This suggests that a study of the nickel and cobalt catalyzed Bosch process may lead to a more efficient reactor.

By measuring the compositions of gas mixtures of carbon dioxide, carbon monoxide, methane, hydrogen and water in equilibrium with deposited carbon, and then comparing these with gas compositions calculated making the assumption that the solid phase is β-graphite, it might be possible to determine if either a carbide or some other form of carbon is affecting the equilibrium.

2.1 Previous Bosch Studies

In the early 1970's researchers at MIT became interested in the Bosch process, especially with the difficulty which NASA scientists had encountered while running Bosch prototype reactors. By running a Bosch recycle reactor using a steel wool catalyst, the conversion of carbon dioxide to water was achieved. However, a large recycle rate was needed considering the low water concentrations present in the reactor. The water concentrations obtained were much lower than that predicted by equilibrium calculations based on a solid phase of β-graphite with a gas phase of carbon dioxide, carbon monoxide,

methane, hydrogen, and water.

2.1.1 $CO-CO_2-Fe-Fe_3O_4$ Equilibrium

Since the gas phase compositions obtained in the prototype reactors had not reached the equilibrium expected at the graphite-gas phase boundary, it was believed that a closer look should be taken at the thermodynamics of the system. To better understand the Bosch process, Manning (1976) began both a thermodynamic analysis and an experimental study of the process. Considering a gas phase of hydrogen, carbon monoxide, methane, carbon monoxide, and water, and a solid phase of carbon, three independent reactions may be chosen to describe the system. As an example, there is the reverse water-gas shift reaction,

$$H_2 + CO_2 \rightleftarrows CO + H_2O,$$

the disproportionation of carbon monoxide,

$$2CO \rightleftarrows C + CO_2$$

and the methanation reaction,

$$C + 2H_2 \rightleftarrows CH_4$$

A phase rule analysis of the system gives a variance of three which allows the temperature, pressure, and gas phase elemental O/H ratio to completely set all other intensive variables. For a metallic steel wool catalyst, calculation of the gas phase concentration in equilibrium with iron and iron oxide phases involves determining the particular iron oxide phase which is expected to be in equilibrium with the metallic phase at a given temperature. At 800K, the stable iron oxide species determined from the Fe-O phase diagram (Muan and Osborn, 1965) is Fe_3O_4. Three independent reactions for the iron-iron oxide

gas equilibria are

$$3Fe + 4H_2O \rightleftarrows Fe_3O_4 + 4H_2$$
$$4CO_2 + 3FE \rightleftarrows Fe_3O_4 + 4CO$$
$$3H_2 + CO \rightleftarrows CH_4 + H_2O$$

Figure 2-1 is an equilibrium phase diagram for a gas phase of carbon dioxide, carbon monoxide, methane, hydrogen, and water at 1 atm and 800K. Both the iron-iron oxide-gas and the graphite-gas equilibrium lines are shown. Above the graphite-gas equilibrium line one expects to deposit carbon, while below the line one would expect carbon removal. The iron-iron oxide phase boundary reveals the stable species of iron which would be expected to be in equilibrium with an equilibrium gas mixture. For a point representing a gas phase composition above the oxide phase boundary, iron is the stable species, below the boundary iron oxide is stable.

In experimental studies, Manning employed a gravimetric differential reactor, which is similar to the one used in this thesis. The catalyst employed in the experiments was grade 2 steel wool supplied by the American Steel Wool Co., Long Island City, N.Y. The concentration of alloying elements in the steel wool was 0.36 wt%C, 0.70wt%Mn, 0.04 wt%P, 0.018 wt%S, and 0.4ppm N. The BET surface area of the catalyst was determined to be 389 cm^2/g from the adsorption of krypton at liquid nitrogen temperatures.

In one experiment, 250 mg of steel wool and approximately 700 mg of deposited carbon at 823K were used to study the equilibrium of the reaction,

$$2\ CO \rightleftarrows C + CO_2$$

Figure 2-2 gives the results in graphical form. Four gas mixtures were passed over the catalyst which resulted in three different phenomena. For a 50:50 $CO:CO_2$ mixture, no carbon depostion was observed and a constant weight measure-

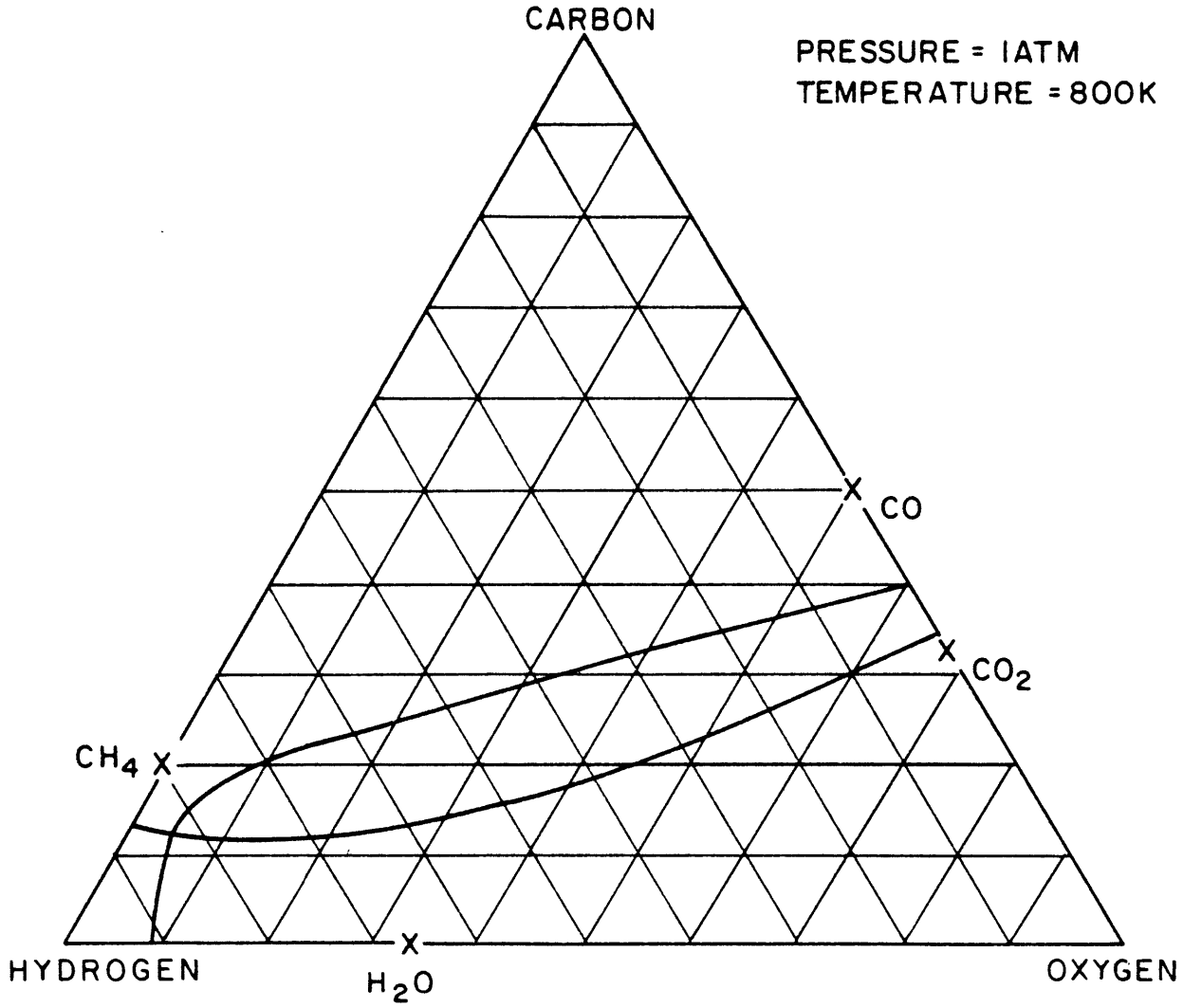

UPPER CURVE: IRON-IRON OXIDE-GAS EQUILIBRIA
LOWER CURVE: GRAPHITE-GAS EQUILIBRIA

FIG. 2-1

Phase Diagram for the Iron-Iron Oxide-Gas and Graphite-Gas Equilibria

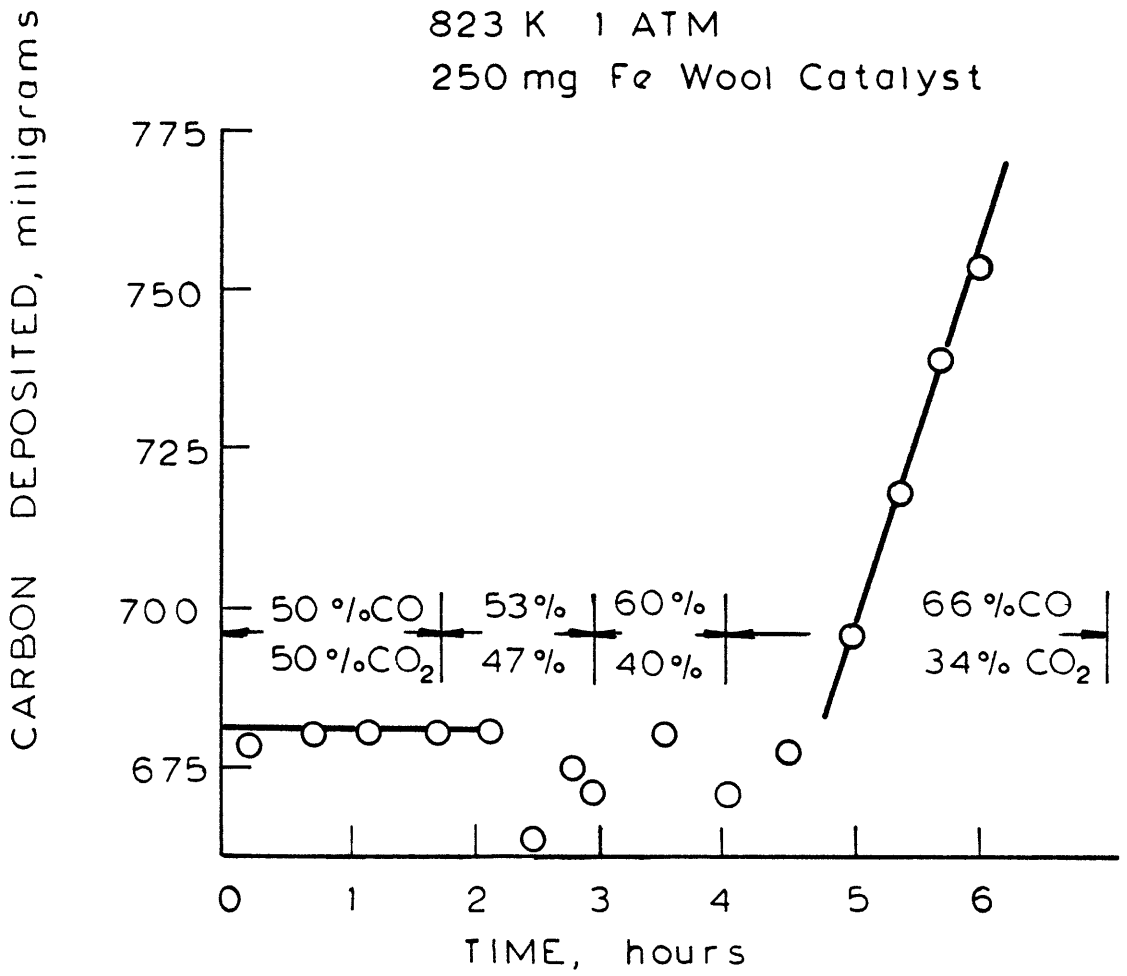

Figure 2-2 Carbon Deposition From $CO-CO_2$ Mixtures (Manning, 1976)

ment was obtainable for almost a two hour period. For the next two hours a 53:47 $CO:CO_2$ and a 60:40 $CO:CO_2$ mixture were passed over the catalyst which resulted in the erratic weight gain and loss. These weight changes were of the order of 10-15% of the total weight. The final gas mixture was a 66:34 $CO:CO_2$ which resulted in a rapid rate of carbon deposition.

To understand the phenomena occuring in this experiment, examine the two reactions, the iron oxidation reaction,

$$3Fe + 4CO_2 \rightleftarrows 4CO + Fe_3O_4$$

and the disproportionation of carbon monoxide,

$$2\ CO \rightleftarrows CO_2 + C$$

At 823K the equilibrium carbon monoxide gas phase compositions for the two reactions are 53 and 13 mole%, respectively. Manning postulated that with a 66:34 mixture of $CO:CO_2$ mixtures iron oxide is converted to its reduced from at which point carbon deposition begins. In the intermediate zone, Manning indicated that the experimental technique did not allow one to differentiate between carbon deposition and catalyst oxidation.

For the most part, Manning's explanation for equilibrium phenomena is quite sound. Experimentally he has given good evidence for the interference of oxides on carbon deposition. Through careful coupling of both theoretical and experimental data, Manning was able to explain on thermodynamic grounds the prevention of carbon deposition on iron oxides which could explain the low water yields in Bosch reactors. Examining his results, it can be seen that during the intermediate phase there occurs no weight gain on loss over the base line which was established during the 50:50 $CO:CO_2$ period. This indicates that there exists two kinds of reactions occuring which cause both weight increases and decreases. Manning believed that they were the deposi-

tion of carbon and the reduction of iron.

2.1.2 The Equilibrium of H_2, CO, CO_2, CH_4, and H_2O with Iron and Iron Oxide

Sacco studied the equilibria of gas mixtures containing carbon dioxide, carbon monoxide, methane, hydrogen, and water over an iron catalyst using the experimental apparatus described in this thesis. Water was added to the gas mixture by means of a saturator. The saturator consisted of three round bottom flasks connected by glass tubes and bubblers. To set water content of the gas stream, the flasks were contained in a constant temperature bath. The partial pressure of water desired was set by the temperature of the bath. The gas was passed through a vertical bed packed with glass beads to remove any entrained liquid water.

Figure 2-3 shows the results of Sacco's experiments at 800K. The phase diagram shows the various equilibrium solid phases and the phase boundries which separate them. The triangles indicate gas compositions which were passed over the catalyst, closed triangles representing weight gain, or carbon deposition, and open ones representing no weight change.

To determine the gas phase composition at which carbon deposition ceased, Sacco used the following logic and technique. Since a differential reactor was used, it was important that the compositions of the gas mixtures were close to equilibrium. Starting from such a point where carbon deposition was possible, the position of the carbon deposition boundary was determined by fixing the O/H ratio and decreasing the C/H ratio of the inlet gas mixture to a point where carbon deposition ceased. This was accomplished in the following manner. Two independent reactions which relate the gas phase components were chosen to be

$$H_2 + CO \rightleftarrows H_2O + CO_2$$

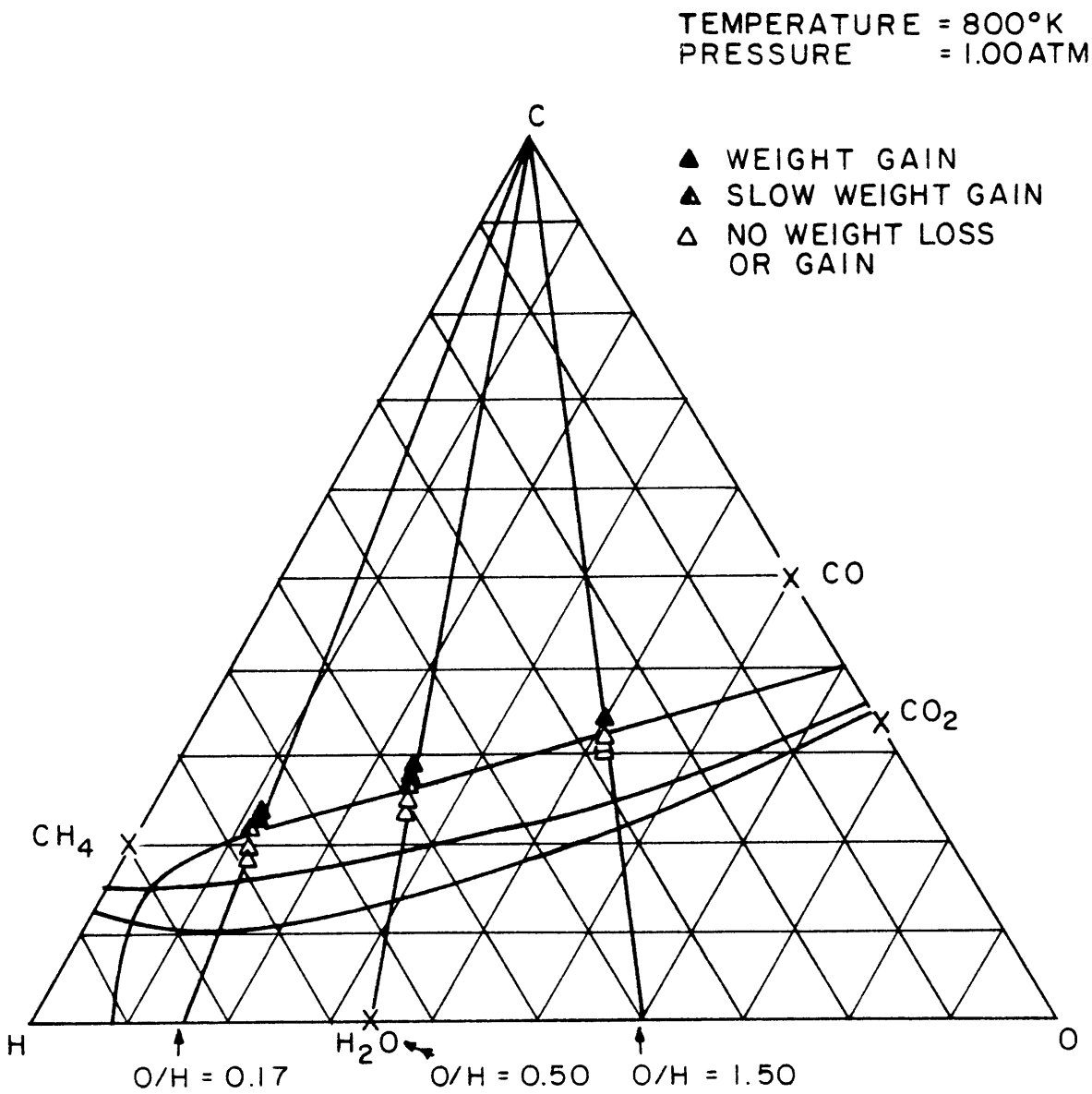

Fig. 2-3 INHIBITION OF CARBON DEPOSITION BY Fe_3O_4 AT VARIOUS O/H RATIOS. (Sacco, 1977)

and

$$3H_2 + CO \rightleftarrows CH_4 + H_2O$$

A phase rule analysis reveals that if the temperature, pressure, and O/H ratio are set, and the C/H ratio varied, only one phase may be present at equilibrium. Using known equilibrium constants,the gas composition would then be calculated. The gas compositions calculated in this manner are not equilibrium compositions but ones which are close to equilibrium. Sacco then used a gas delivery system to make up gas mixtures of the desired composition.

As can be seen from Figure 2-3, as long as the gas compositions were above the oxide equilibrium and therefore iron was the stable phase, carbon deposition occurred. Once below the line, carbon deposition was stopped.

The work by Sacco is very significant since it gives further evidence of Manning's hypothesis of the role of oxides in carbon deposition. With the close approach of the oxide equilibrium line it becomes quite clear that Fe_3O_4 does not catalyze carbon deposition.

Sacco also investigated the carbon deposition boundary at 900K and various O/H ratios as shown in Figure 2-4. It was found that FeO inhibited carbon deposition. Figure 2-4 shows how carbon deposition was controlled by adjusting the C/H ratio. Since the three different phase lines are very close together at 900K, it is easier to observe the experimental results in a form which is presented in Figure 2-5. Here the precentage of the theoretical equilibrium P_{H_2}/P_{H_2O} ratio is plotted against the experimental P_{H_2}/P_{H_2O} ratio, for various O/H values. Since the P_{H_2}/P_{H_2O} ratio is defined by the equilibrium constant for the oxide reaction,

$$Fe + H_2O \rightleftarrows H_2 + FeO$$

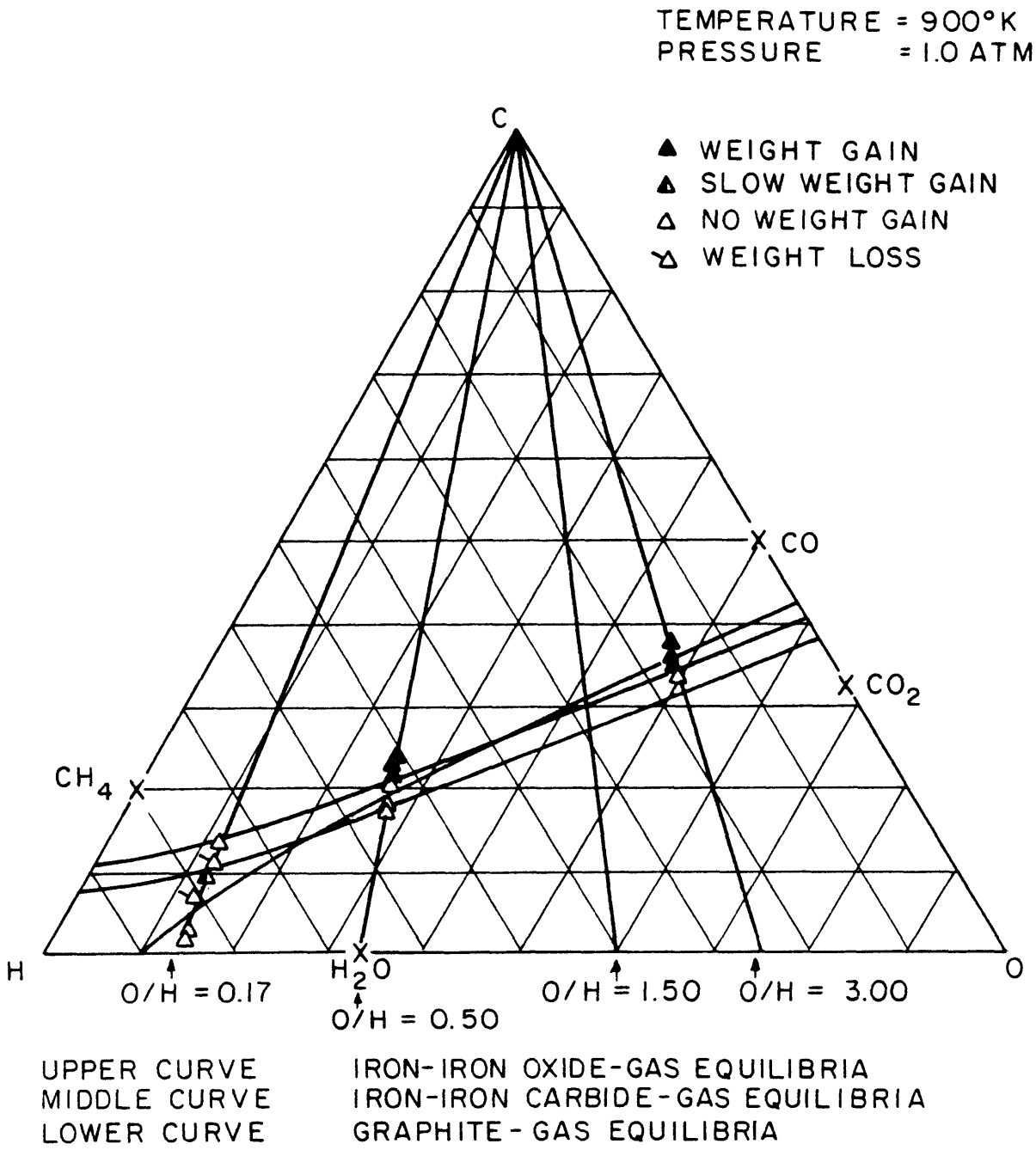

Fig. 2-4 DETERMINATION OF THE IRON/WUSTITE PHASE BOUNDARY IN A FIVE COMPONENT GAS MIXTURE AT VARIOUS O/H RATIOS. (Sacco, 1977)

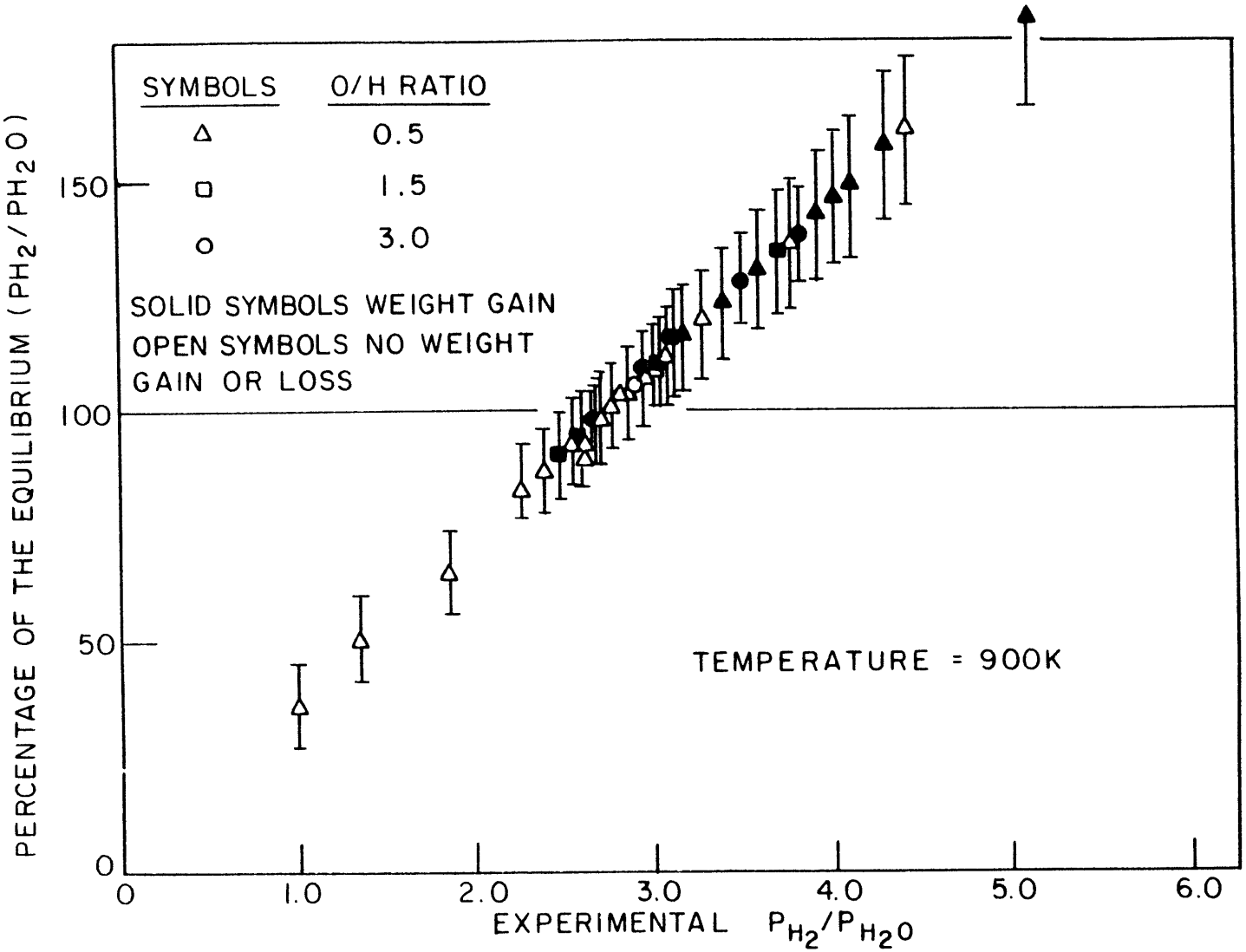

Fig. 2-5 PERCENTAGE OF THEORETICAL $P_{H_2}/P_{H_2O}|_{eq}$ VERSUS EXPERIMENTAL P_{H_2}/P_{H_2O} FOR VARIOUS O/H VALUES (Sacco, 1977)

at 900K, the equilibrium ratio is idependent of the gas phase composition. Error bars which indicate the maximum possible error due to the experimental method are given. This error was calculated to be 11%. Most of the data fall within 10% of the equilibrium P_{H_2}/P_{H_2O} ratio. Since a propagation of error analysis indicates the maximum possible error, Sacco suggested that some of the scatter reflected another process.

Sacco suggested the possiblility of the formation and reduction of multiple oxides phases. At 900K, under an atmosphere of carbon dioxide and water, he detected the formation of both hematite (Fe_2O_3) and wustite (FeO) after an inlet leak in reactor was detected and reactor shut down was necessitated. Although an interesting phenomena, multiple oxide formations at this point do not seem reasonable.

2.2 Nickel and Cobalt as Catalysts in the Bosch Process

Due to the oxide limitations fo the iron catalyzed Bosch process an investigation of the process using either nickel or cobalt as a catalyst could possibly yield a more efficient design. Since the water concentration of the graphite-gas equilibrium is higher than that of the iron-iron oxide-gas phase boundary, a catalyst which achieved the conversion of gases to the graphite equilibrium would have an overall lower gas recycle ratio.

2.2.1 Thermodynamics of the Ni-O_2 and Co-O_2 Systems

A thermodynamic analysis of the nickel-nickel oxide-gas and the cobalt-cobalt oxide-gas equilubria can be done in the same way as the one carried out on the iron system by Manning (1976). Figure 2-6 shows the phase diagram for the nickel-oxygen system. The phase diagram reveals that in going from a reducing medium to an oxidizing one, NiO is the oxide species of nickel which will be formed first (Bogatski, 1951). No Co-O phase diagram exists, however, there do exist Gibbs energy data for two different species of cobalt oxide. Figure 2-7 shows a plot of ln K_p ($\ln P_{O_2}$) versus 1/TK for the reaction

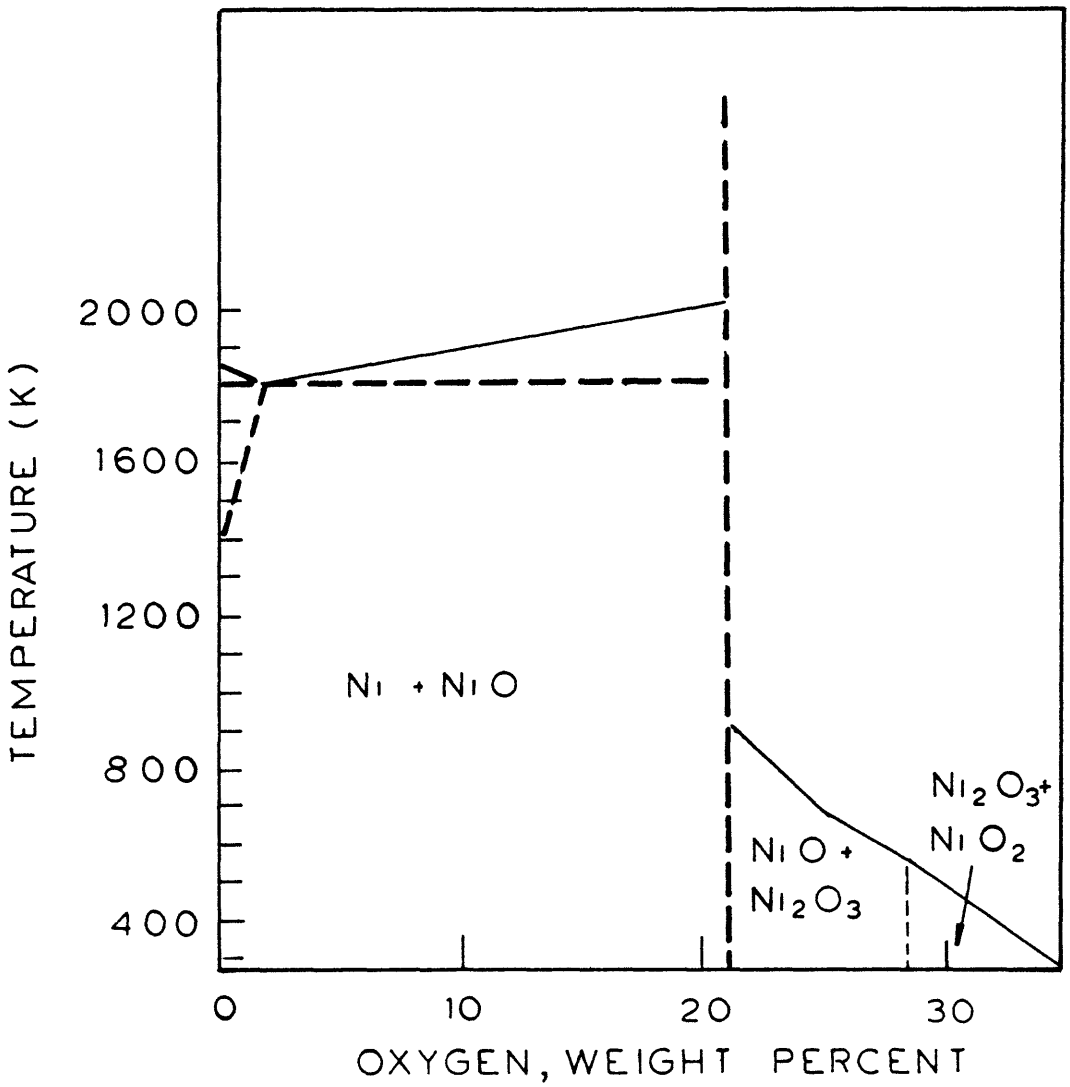

Fig 2-6 Nickel - Oxygen Phase Diagram
(Bogatski, 1951)

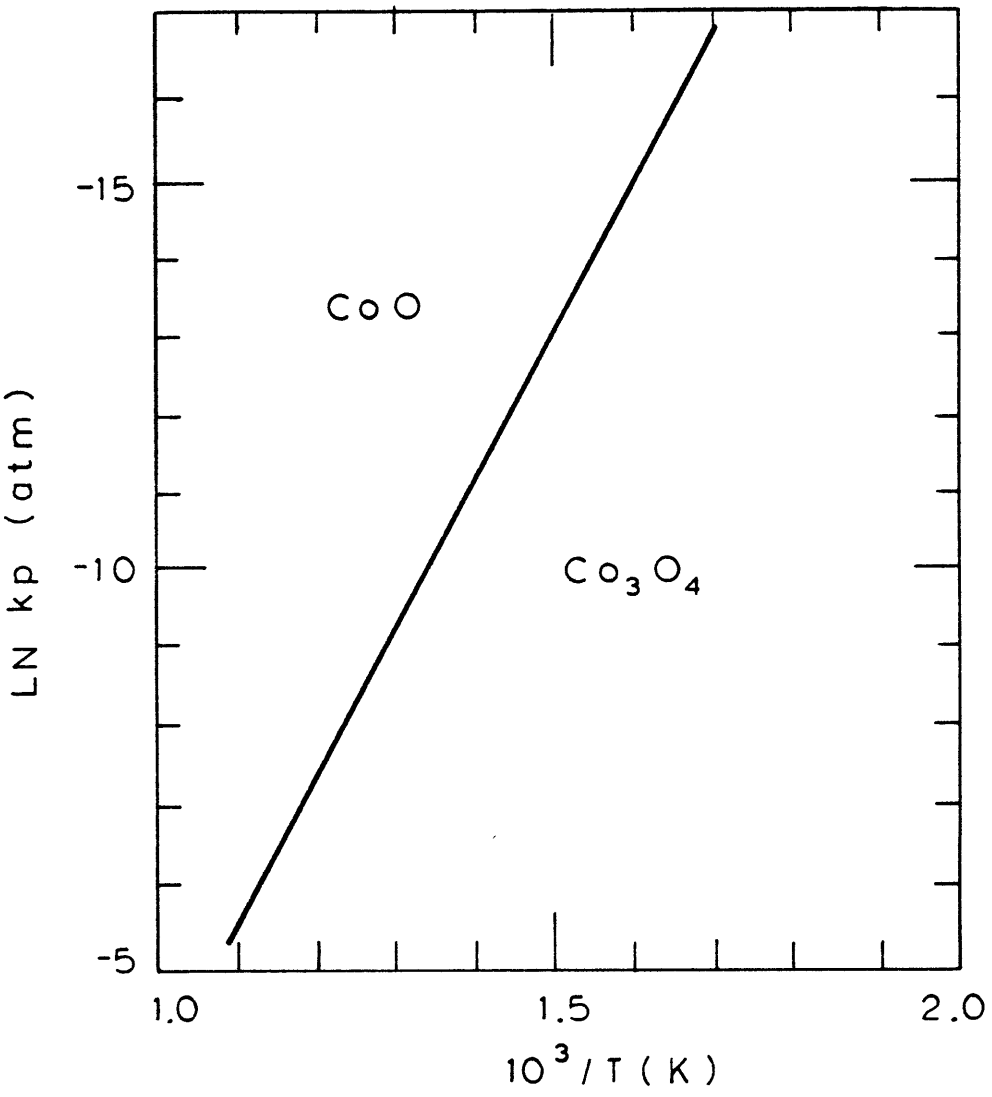

Fig 2-7 Equilibrium Constant for the Reaction $2Co_3O_4 \rightleftharpoons 6CoO + O_2$
(Kubaschewski, 1967)

$$2\ Co_3O_4 \rightleftarrows 6\ CoO + O_2$$

The equilibrium diagram reveals that CoO is formed at a lower partial pressure of oxygen than Co_3O_4. This indicates that in going from a reducing atmosphere to an oxidizing one, CoO will be formed before Co_3O_4. In other words in determining whether or not cobalt oxide will interfere with the graphite-gas equilibria, the Co-CoO-gas equilibrium must be considered. Although another species, Co_2O_3, also exists, no thermodynamic data are available. In the next paragraph, calculations show that the equilibrium line is so far removed from the graphite line that any small differences in Gibbs energy of Co_2O_3 would make very little change in the phase diagram of figure 2-8.

Three reactions may then be chosen to relate the components of the equilibrium system.

$$Ni + H_2O \rightleftarrows NiO + H_2$$

or

$$Co + H_2O \rightleftarrows CoO + H_2$$

$$Ni + CO_2 \rightleftarrows CO + NiO$$

or

$$Co + CO_2 \rightleftarrows CO + CoO$$

and

$$3H_2 + CO \rightleftarrows CH_4 + H_2O$$

Thermodynamic data on the oxide reactions are as follows

$$Ni + 1/2\ O_2 \rightleftarrows NiO$$

$$\ln K_p = 2.905\times10^{4}/T - 2.040\ \ln T + 3.786\times10^{-3}T - 1.425\times10^{-6}T^2 + 2.486\times10^{-10}T^3$$

$$Co + 1/2\ O_2 \rightleftarrows CoO$$

$$\ln K_p = 2.786\times10^{4}/T - 1.447\ \ln T + 2.452\times10^{-3}T - 7.9;6\times10^{-7}T^2 + 1.055\times10^{-10}T^3$$

(Kubaschewski, 1967; Barin and Knacke, 1973). In the equilibrium calculations,

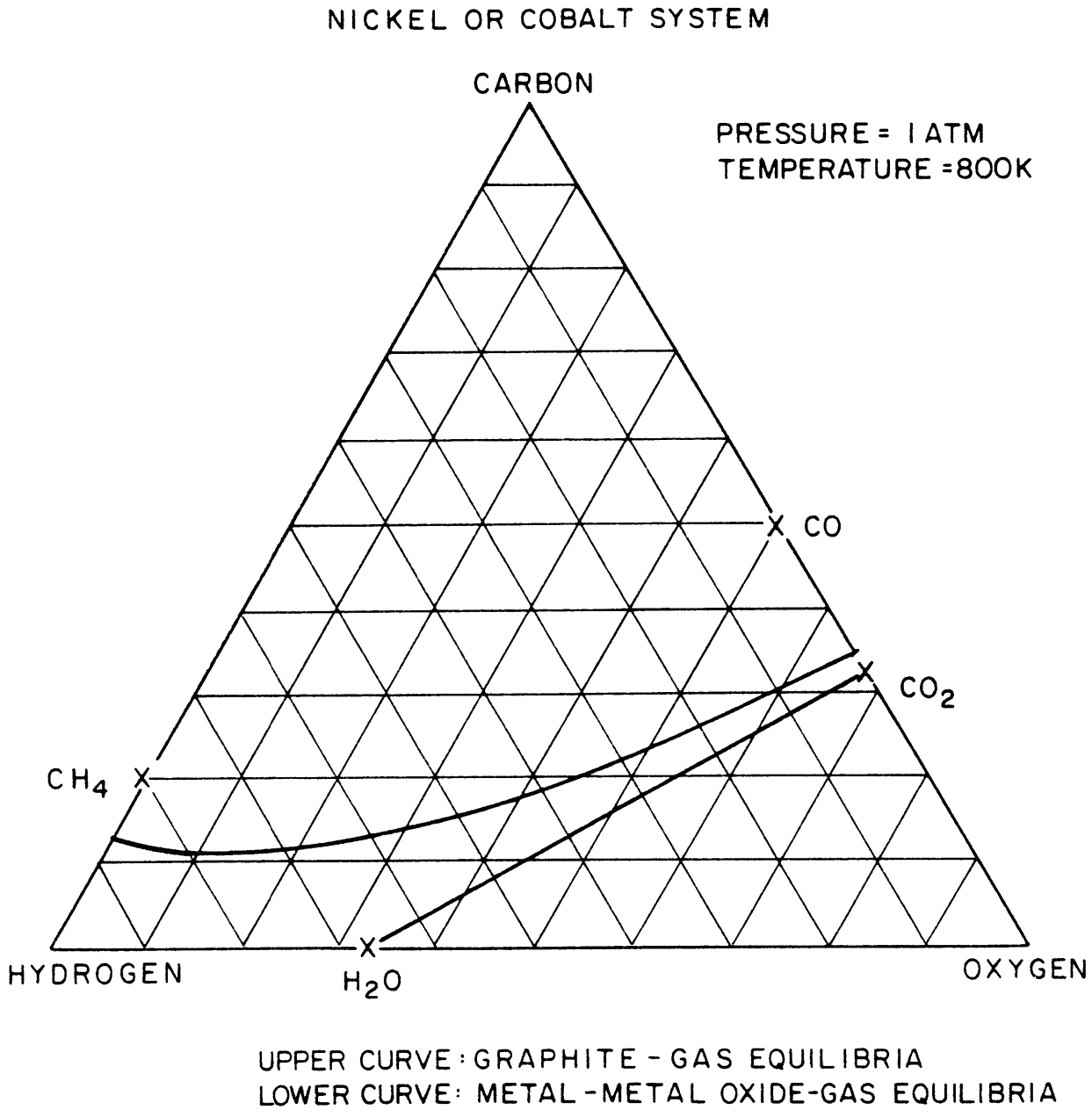

FIG. 2-8

Phase Diagram for the Metal-Metal Oxide-Gas Equilibria for the Nickel or Cobalt System

it was assumed that the activity of the solid phases was unity and that no solid solution existed. By setting the temperature, pressure, and C/H or O/H ratio, the phase rule has been satisfied and a phase diagram may be constructed. Figure 2-8 shows the equilibrium phase boundaries for the graphite-gas and either the nickel oxide or cobalt oxide systems. There is essentially no difference between the oxide boundaries. The gas composition necessary to cross the oxide phase boundaries is a partial pressure of water plus carbon dioxide of greater than 99%. If the phase diagrams for other temperatures between 600 and 900K are examined it is observed that the above condition for the oxidation of both nickel cobalt still holds.

If the nickel or cobalt system is compared with the iron Bosch system, the most obvious difference is the location of the oxide equilibria. In the nickel or cobalt system the oxide phase boundary never crosses the carbon deposition boundary; it is always below it. The significance of the calculations for the nickel and cobalt systems, making the assumption that the oxide forms of nickel and cobalt, as with iron, are not catalysts for carbon deposition is that the graphite-gas equilibrium can be reached.

2.2.2 Thermodynamics of the H_2-CO-CH_4- CO_2-H_2O-Carbon System

Since it has been shown in the previous section that oxides of nickel or cobalt will not interfere with the Bosch process, an equilibrium study of the carbon-gas system should indicate their advantages over an iron catalyst. Manning (1976) has shown how to calculate equilibrium gas compositons assuming the gas is in equilibrium with graphite. A phase rule analysis revealed that the temperature, pressure, and some elemental ratio in the gas phase must be fixed in order to define completely the system.

Equilibrium studies of previous nickel and cobalt catalized carbon (or carbide) - gas systems have been carried out. These studies have included

the methane-hydrogen-carbon (or carbide) system, the carbon monoxide-carbon dioxide-carbon (or carbide) system, and one study which examined a five-component (H_2,CO,CH_4,CO_2 and H_2O) system. The results of these studies indicated that the equilibrium resulted from a reaction of the gas phase species with a solid phase which might range from β-graphite to a solid phase, which included carbon, which had a Gibbs energy 7.0 kcal/mole greater than β-graphite. In other words, the investigators believed they were studying an equilibrium with β-graphite, a carbon with a Gibbs energy greater than β-graphite, or a nickel or cobalt carbide.

Dent (1945) and Rostrup-Nielsen studied both the CO-CO_2-C and CH_4-H_2-C equilibria over nickel catalysts. Dent included in his studies measurements of some five-component gas-carbon systems. These two investigations covered the temperature range from about 600 to 1200K. Although Dent only approached the equilibrium point from the carbon depositing side, Rostrup-Nielsen claims to have observed both sides of the equilibrium point in his experiments.

The other studies discussed in this chapter involve the methane-hydrogen equilibrium. The authors claimed that the solid phase in the system was either carbon or carbide. These studies include Schenck (1927), and Browning and Emmett (1952), and covered a temperature range of 450 to about 1000K.

In this thesis, a notation common to both Dent and Rostrup-Nielsen's results is ΔG_c, the Gibbs energy of a carbon formed in a given experimental system, where ΔG_c for β-graphite is equal to 0.0 kcal/mole.

$$\Delta G_c = G^\circ_{\text{EXPERIMENTAL CARBON}} - G^\circ_{\beta\text{-GRAPHITE}}$$

The equilibrium constant for a given reaction is thus related to ΔG_c by the equation

$$\Delta G_c = -RT \ln K_{p_{EXPERIMENTAL\ CARBON}} - RT \ln K_{p_{\beta\text{-Graphite}}}$$

For the systems of interest, the equilibrium constants may be calculated using any of the three carbon deposition reactions which are applicable.

$$H_2 + CO \rightleftarrows C + H_2O,\ K_p = \frac{P_{H_2O}}{P_{H_2} P_{CO}}$$

$$CH_4 \rightleftarrows C + 2H_2,\ K_p = \frac{P_{H_2}^2}{P_{CH_4}}$$

$$2CO \rightleftarrows C + CO_2,\ K_p = \frac{P_{CO_2}}{P_{CO}^2}$$

Although the function ΔG_c was defined to represent the Gibbs energy change resulting from any stuctural or compositional differences between an experimentally observed carbon and graphite, it can also be used to represent the Gibbs energy change of the carbide formation reaction

$$Me + C_{\beta\text{-graphite}} \rightleftarrows Me_nC$$

where Me represents either cobalt or nickel. In this case, the Gibbs energy change of the metal-carbide-gas equilibrium

$$CH_4 + nMe \rightleftarrows Me_nC + 2H_2$$

is equal to

$$\Delta G = \Delta G_c + \Delta G^\circ_{\beta\ graphite}$$

where $\Delta G^\circ_{\beta graphite}$ is the Gibbs energy change for the decomposition of methane to β-graphite plus hydrogen. This follows from stoicheometry

$$CH_4 \rightleftarrows 2H_2 + C_{\beta\text{-graphite}}$$

$$\frac{C_{\beta\text{-graphite}} + nMe \rightleftarrows Me_nC}{CH_4 + nMe \rightleftarrows Me_nC + 2H_2}$$

As referred to in a previous section, Sacco (1977) determined the iron-iron oxide-gas phase boundary by choosing two independent reactions and setting the temperature, pressure, and O/H ratio in the feed stream, and then varying the C/H ratio. By starting a given experimental run with a high C/H ratio and proceeding to a lower one, the point at which iron oxide first appeared was determined by the cessation of carbon deposition. In this thesis, a mathematically equivalent method was used. Three reactions were chosen, one being a carbon deposition reaction. Then the temperature, pressure, and O/H ratio were set and the Gibbs energy of the carbon deposition reaction was varied according to the equation

$$\Delta G_c = - RT \ln K_{p_{observed}} + RT \ln K_{p_{graphite}}$$

The variation of ΔG_c is equivalent to changing the C/H ratio in the gas feed. Since equilibrium calculations are based on ΔG_c, (which is assumed to be independent of gas phase) the results obtained from a two-component gas experiment can be applied to a five-component gas system.

2.2.2.1 Dent's Study of the Carbon-Gas Equilibrium

Dent (1945) studied the catalytic synthesis of methane from carbon monoxide and hydrogen to determine the conditions necessary to obtain an adequate catalyst life and to avoid carbon deposition, typically referred to as coking. For this, an important factor is the carbon-gas equilibrium.

To study the equilibrium system, Dent employed a column reactor at a residence time of 30s. The nickel catalyst used was prepared by adding 25

parts by weight of china clay to an aqueous solution containing 100 parts of nickel nitrate, 20 parts maonganese nitrate and 13.6 parts aluminium nitrate. The metals were then precipitated as basic carbonates or hydroxides by the addition of a solution of 97 parts potassium carbonate to the catalyst solution. The solution was boiled and filtered. The filter cake was then washed, dried, crushed and sieved.

Dent's first experiments involved the measurement of $CO-CO_2-C$ equilibrium at temperatures between 623 and 1173K, and pressures of 1.0 and 20 atm. Figure 2-9 gives the results in graphical form for an experiment at 773K and 1.0 atm. The experiments were run by passing a carbon monoxide-carbon dioxide mixture over fresh catalyst at constant space velocity while following the reactor outlet composition with time. The compositional change with time, as shown in Figure 2-8, resulted from the catalyst area change which occurred from the deposition of carbon. Gas mixtures of 16, 15, 14, and 13% carbon monoxide were passed over the catalyst bed. Close examination of the results indicate that the outlet composition resulting from the 16 and 15% carbon monoxide mixtures arrived at a final outlet composition of 11.5%, while the 14% mixture finished at 11.0%. The explanation of the 13% mixture's failure to react was that the CO concentration was so low so that equilibrium constrants applied. An alternate explanation is that the reaction was not allowed to proceed for a long enough time so as to allow the area of the catalyst, and hence the kinetics, to increase from the deposition of carbon. Dent argued that since different initial gas compositions all arrived at the same final composition, 11.0% carbon monoxide was the equilibrium point. Upon analyzing the data, the question arises as to the validity of "the same final composition". Figure 2-10 give his results at the other experimental conditions.

The CH_4-H_2-C equilibrium was measured using the same technique described

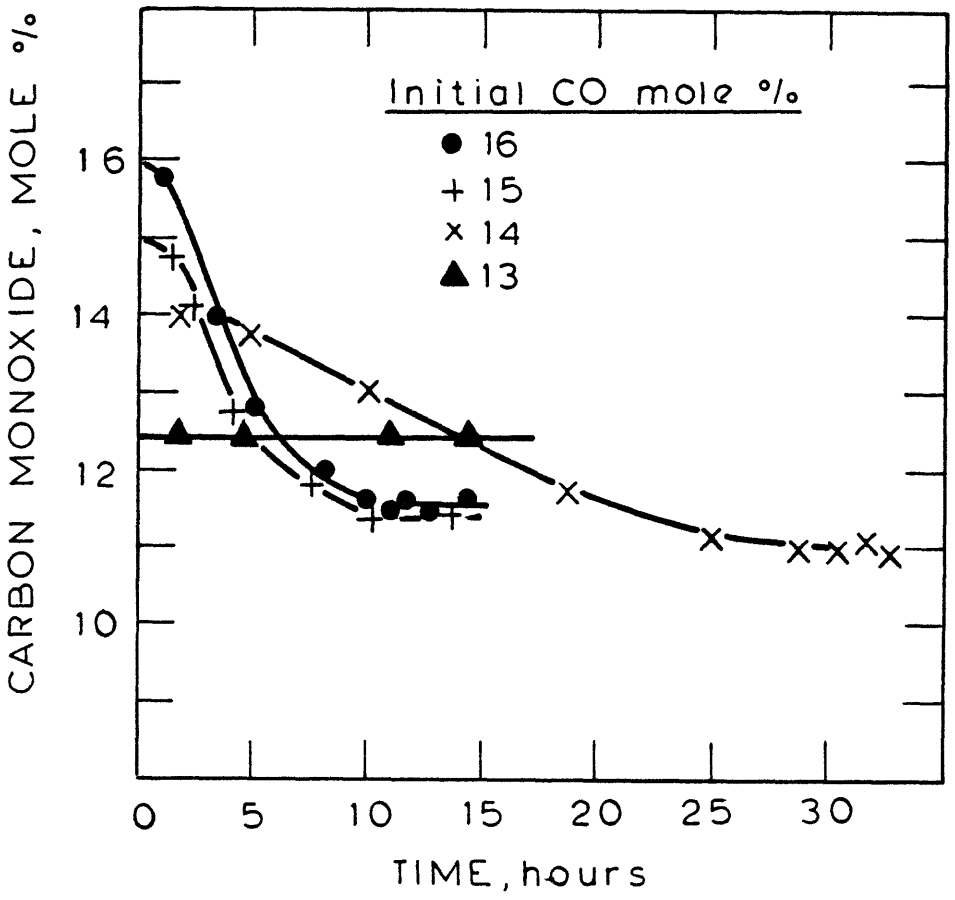

Fig. 2-9 The Decomposition of Carbon Monoxide over a Nickel Catalyst (Dent, 1945)

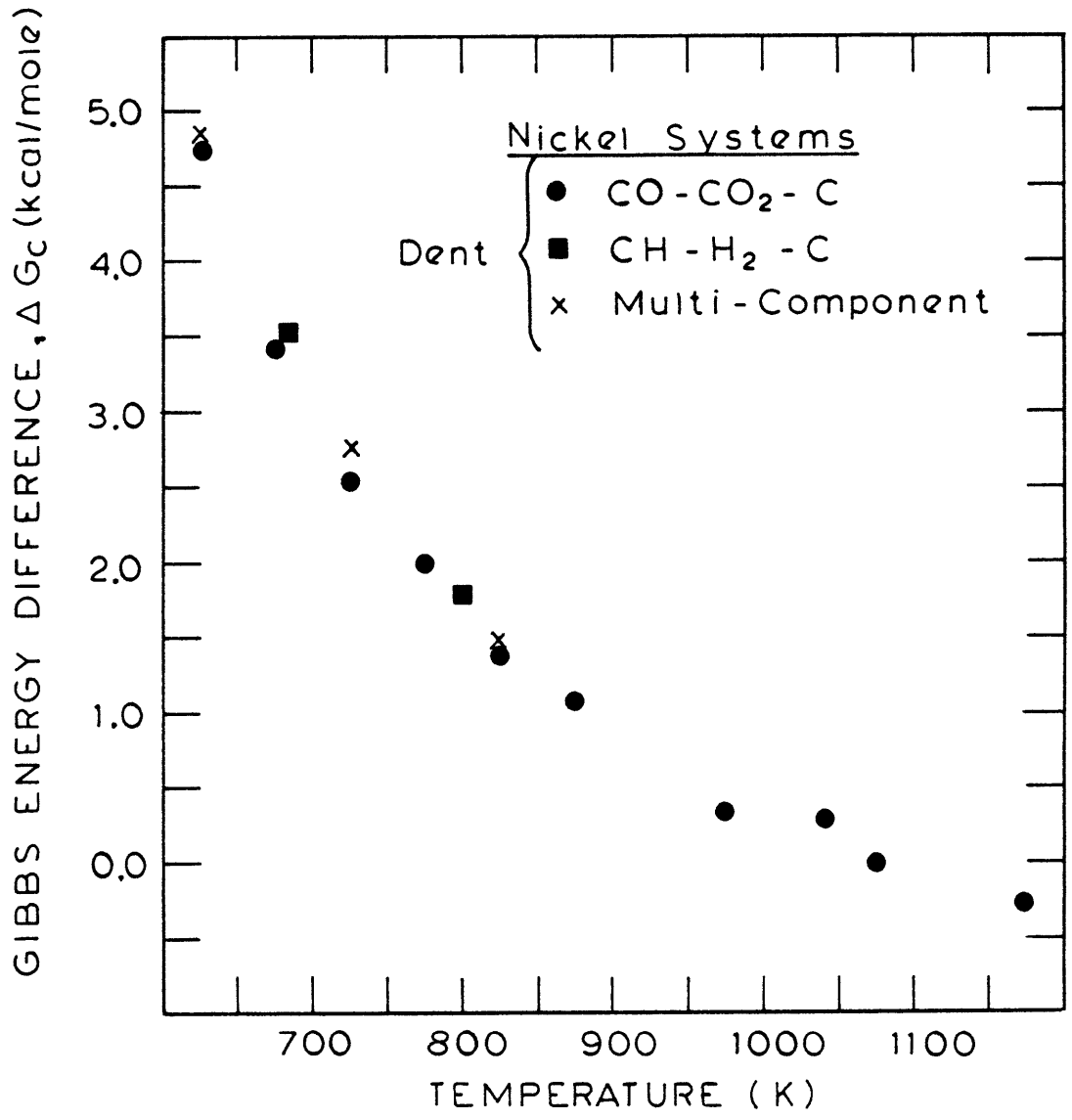

Fig. 2-10 Gibbs Energy Difference for Carbons Formed from Various Gas Mixtures (Dent, 1945)

for the $CO-CO_2-C$ system. The results are given in Figure 2-10. The experiments were run from the methane-rich side of equilibrium such that carbon deposition was occurring.

Dent also ran experiments with gas feeds of hydrogen and carbon monoxide, and of methane and water. These mixtures were studied because of his interest in the catalytic formation of methane and the associated problems of catalyst coking. Three mixtures were run, one at 623K and 1 atm was a equimolar mixture of hydrogen and carbon monoxide. A second mixture of 95% methane and 5% water was reacted at 723K and 1 atm. A third gas mixture of 66% hydrogen and 33% carbon monoxide was reacted at 823K and 1 atm. When these mixtures were used with a nickel catalyst, the reactor outlet compositions were measured and are compiled in Table 2-1. In the table, ΔG_c for the reactions

$$H_2 + CO = C + H_2O$$

$$CH_4 = C + 2H_2$$

$$2CO = C + CO_2$$

was calculated using the outlet gas compositions. These results are listed in the table and the average values of ΔG_c are also graphed in Figure 2-10. Table 2-1 shows that ΔG_c is invariant with respect to the equation used to calculate it. This indicates that the system is at equilibrium. Although only three equations are needed to specify the equilibrium system, the equilibrium constant for the gas reaction

$$CH_4 + H_2O = CO + 3H_2$$

is given and also the corresponding temperature. Note the agreement between

Table 2-1 Carbon Equilibrium in a Methane Synthesis System (Dent, 1945)

Temperature, K	623	723	823
Pressure, Atm	0.985	0.991	0.996
Initial Gas	CO/H_2 (1/1)	CH_4/H_2O (95/5)	CO/H_2(1/2)
Final outlet composition		(mole %)	
CO_2	46.8	0.7	14.1
CO	1.3	0.6	8.7
H_2	1.5	15.9	34.5
CH_4	46.1	79.9	36.5
N_2	1.7	0.3	0.2
H_2O	2.6	2.6	16.0
Log K_p of			
$CO + 3H_2 = CH_4 + H_2O$	-6.45	-3.075	-2.92
Corresponding Temperature, K	623	727	824
ΔG_c ($CH_4 = C + 2H_2$) kcal/mole	4.56	2.48	1.36
ΔG_c ($2CO = C + CO_2$)	4.84	3.03	1.43
ΔG_c ($H_2 + CO = C + H_2O$)	5.01	2.92	1.51

the calculated and experimental reaction temperature. Figure 2-10 shows how the ΔG_c from these three experiments have good agreement with the CO-CO_2-C and CH_4-H_2-C systems. These results indicate that equilibrium was being measured and that it is independent of the O/H ratio in the mixture. Since reaction rates diminish as equilibrium is approached, it is possible that Dent's reaction had not gone to equilibrium. To have removed this uncertainty, the equilibrium should have been approached from the carbon removal side.

Dent had no conclusive explanation of why the equilibrium in the systems he studied did not agree with calculations which assumed a solid phase of graphite. He did, however, indicate that an explanation could be found which was based on either the structural differences between the carbon formed in his system and that of β-graphite, or the formation of a nickel carbide.

The importance of Dent's work is two-fold. First it shows that in making equilibrium calculations in either of the two binary systems or a multicomponent one a Gibbs energy value for the carbon at a give temperature can be used. Secondly, that in making equilibrium gas compositions calculations for the Bosch process, the assumption of a Gibbs energy value, equal to that of graphite, may be an erroneous one.

2.2.2.2 Rostrup-Nielsen's Study of the CO-CO_2-C and the CH_4-H_2-C Equilibrium

Rostrup-Nielsen (1972) studied the CO-CO_2-C and CH_4-H_2-C equilibrium over nickel. The work was part of a study on coking of naphtha-steam reforming catalysts caused by the decomposition of carbon monoxide and methane. Since coking can be eliminated by operating with an excess of steam, so that thermodynamics predicts no formation of carbon, a measurement of the Gibbs energy of the carbon present is important.

To study the equilibrium, Rostrup-Nielsen employed a thermogravimetric reactor to follow the deposition and removal of carbon. The catalyst was suspended in a basket from an electrobalance which allowed continuous weight measurement. The principle catalyst used was a nickel (25 wt%) on magnesia, labeled A-1. Other catalysts examined were modified A-1 catalysts, nickel on magnesia catalysts with varying nickel content, and nickel catalysts made with other supports such as magnesium aluminum spinel, η-alumina, and α-alumina.

The experimental procedure involved passing pure carbon dioxide or hydrogen through the system, then adding, stepwise, carbon monoxide or methane until carbon deposition accurred. At that point, the carbon monoxide or methane was decreased until carbon removal occurred. By extrapolating to a point of no weight change, the equilibrium point was determined. Figure 2-11 shows the resultant Gibbs energy difference, ΔG_c, plotted against temperature.

The study carried out over the A-1 catalyst is represented in Figure 2-11 by squares ($CO-CO_2-C$) and circles (CH_4-H_2-C). The range of the values of the results of all catalysts for the $CO-CO_2-C$ system at 773 and 873K are shown in the figure by verticla bars. The same is done for the CH_4-H_2C system at 773K.

From Dent's results it was shown that the same Gibbs energy of carbon was determined at a given temperature, to be independent of the equilibrium system which he studied. For Rostrup-Nielsen's results, it is seen in Figure 2-11 that the equilibrium point for the $CO-CO_2-C$ and CH_4-H_2-C system are different. While the $CO-CO_2-C$ equilibrium is in good agreement with Dent, the CH_4-H_2-C is observed closer to graphite at higher temperature. Below 750K, the results of the methane reaction are seen to approach that of carbon monoxide. It is not clear, at this point, why this would occur.

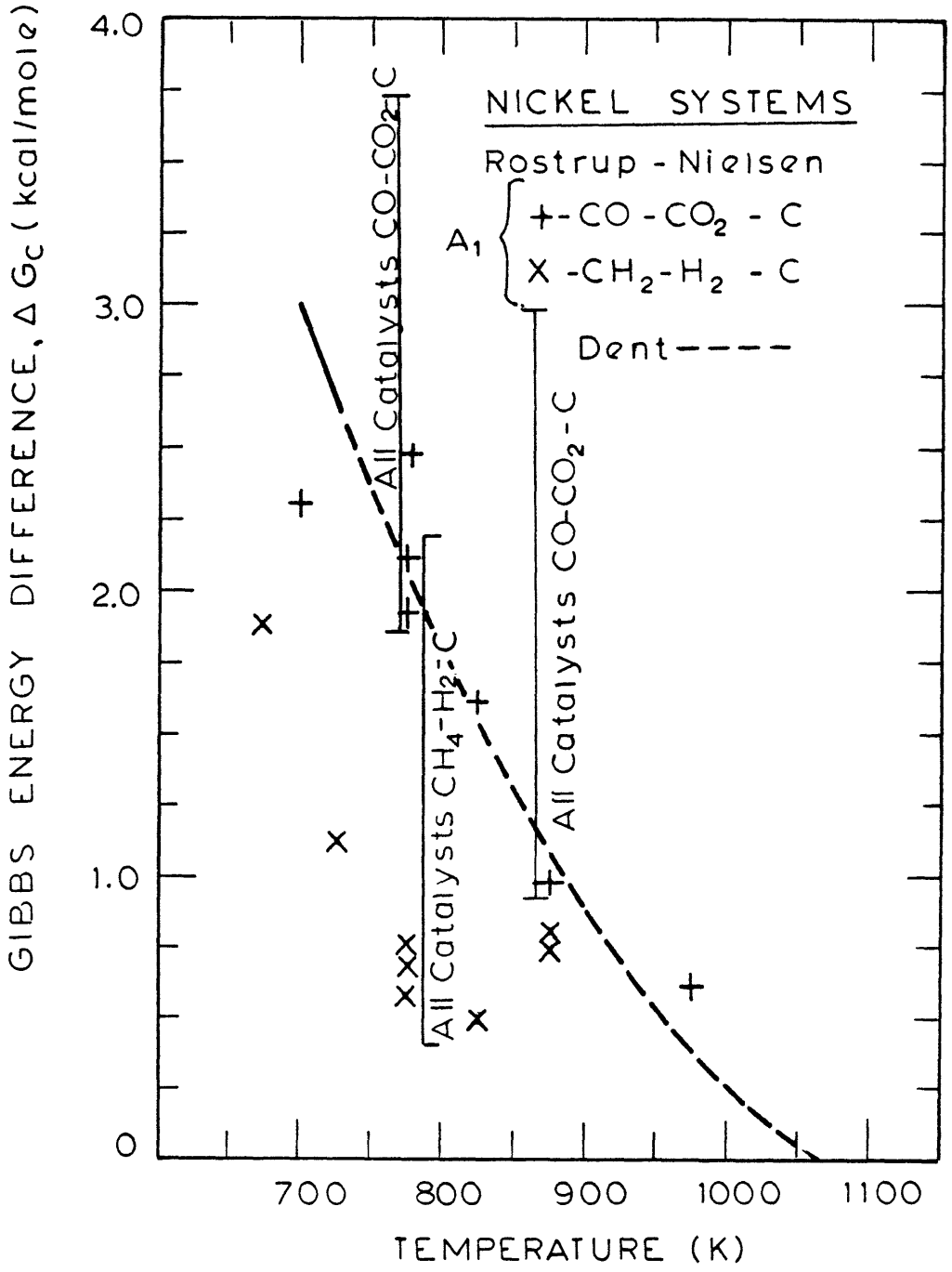

Figure 2-11 Gibbs Energy Difference for Carbon Formed in the $CO - CO_2 - C$ and $CH_4 - H_2 - C$ Equilibrium (Rostrup - Nielsen, 1972)

Observing the range of values obtained for the various catalysts (Figure 2-11), it can be seen that the lowest value for either of the two gas systems ($CO-CO_2-C$ at 773 and 873K, CH_4-H_2-C at 773K) falls close to the value obtained for the corresponding experiment over the A-1 catalyst. The other values occur at gas compositions richer in the carbon depositing gas, carbon monoxide or methane. An alternative explanation to that Rostrup-Nielsen's involving a Gibbs energy contribution due to nickel crystallite sizes (discussed in the next paragraph) is that these other catalysts which were studied were less active than the A-1 and thus needed a gas mixture richer in carbon monoxide or methane in order to dectect carbon deposition. This reasoning assumes that the removal of carbon was slow, and that the point at which carbon deposition first ceased was taken as the equilibrium point. This explanation follows from experimental observations of the work of this thesis which indicated that under certain conditions, carbon removal was not detectable.

As was discussed, the experiments (Figure 2-11) using various catalysts for the $CO-CO_2-C$ system at 773 and 873K, and for the CH_4-H_2C system at 773K show a wide variation in ΔG_c. Observations made in the electron microscope showed that the diameter of a carbon whisker, formed from carbon monoxide or methane decomposition, was close to, but not greater than, that of the nickel crystallite from which it grew. From this observation, Rostrup-Nielsen concluded that the Gibbs energy difference between the observed carbon and graphite, could be attributed to surface energy contributions resulting from the cylindrical form of a carbon filament. He assumed that the carbon filament could be modeled as an infinite cylinder for which the Kelvin equation expresses the difference between the Gibbs energy, μ, of a cylinder with a radius r, and the Gibb energy, μ_o, of a cylinder of infinite radius,

$$\mu - \mu_o = \frac{\gamma M}{r \rho}$$

where γ is the surface tension of graphite, M its molecular weight, and ρ its density. In the model ΔG_c is equated to the surface energy difference,

$$\Delta G_c = \mu - \mu_o + \mu^*$$

plus a constant term μ^* which is equal to the Gibbs energy difference between the experimentally observed carbon and graphite for a carbon fiber of infinite radius. μ^* reflects any structural and compositional differences which are independent of r.

The final equation is

$$\Delta G_c = \frac{\gamma M}{\rho} \frac{1}{r} + \mu^*$$

Thus a straight line should result when ΔG_c is plotted versus 1/r. Rostrup-Nielsen used this equation to analyze his data and to explain the wide varation of ΔG_c with respect to the catalyst type, Figure 2-12 shows his results. Although a general functionality of ΔG_c with 1/r is observed in the two sets of experiments, the correlation is poor and it is questionable whether or not the model is correct. The explanation involving slow rates of carbon deposition previously discussed seems to be more plausible.

From the experimental data of Rostrup-Nielsen one may obtain expressions for the Gibbs energies of carbon at 823K. For the disproportionation of carbon monoxide

$$\Delta G_c = 2 + \frac{222}{d} \text{ kcal/mole}$$

and for the decomposition of methane

$$\Delta G_c = 0.7 + \frac{219}{d} \text{ kcal/mole}$$

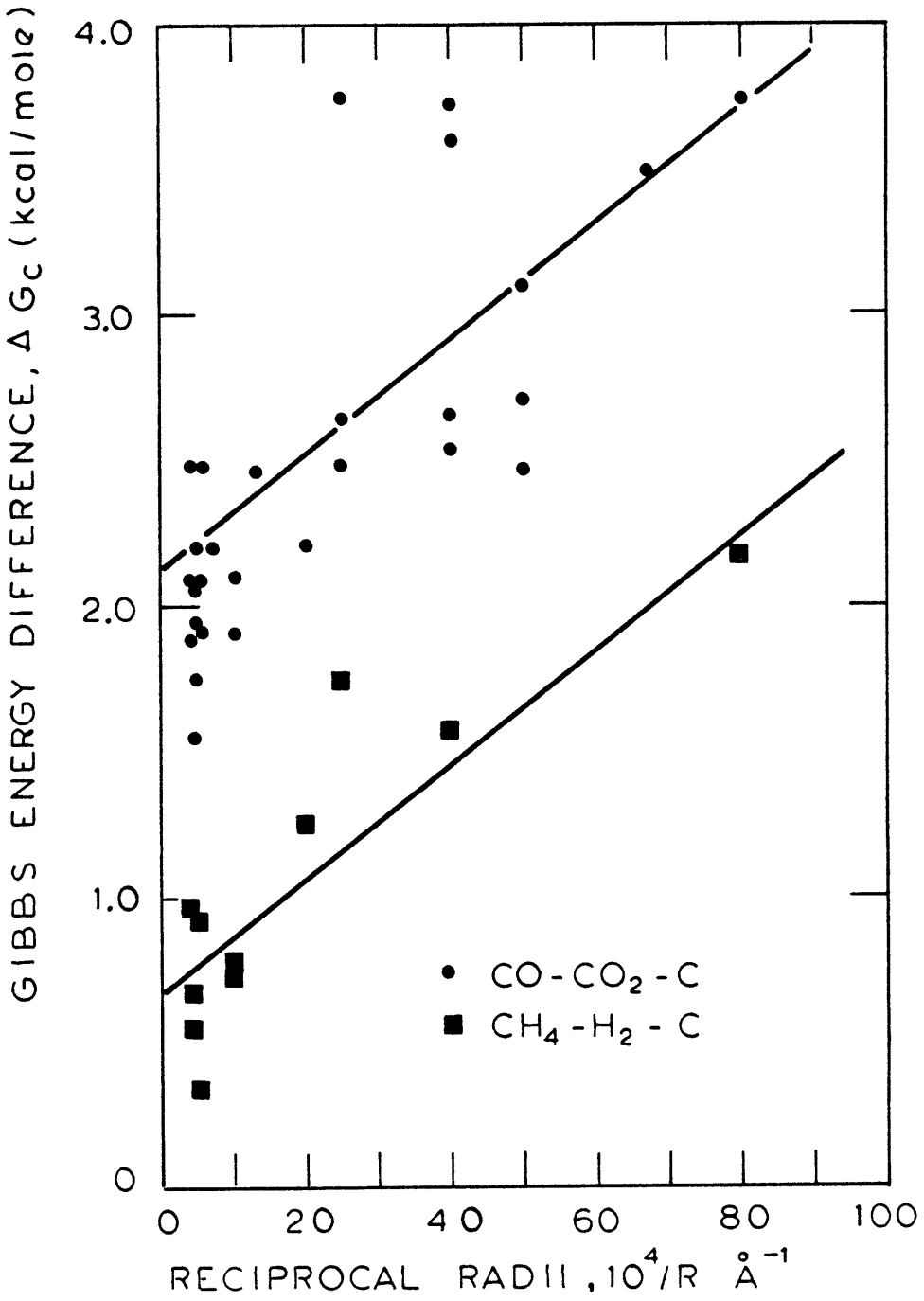

Fig. 2-12 Variation of the Gibbs Energy Difference as a Function of the Reciprocal Radii of the Catalyst Particle (Rostrup-Nielsen, 1972)

where d is the diameter of the carbon filament in A. As shown previously, these equations resulted from a model which assumed that a carbon fiber could be represented as a solid cyliner. Another interesting model was developed by Renaud and Bonnetain (1974) which assumed that the carbon fiber could be represented by a annulus which formed about a nickel crystallite. The length and inner diameter of the annulus and the diameter of the nickel particle were assumed to all equal d (A). The wall thickness was equal to h (A). The authors showed how the excess Gibbs energy of the carbon can be approximated by

$$\Delta G_c = \frac{M}{\rho} \left(\gamma_{0002} + \gamma_{0002,\ Ni}\right) \frac{1}{h} + 2\gamma_{0100} \frac{1}{d}$$

where M is the molecular weight and ρ is the density of carbon, γ_{0002} is the surface tension of the 0002 plane of graphite, $\gamma_{0002,\ Ni}$ is the interfacial tension of the 0002 plane of graphite in contact with nickel, and γ_{0100} is the surface tension of the 0100 plane of graphite. Using literature sources, these values were estimated and their final expression is shown below

$$\Delta G_c = \frac{16.5}{h} + \frac{206}{d} \text{ (kcal/mole)}$$

The 1/d multiplier in the above equation agrees within 10% of the two equations of the equations of Rostrup-Nielsen. The constant terms in his two equations 2 and 0.7 kcal/mole allows h to be calculated as 8 and 24 A. Electron micrographs of hollow filaments (Rostrup-Nielsen, 1972) reveal that the diameter of the hollow portion of the filament is smaller than 1/2 the diameter of the filament, so h ~ 1/2 d. Since the d values observed were between 100 and 2500 A, h values of 8 and 24 A, calculated previously, are comparatively too low.

2.2.2.3 Methane-Hydrogen Equilibrium Over Various Solid Phases

The methane-hydrogen equilibrium has been studied by many researchers over both nickel and cobalt at temperatures between 450 and 1000K. They believed they were studying the equilibrium of methane and hydrogen with graphite, a carbon with a higher Gibbs energy than graphite, or a nickel or cobalt carbide. In this section, their work is reviewed to determine the solid phase which would be in equilibrium with gas species in a Bosch process. This is important since calculations show that the ΔG_c's which have been observed can have large effects in decreasing the equilibrium water concentrations exiting from a Bosch reactor (Section 4.2).

The CH_4-H_2-C system was studied by both Dent (1952) and Rostrup-Nielsen (1972) over nickel. Their work was discussed in Section 2.2.2. Their results are plotted for comparison in Figure 2-13a. It can be seen that Rostrup-Nielsen's results are about 1.0 kcal/mole closer to graphite. However, the two sets of data follow the same general trend. Of course, the disagreement could be due to experimental scatter.

Browning and Emmett (1952) studied the equilibrium of the reaction

$$3Ni + CH_4 \rightleftarrows Ni_3C + 2H_2$$

in the temperature range of 499 to 558K and the reaction

$$2Co + CH_4 \rightleftarrows Co_2C + 2H_2$$

in the range of 463 to 717K, at total final pressures from 1.3×10^3 to 7.0×10^4 N/m^2. The reaction was carried out in a quartz recycle reactor which was described by them in a previous publication (Browning et al., 1950). The nickel and cobalt samples were precipitated catalysts made from the corresponding nitrate, soduim carbonate, and thorium nitrate. The catalysts were calcined and reduced after precipitation. Prior to placement

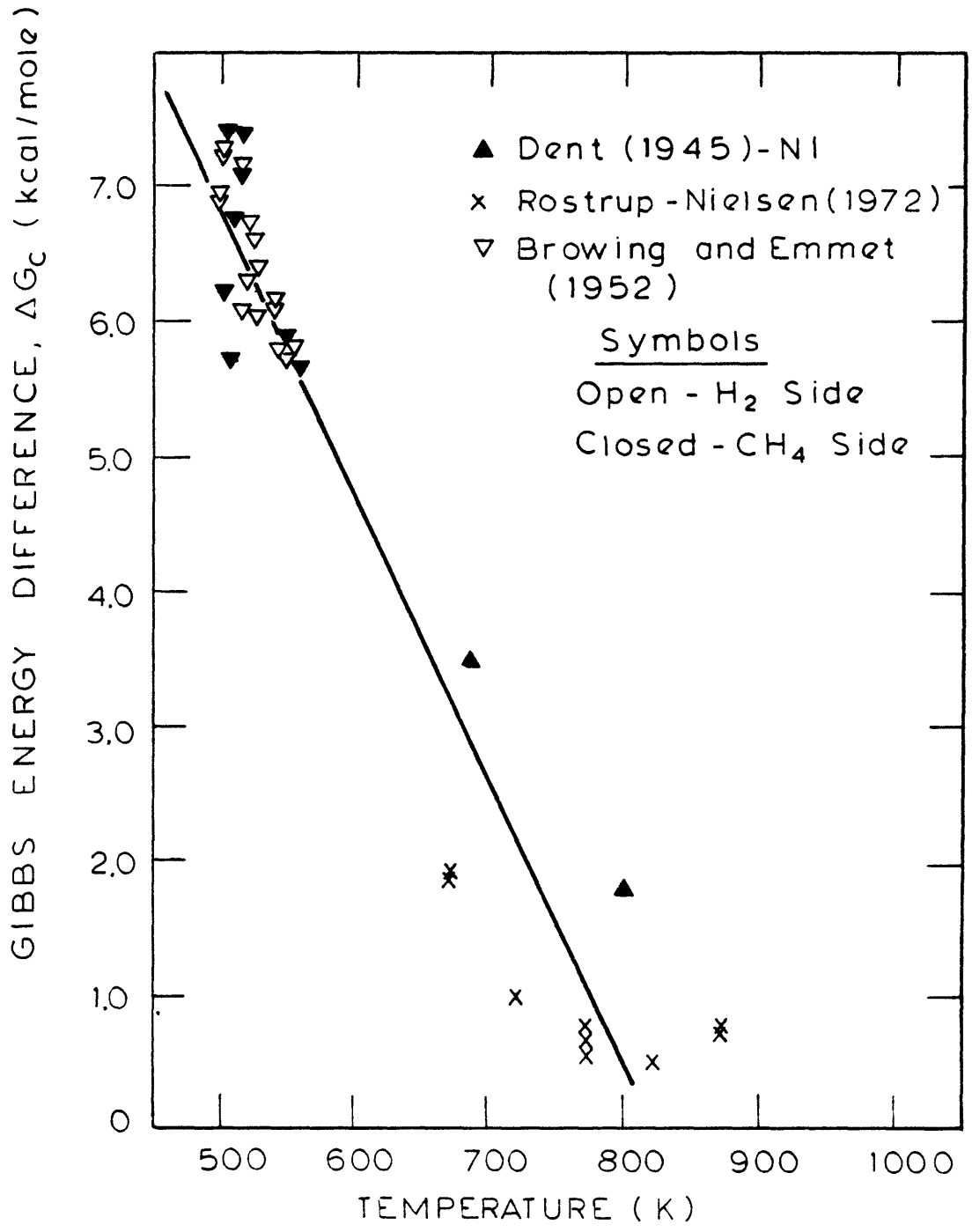

Figure 2-13 A Gibbs Energy Difference for the CH_4-H_2-C or-Nickel-Nickel Carbide Equilibrium

of the samples into the reactor for equilibrium studies, the samples were carbided in carbon monoxide at 493K. X-ray patterns indicated complete carburization of the nickel.

The results of the nickel experiments have been presented in Figure 2-13a. In viewing the equilibrium values for the reactions over the carbided nickel catalyst, it is observed that the results of Dent and Rostrup-Nielsen form a straight line. Much scatter is noted about the line; however, over the large temperature range, the correlation appears to be good.

When examining the results for the Co_2C equilibrium it is important to note that Browning and Emmett observed results which indicated the relative stability of the nickel and cobalt carbides which they prepared in their laboratory. First, when x-ray patterns of carbided cobalt were examined it was noted that the cobalt was only 50% carburized. This could have resulted from the decomposition of cobalt carbide to carbon and free cobalt. In discussion of the experimental technique for measuring the cobalt carbide equilibrium at the highest temperature, Browning and Emmett indicated their suspicion that some of the carbide decomposed. They stated, "the value at the highest temperature (717K) was obtained by carbiding a sample of cobalt at 493K and then raising the temperature as quickly as possible and circulating hydrogen over the sample for an additional hour after the pressure remained constant. Apparently enough carbide remained to allow equilibrium to be established, since the value of K_p obtained lies within an extrapolation of the approximate range of the other values..." In their studies of the thermal stabilities of the carbides, they indicated that Ni_3C was shown by x-ray analysis to decompose completely after 24 hr at 643K, while Co_2C decomposed at a relatively low temperature of 513K after 48 hr. This indicates the metastable behavior of both carbides; the stability

is discussed further in Section 2.2.3.

For the cobalt system, the equilibrium values can be seen to range from the graphite equilibrium (ΔG_c = 0.0 kcal/mole) to the equilibrium line which Browning and Emmett measured for the nickel carbide study (Figure 2-13b). Also, the experiments from the hydrogen rich side of equilibrium are observed closer to the graphite line than the experiments from the methane rich side, which tend to favor the nickel carbide line. An explanation of the scatter in the data may lie in the instability of the cobalt carbide. Since the presence of either the carbon or carbide will cause the gas compositions to approach the corresponding equilibrium, transients, which occur, such as the slow decomposition of the carbide phase, will cause experimental values of the equilibrium constant to lie between the two equilibrium lines. Here the implication of a competitive process between the carbon reaction,

$$CH_4 \rightleftarrows C + 2H_2$$

and the carbide reaction,

$$CH_4 + 2Co \rightleftarrows Co_2\,C + 2H_2$$

is made. This indicates that these observations result from reaction rates rather than equilibrium. This is supported by the phase rule which reveals that either, but not both, a carbon or a carbide plus metal phase may exist at equilibrium, at constant temperature and pressure.

Schenck (1927) studied the equilibrium of methane and hydrogen over a cobalt catalyst for the temperature range of 633K to 1013K. He reported results for the equilibrium system

$$CH_4 \rightleftarrows H_2 + C$$

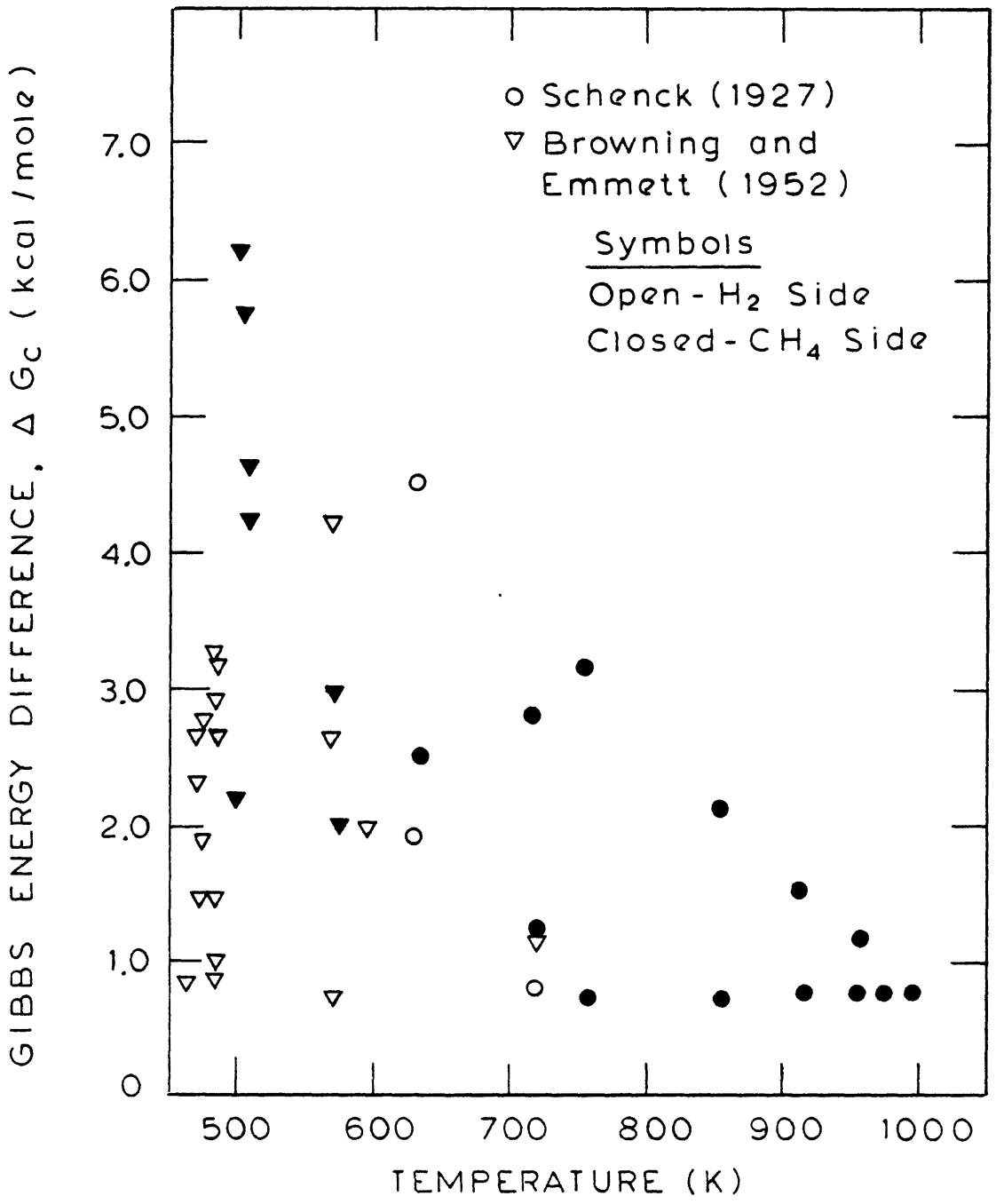

Figure 2-13 B Gibbs Energy Difference for the CH_4 - H_2 - C or - Cobalt - Cobalt Carbide Equilibrium

and the carbide system

$$3Co + CH_4 \rightleftarrows Co_3C + 2H_2$$

No description of the experimental system was given. The results were presented in tables which gave reaction time and temperature, flow rate, and final gas compositions reported as precentages. Flow rates were reported to be, for the most part, 0.0 cm^3/min. a static system, but were as high as 3.0. Reaction times ranged from 1 to 114 hr.

The results are given in Figure 2-13b for the carbon and the carbide equilibrium. As can be seen, only in the former was the equilibrium approached from both the methane and hydrogen side. Since Schenck did not state how he distinguished between the carbon and carbide equilibrium experiments, it is difficult to interpret his results.

The total carburization of Co to Co_3C results in a weight increase of only 6%. From this fact one can hypothesize that the measurements of the carbide equilibrium were made with little carbon deposited in the form of carbide, while measurements of the carbon equilibrium were made after a weight of carbon equal to a large fractional weight of the cobalt had been deposited as free carbon.

Throughout this section experimental data from the literature have been reviewed which was obtained by passing hydrogen and methane over cobalt or nickel. The values of the equilibrium constants ranged from those calculated using Gibbs energy data for graphite to that which appears to be an extension of the line formed by the results Browning and Emmett obtainted over nickel. It is quite clear that at the low temperatures which Browning and Emmett studied the reactions, nickel carbide and free nickel rather than carbon, were in equilibrium with the gas phase. The data of

Browning and Emmett, Dent, and Rostrup-Nielsen have been shown to form a straight line (Figure 2-13a). Thermodynamics reveal that a plot of ΔG versus temperature yield a straight line when ΔH and ΔS are constant ($\Delta G = \Delta H - T\Delta S$). All this is consistant with the reasoning that it is nickel carbide, rather than carbon which is controlling the equilibrium in the various nickel catalyzed processes which have been discussed.

The results which Browning and Emmett (1952), and Schenck (1927) had for cobalt both reveal much scatter. It is therefore difficult to conclude upon what might be expected in a Bosch reactor. This indicates the importance of the experimental work using cobalt in this thesis.

2.2.3 Carbons and Carbides

2.2.3.1 The Formation and Decomposition of Cobalt and Nickel Carbide

Hofer et al. (1949, 1950) studied the isothermal decomposition of both nickel and cobalt carbide using a reactor system equipped with a magnetic balance. The decomposition could be followed easily because of the high magnetic moment of the metallic phase and the low moment of the carbide. In the study, a cobalt-thoria-kreselguhr (100:18:100) catalyst was reacted with carbon monoxide at 480K. After 72 hr the reaction ceased. The sample was then reacted for an additional 48.5 hr with virtually no weight increase. X-ray analysis revealed only cobalt carbide lines (no free carbon or cobalt) which represented the lattice structure of Co_2C. The quantity of carbon taken up during reaction by the sample (10.03g C/100g of cobalt metal) corresponded to the complete conversion of Co to Co_2C (10.17g C/100g Co).

The decomposition rates of cobalt carbide were measured at six temperatures between 573 and 632K in vacuo. The results are plotted in Figure 2-14. For cobalt carbide weight percentages between 20 and 100, the rate of carbide decomposition is linear with time. This indicates a zero order reac-

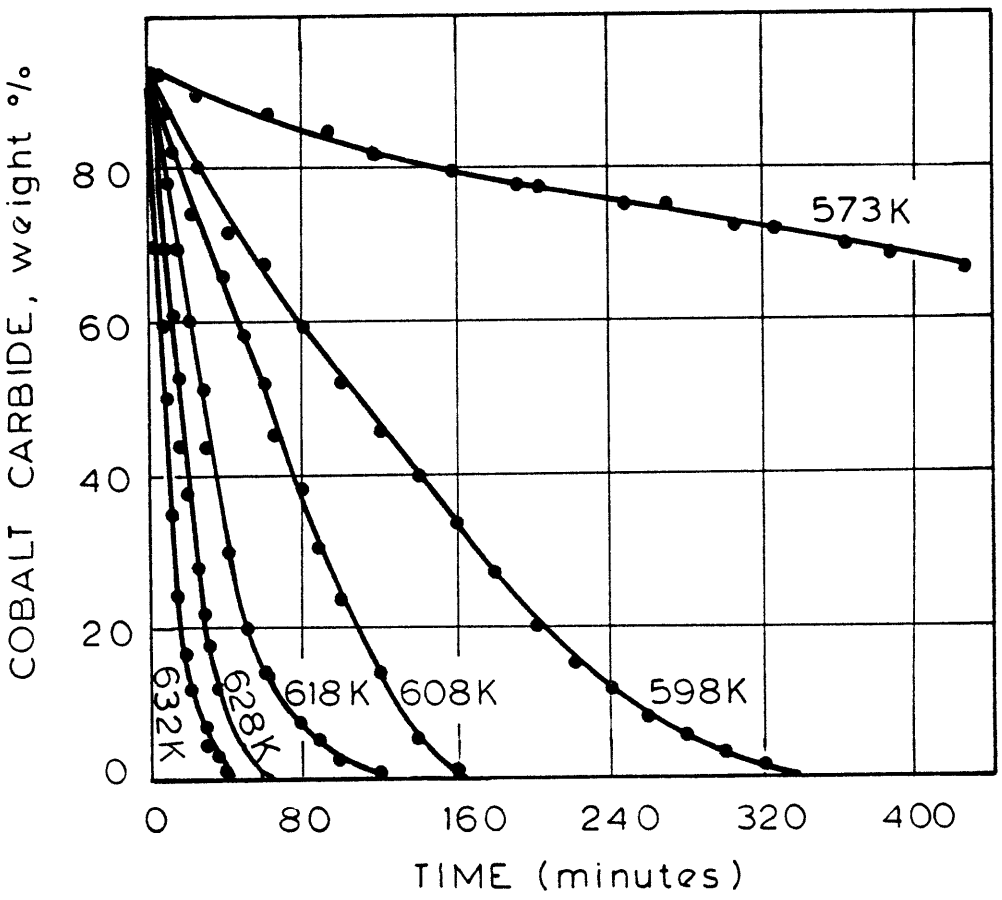

Figure 2-14 The Decomposition of Cobalt Carbide at Various Temperatures (Hofer et al, 1949)

Table 2-2

Induction Period and Quasi-Zero-Order Rate Constants for Decomposition of Fully Carburized Ni_3C

DECOMPOSITION TEMPERATURE	INDUCTION PERIOD	APPARENT SPECIFIC REACTION-RATE CONSTANT, k
K	min.	$sec.^{-1}$
596	1320	3.4×10^{-5}
596	960	3.9×10^{-5}
596	660	4.0×10^{-5}
606	540	7.8×10^{-5}
606	420	9.7×10^{-5}
606	420	11×10^{-5}
616	180	23×10^{-5}
616	240	19×10^{-5}
628	100	51×10^{-5}

tion rate. Below 20 wt%, the reaction order changes. The reaction rate constant was defined for a zero order reaction as

$$- (C_{wt_1} - C_{wt_2}) / (t_1 - t_2)$$

where C_{wt} is the weight percent carbide and t the time in seconds, are given in Figure 2-15. An Arrhenius plot indicates an activation energy of 54.3 kcal/mole for the decomposition.

A precipitated nickel hydroxide catalyst reduced for 85 hr in hydrogen to constant weight served as the catalyst in the nickel study. It was carburized with carbon monoxide at 523K for 22.5 hr, and then for an additional 91 hr which resulted in no weight gain. X-ray analysis showed only the lines of hexagonal close-packed nickel carbide, Ni_3C. The carbon-nickel weight ratio was found to be 0.0725, an excess over the ideal stoichiometric ratio of 0.0682.

The fully carburized nickel was decomposed in vacuo at four different temperatures between 596K and 628K. The decomposition was preceeded by an induction period, for consistency it was defined as the time it took for 5% of the carbide to decompose. Table 2-2 gives the induction period and zero-order reaction rate constant as a function of decomposition temperature. Figure 2-16 shows the results for the decomposition of nickel carbide at 596K. As can be seen, a linear rate of decomposition occurs between 70 and 10 wt% nickel carbide. As with the cobalt carbide experiments, a zero order rate constant was determined from this portion of the curve. Although the cobalt carbide decomposition showed no induction period, zero-order rate constants at a given temperature, for the two systems are similar. Figure 2-17 is an Arrhenius plot of the decomposition and of the induction period,

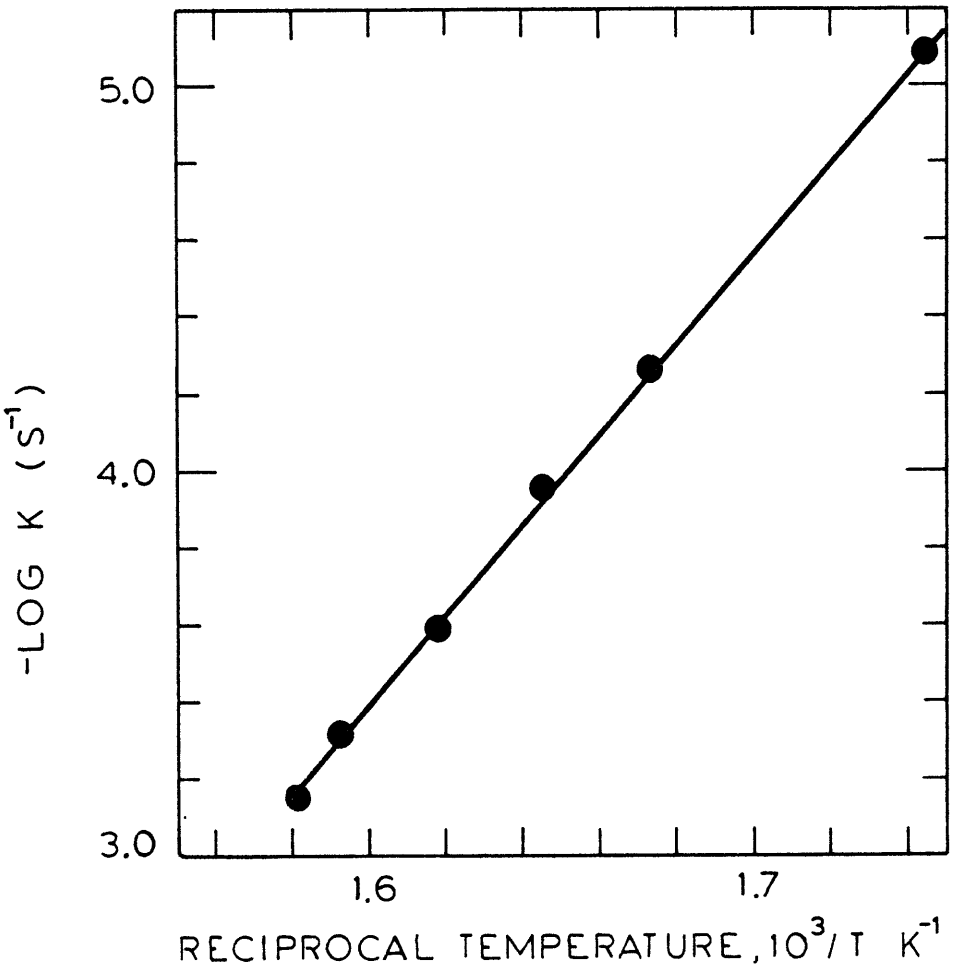

Fig. 2-15 An Arrhenius Plot for the Decomposition of Cobalt Carbide (Hofer et al., 1949)

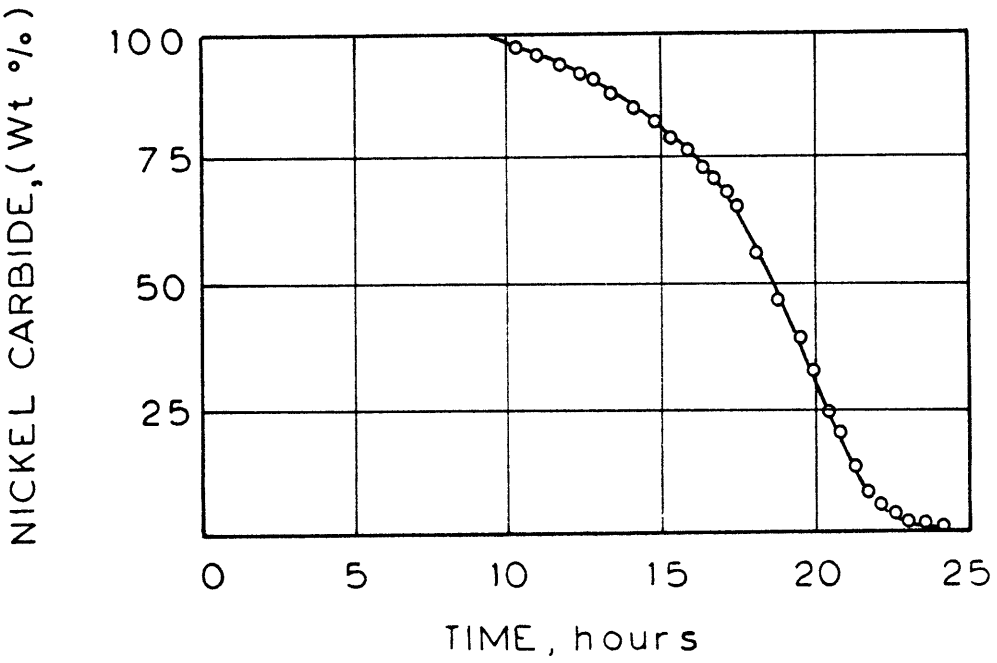

Fig. 2-16 The Decomposition of Nickel Carbide at 596 K (Hofer et al. 1950)

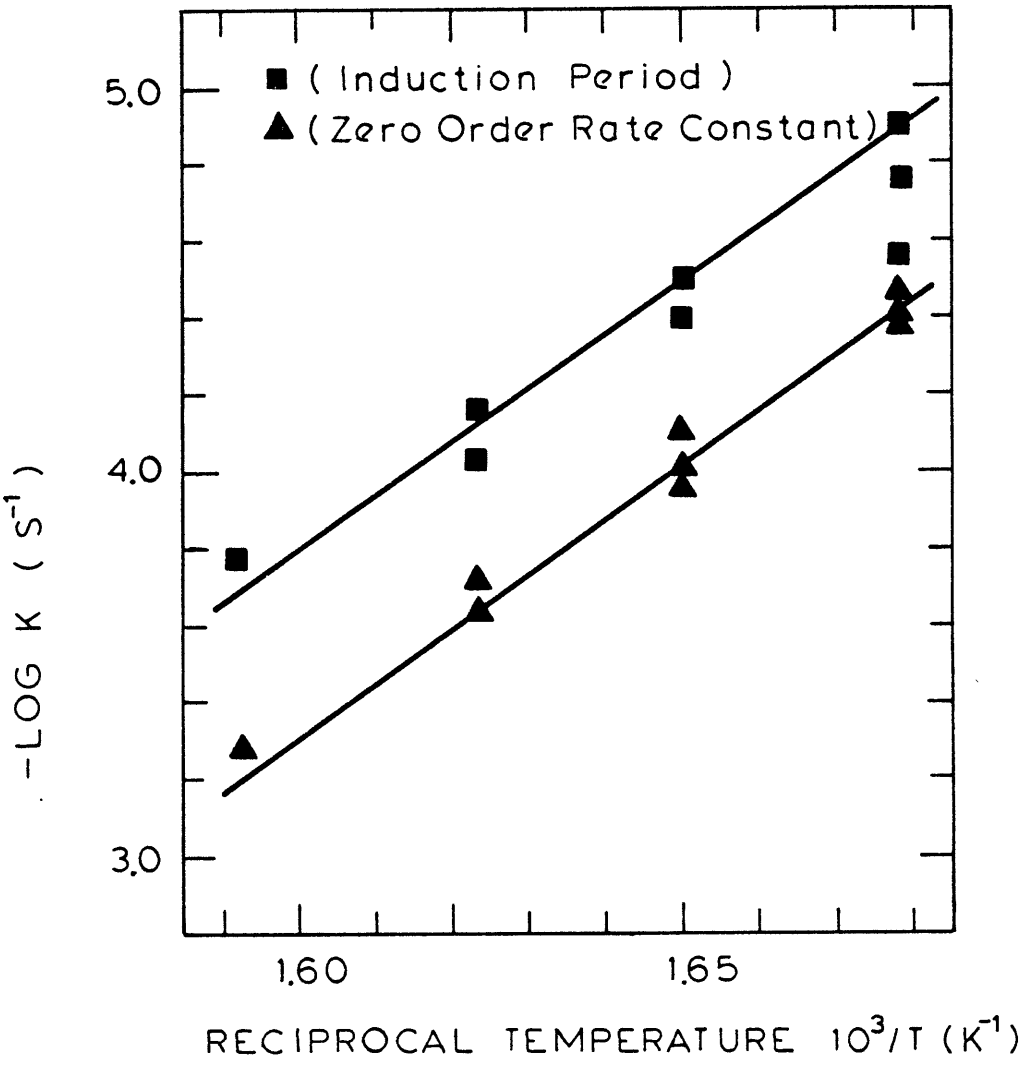

Fig. 2-17 An Arrhenius Plot for the Decomposition of Nickel Carbide (Hofer et al., 1950)

the activation energy of which is 61 and 55 kcal/mole, respectively.

The formation and decomposition of both nickel and cobalt carbide were studied by Nagakura (1957, 1961) using electron diffraction. Thin nickel films, formed by evaporation, were carburized in carbon monoxide at temperatures between 523 and 773K at 50K intervals. The progress of carburization was followed by preparing a sample at a give temperature, cooling, and then observing the sample with an electron diffraction camera. Results showed that below 723K carbide was formed although nickel rings of appreciable intensity always remained. At 773K, only amorphous carbon deposits were observed. From the intensities of the carbide rings, it was found that the maximum rate of carbide formation occurred at about 623K. The thermal decomposition of nickel carbide was studied non-contiuously using electron diffraction. The samples were heated in vacuum at a given temperature for varying periods of time. When completely carburized films were kept at 573K for 21 hr, the diffraction pattern still consisted almost entirely of the carbide rings, though a trace of nickel rings appeared. At 673K, heating for 30 min produced also no remarkable change, but after 2-4 hr of heating, the carbide decomposed completely. At 773K the decomposition occurred more rapidly than at 673K. In another experiment, the continual decomposition of nickel carbide was followed using a high temperature electron diffraction camera. Previously carburized films were continuously heated, starting at 289K, at a rate of 2-4 K/min. At 704K, decomposition had already begun. Around this temperature nickel and diffuse carbon rings become stronger, while the carbide rings weakened, indicating that the decomposition of the carbide had begun. Two minutes later, at 706K, no carbide rings were found.

Nagakura's (1961) study of cobalt carbide was carried out using thin

cobalt films carburized in town gas. The gas was composed of 25 mole% CO, 5%CH_4, 40% H_2, and 30% N_2. Both forms of cobalt carbide, Co_2C and Co_3C, were observed. In the study of Co_2C, no carbide was produced after 5 hr for temperatures below 673K. At 723K, the film was carburized to Co_2C, leaving small amounts of α-Co, while at 773K complete carburization occurred. At his temperature free carbon was observed. Above 823K the diffraction pattern was composed of rings due to α-and β-Co and graphitic carbon. The decomposition of Co_2C was studied in the same manner as nickel carbide. The decomposition began at 723 and finished at 742K, leaving the rings due to α-Co and graphitic carbon.

Nagakura also studied the electron diffraction patterns and the thermal stability of Co_3C. This carbide's structure and diffraction pattern were shown to be very similar to the iron carbide, Fe_3C. Thermal studies indicated that the maximum rate of formation occurred between 723 and 773K. When heating at a rate of 2-4K/min, decomposition of Co_3C occurred between 750 and 764K.

2.2.3.2 The Occurence of Carbides During Carbon Formation

Renshaw et al. (1971) studied the catalytic disproportionation of carbon monoxide, in the presence of Ni and Co single crystals, for a temperature range of 673 to 1073K. The carbonaceous products from disproportionation were studied in one of two forms; either as bulk products or as a stripped film. Bulk products refer to a large buildup of material on the metal surface; this product material was then removed, ultrasonically dispersed in distilled water, and supported on electron microscope grids. The thin films examined were stripped from the crystal surface by direct chemical attack of the metal substrate using a saturated solution of iodine in potassium iodide. The film was then washed in methanol.

Stripped films were prepared over nickel at 673K on the (111) surface with a CO-9.4% H_2 mixture. A most interesting observation was the hexagonal platelets formed which had diameters of about 1000A. Selected area electron diffraction yielded spot patterns indicating their single crystal nature, an analysis of which showed that it corresponded to the (0001) reciprocal lattice plane in nickel carbide, Ni_3C. Other parts of the film gave selected area diffraction patterns which corresponded to polycrystalline graphite. The crystallite size was of the order of a few hundred Angstrom units.

Stripped carbonaceous films were prepared at 1073K on the nickel (111) surface. After 20 hr the authors reported the formation of individual grains whose average size were of the order of 2000 A. No diffraction analysis was performed on these grains, but it is interpreted that the authors believed this was single crystal graphite. At a later stage in the reaction (48 hr), platelike material began to form in the vicinity of the grain boundaries. Selected area diffraction give single crystal spot patterns which, on analysis, proved to result from a graphite lattice. Areas of dark contrast observed in the electron microscope were believed to be either free nickel or a Ni-C solid solution. It was hypothesized that these situations could have arisen from the decomposition of an intermediate carbide phase. Selected area diffraction of a region of the film gave a ring pattern, d spacings of which corresponded to polycrystalline graphite. However, since Ni_3C has some d (distance between diffracting planes) spacings close to those of graphite, the possibility that some of the rings correspond to carbide cannot be ruled out. In general, both electron and x-ray diffraction easily distinguish between graphite and nickel or cobalt carbide (Nagakura, 1957, 1961; Andrews et al., 1971; ASTM, 4-0850, 5-0704, 5-0727, 6-0697,15-806,

23-64, 25-284, 26-450).

Bulk studies were carried out over nickel at 823K, the temperature for the fastest rate of product growth. Observations in the electron microscope revealed products typical of this reaction, a platelike material and a highly fibrous material. Selected area diffraction of the platelike material gave rise to single crystal spot patterns that have been shown to correspond to the (0331) reciprocal lattice plane in Ni_3C. The dimensions of the plates were comparable to those found in the stripped films at 673K. The fibrous material was shown to be graphite.

A cobalt crystal was reacted in the carbon monoxide-hydrogen mixture at 973K. The stripped product film was shown to be platelike material with a well-defined hexagonal morphology. Selected area diffraction revealed the product to be polycrystalline graphite. Although electron diffraction failed to produce any evidence that would indicate the presence of a carbide phase, an interesting observation caused the authors to speculate on the possibility that one had existed. When the electron beam was centered on a triangular shaped nuclei during diffraction studies, they appeared to decompose suggesting that they were not composed purely of carbon. A pronounced outer shell surrounding most of the nuclei suggested to the authors that the decomposition of a carbide phase had occurred.

A bulk product study was done on cobalt at 723K. Selected area diffraction revealed that most of the plate and filamentary material was composed of polycrystalline graphite. Single crystalline graphite flakes were occasionally found. Within the products many hexagonal shaped plates were observed. When these were subjected to diffraction analysis, assignment of the carbide structure Co_3C was made. Furthermore, the newly discovered carbide was designated β-Co_3C to distingish it from the known α form. A detailed

crystallographic analysis was given.

Renshaw et al. (1971) proposed a mechanism for carbon formation over the range of their study. At low temperatures it was believed that carbon was formed from the decomposition of the metastable nickel or cobalt carbide. Although no conclusive evidence of the existance of a carbide was found at high temperatures over nickel and cobalt, the observation of the hexagonally shaped graphite single crystals at high temperature are reminiscent of the hexagonally shaped nickel carbide single crystals at low temperature. Over nickel, the observation that the average grain size is much larger in films grown at 1073K, relative to those grown at 673K, was believed to indicate they resulted from the breakdown of the large nickel carbide crystals at 673K. The argument given was that the recrystallization of the smaller crystallites to form larger ones would not occur at these temperatures. An additional argument for the intermediate cobalt carbide at the higher temperature was the observed decomposition of the triangular shaped nuclei in the electron beam.

The observation of carbides at 673 and 823K over nickel, and 723K over cobalt was conclusive in this study. Platelike material, hexagonal in shape, was shown to correspond to a carbide in stripped films formed over nickel at 673K and bulk studies at 823K. This is a relatively high temperature for nickel carbide. Over cobalt, hexagonal platelets of β-Co_3C was formed at 723K.

The importance of the material presented in Section 2.2.3 is that it substantiates the metastable nature of both nickel and cobalt carbides. Although Hofer et al. (1949, 1950) clearly have shown that both carbides decompose readily at temperatures of 630K, the time required is still finite (40 minutes). Nagakura (1957, 1961) reported that the time required for

the decomposition of Ni_3C was finite at 773K and that in a temperature programmed study, decomposition did not occur until 704K. He also indicated that maximum rate of carbide formation occurred at 623K. For the cobalt system, the decomposition of Co_2C occurred at 723K and at 750K for Co_3C. The maximum rate of formation of both carbides occurred at temperatures between 723 and 773K. It should also be repeated that Renshaw et al. (1971) observed Ni_3C at temperatures as high as 823K. In Nagakura's study, only free metal and carbon were observed at temperatures above 772K for Ni and 823K for Co.

2.2.3.3 The Hydrogen Content of Carbon Formed Over Iron.

Although no analysis has been made of the hydrogen content of carbon formed over cobalt and nickel, Walker et al. (1959) reported the C/H ratios determined from carbon formed from hydrogen-carbon monoxide mixtures over iron. The catalyst used was a Baker reagent grade iron powder prepared by reducing iron carbonyl in hydrogen. The powder consisted of spherical particles having an average diameter of about 10μm and a B.E.T. surface area of $0.99m^2/g$. The carbon samples were prepared by reacting hydrogen and carbon monoxide in a flow reactor. The weight increase due to carbon was determined by a before and after measurement made outside the reactor.

In the first set of experiments varying compositions of hydrogen and carbon monoxide. 0.8 mole % to 65.9% H_2, were reacted over iron at temperatures between 743 and 973K. The results shown in Table 2-3 reveal that at a given hydrogen concentration in the gas phase, the C/H ratio is proportional to temperature. If the results are examined at constant temperature, although not dramatically, the C/H ratio is seen to be inversely proportional to hydrogen concentration in the gas phase. In their publication, Walker et al. explained the low temperature C/H ratios with the following argument.

Table 2-3

Effect of Carbon Monoxide-Hydrogen Composition and Temperature on the Atomic Carbon-Hydrogen Ratio of Carbons (Walker et al, 1959)

Formation temp., K	Atomic carbon-hydrogen ratio of carbons produced from various carbon monoxide-hydrogen mixtures						
	0.8%H_2	2.2	5.2	9.0	19.9	39.8	65.9
743	14.4	13.1	11.4	. .	. .	. .	. .
773	21.5	16.4	14.1	9.6	11.4	7.3	9.0
801	25.3	15.4	19.5	10.8	13.3	10.1	9.6
849	27.3	21.1	21.6	23.2	17.3	14.3	12.2
875	. .	27.4	26.2	27.4	28.1	16.4	20.4
903	34.2	. .	. .	34.5	35.2	. .	34.6
973	. .	. .	. .	. .	52.7	53.0	. .

He postulated that the hydrogen content of the carbon could result from the chemisorption of hydrogen atoms on the edge atoms of a crystal. Although this may have been the true it would be relatively difficult to determine experimentally.

Walker et al. also measured the change of properties of carbon with mass of carbon deposited on 0.1 g of iron at 801K. The gas mixture used was 0.8% hydrogen in carbon monoxide. Table 2-4 lists the L_c (crystal dimension perpendicular to the basal plane), interlayer spacing of the carbon basal planes, the surface area, and the C/H ratio. The values for L_c indicate that as more and more carbon is deposited, the crystals formed are smaller; the interlayer spacing, however, remains constant. The change of surface area observed can be explained by assuming that the surface area measured is equal to a mass weighted average of the surface area of the iron and the carbon. Within experimental error, the C/H ratio is seen to be independent of mass of carbon.

2.2.4 Carbon Fiber Formation Mechanism

2.2.4.1 Dissolution - Diffusion Mechanisms for Filamentary Growth

Baker et al. (1972) studied the catalytic decomposition of acetylene over silica films and single crystal graphite supported nickel employing controlled atmosphere electron microscopy (CAEM) at temperatures between 825 and 1300K. Within the study, a model was developed which could account for many of the observed phenomena.

When acetylene was pyrolyzed over nickel, three forms of carbonaceous deposits were observed; amorphous, filamentary, and graphitic. At 850K, a flocculent amorphous deposit of carbon formed about the nickel particles (~30nm diameter) in the presence of $0.05 kN/m^2$ acetylene. Upon raising the temperature to 870K, the nickel particles became mobile and filaments were

Table 2-4

Change of Properties of Carbons with Weight Formed from a 99.2% CO-0.8% H_2 Mixture at 801K over 0.1 Gram of Carbonyl Iron (Walker et al 1959)

Carbon formed. g.	L_1. A.	Interlayer spacing. A.	Surface area. m^2/g.	C/H
0.09	145	3.365	83	8.5
0.92	124	3.370	110	25.3
2.05	110	3.374	117	18.5
3.39	94	3.383	131	16.3
4.63	97	3.384	143	17.3
6.87	87	3.384	144	18.2

observed to grow beneath them, at which point they lost contact with the support. One important observation was that the diameter of the filament was always the same as the nickel particle from which it grew. Each nickel particle had only one filament growing out of it. The filaments grew randomly, forming loops, knots, and interconnected networks. They had a hollow channel running their length and the nickel particle was "pear-shaped" with its base in the direction of growth. The filament growth would cease when the particle became encapsulated in carbon. The growth could be reactivated by subjecting the system to either hydrogen or oxygen, which served to clean the catalytic surface of carbon and allow the further decomposition of acetylene and growth of the fiber. By reacting the fibers with oxygen their structure was uncovered. During this oxidation, the fiber was shown to consist of an easily oxidizable central core and a more dense and relatively stable outer tube.

In their mechanism, Baker et al. gave an explanation for the sigmoidal type growth curve (Figure 2-18) and the formation of carbon filaments and their properties (Figure 2-19). The process is presumed to begin with the formation of flocculant amorphous carbon which accumulates about the base of the nickel particle. The formation of the fiber and the accelerating portion of the growth curve begin with the decomposition of acetylene on the exposed upper surface of the particle. Because of the large amount of heat released, -223.6 kJ/mole for the $-\Delta H_f$ of acetylene and -40.5kJ/mole for ΔH_{soln} for C in Ni (Stull et al., 1969), a temperature gradient is developed within the particle. At this point the fiber grows from continual acetylene decomposition on the face of the particle, dissolution and diffusion along the temperature gradient and then precipitation of carbon on the fiber side of the particle. An acceleration of the growth curve was reported to result

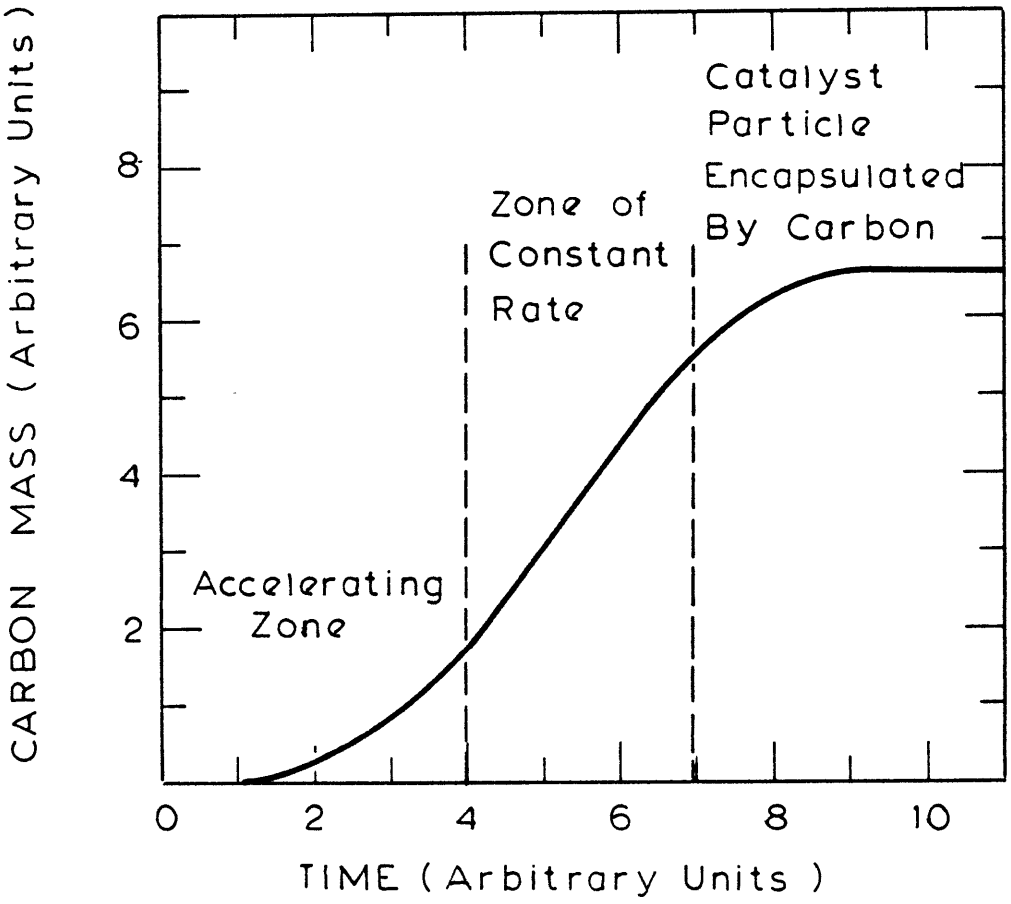

Fig. 2-18 Sigmoidal Growth Curve for Carbon Deposition

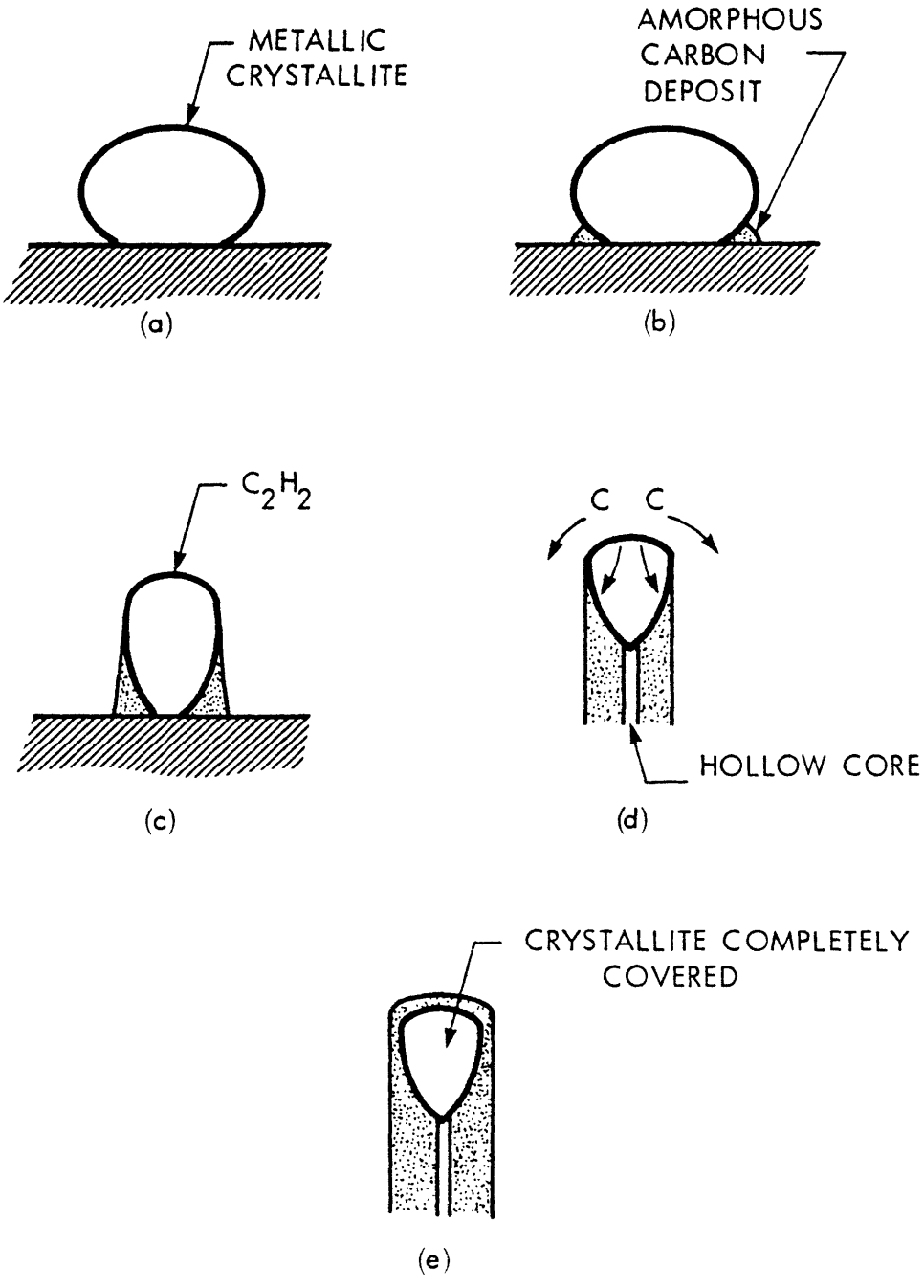

FIGURE 2-19

FIBER GROWTH MECHANISM (BAKER et al.,1972)

from the temperature rise. This resulted from the increased heat load when the particle became detached from the support, which served as a heat sink, and the insulation of the particle upon the growth of the carbon filament. The two forms of carbon believed to constitute the fiber, which were observed during oxidation studies, were reportedly formed by two processes. The inner, less stable carbon structure, resulted from the diffusion of carbon through the nickel particle along the hypothesized temperature gradient. The outer, more stable structure, was hypothesized to be formed by carbon which was transported via the surface of the particle. No substantiation of this idea was given.

The middle, constant portion of the growth curve (Figure 2-18) was believed to result from a steady state temperature of the particle, where the net heat flux to the particle equaled zero. The third, and final zone of the growth curve results from the cooling of the particle when acetylene decomposition ceases due to the encapsulation of the catalytic particle by carbon.

To further test the validity of Baker et al.'s (1972) mechanism and more specifically the criterion that heat be given off upon the decomposition of hydrocarbons in order that carbon fibers form, fiber formation from many exothermic systems was measured. Baker et al. (1975a) measured the yield of carbon filaments from the decomposition of various hydrocarbons with positive heats of formation. In the experiments specimens of cobalt coated stainless steel mesh discs were maintained at 998K and exposed to flowing hydrocarbons at 8.0kN/m^2 pressure. In the case of benzene, transfer into the reaction zone was made with hydrogen as a carrier gas. The reaction time was 30 min. Carbon filament yield was taken to be proportional to the weight gain of carbon. Table 2-5 shows how the carbon filament yield is proportional to ΔH_f.

The correlation is very good.

Following the carbon deposition, the samples where subjected to 700N/m^2 of oxygen at 973K upon which the inner portions of the filaments were oxidized leaving a dense oxidation resistant tube. From the video recordings of the CAEM, filament radii (r_2), and wall thicknesses ($r_2 - r_1$) were measured for fifty filaments in each of the different hydrocarbon systems. Since the inner core was believed to have been formed from carbon which diffused through the catalyst particle, and the outer to result from the transport of carbon via the surface, the measurements r_2, and $r_2 - r_1$, permitted the calculation of the mass of carbon formed through each process. Table 2-5 lists the (Cross Sectional (XS) Area of Filament Wall/XS Area of Filament) for the various hydrocarbon systems. This ratio may be calculated since it is equal to

$$\frac{\pi r_2^2 - \pi r_1^2}{\pi r_2^2}$$

dividing top and bottom by πr_2^2 and setting $R + r_1/r_2$ gives

$$1 - R^2$$

The value R is also listed in Table 2-5. The above equation is equal to the ratio of the volume of carbon formed via surface diffusion to the total volume of the fiber, since the volume of a cylinder is equal to its length times its cross sectional area. As can be seen, the higher the value of ΔH_f, the larger the value of R, indicating the favoring of carbon formation via diffusion through the particle.

It follows from Baker et al.'s (1972) mechanism that hydrocarbons which decompose endothermically, such as methane, will not form carbon fibers.

Table 2-5

Variation of Filamentous Carbon Yields and Structure with Various Hydrocarbons (Baker et al., 1975a)

Hydrocarbon	Carbon Filament Yield Relative to that from Acetylene	XS Area of Filament Wall x 100 / XS Area of Filament	$\Delta H_f(\frac{kcal}{mole})$	R
Ethylene	0.01	42.2	9.21	0.76
Benzene	0.03	37.4	14.82	0.79
1, 3-Butandiene	0.10	36.0	22.74	0.80
Allene	0.16	39.7	43.23	0.84
Methylacetylene	0.59	31.6	41.53	0.83
Acetylene	1.00	25.2	53.29	0.87

$R = r_1/r_2$

XS = Cross Sectional

Although there have been reports of fiber formation in methane decomposition studies (Rostrup-Nielsen, 1972), it is believed that this was caused by impurities which would decompose exothermically. Evans et al. (1973) studied the thermal decomposition of commercial and research grade methane and high purity acetone. The reactions were run over iron, nickel, and stainless steel surfaces at temperatures between 673 and 1173K. They came to the conclusion that filamentary formation during methane decomposition resulted from impurities. Carbon formation was observed by transmission electron microscopy.

When commercial grade methane was heated over stainless steel, filamentary growths were observed at temperatures as low as 823K. The filaments were hollow, graphitic in nature and bearing an electron dense tip. In a similar experiment, ultra pure methane was pyrolyzed. Over nickel and iron, no filamentary growth was observed until temperatures of 1173K were reached. These filaments were similar to the ones formed over stainless steel. Carbon platelet formation was also observed.

Evans et al. believed that acetone was a contaminant of commercial grade methane, and because of the ΔH_f° = 51.79 kcal/mole (at 298K) it could explain the occurrence of filamentary growth. Typically, acetone is not found to be a contaminant in commercial grade methane (Matheson, 1979), however, a study of its decomposition is interesting since it does decompose exothermically and might further support the hypothesis that filamentary growth requires this condition. In general, filamentary growth was observed on the metallic surfaces, with acetone, at much lower temperatures than that found with ultrapure methane. Although lamellar carbon was formed over iron at 673K, nickel and stainless steel were found to be inert, at 773K pyrolysis of acetone gave rise to filamentary growth over all three

metals.

Certainly there are many useful and interesting experiments which might prove or disprove the assumptions that have been employed to develop a theory to explain carbon fiber growth. One such investigation, by Baker et al. (1975b), studied the transfer of carbon through 0.25mm thick nickel foil. The experiments were carried out in a reactor tube which was constructed from nickel foil. During an experiment methane was passed through the nickel tube. The reactor tube was encased in a silica tube which was purged with argon. The whole assembly was then placed in a furnace. This design allowed the two sides of the nickel foil to be exposed to different gases, a reactive one and an inert.

Methane was passed through the inner tube and reacted at 1273K while argon passed through the outer casing. After 1 hr, the nickel tube was cooled to room temperature and split open. The inner surfaces were black and had a sooty accumulation of carbon. The outer surfaces were matt grey and covered with a thin adherent film. The carbon film from the outside of the tube was stripped and examined by transmission electron microscopy. An analysis of the carbon by electron diffraction yielded graphite patterns. The morphology of the carbon deposits followed the nickel grain sturcture and heaviest deposits were formed on the grain broundaries. The deposits were a combination of laminar graphite covered with well aligned crystallites.

From this experiment and the morphological studies, Baker et al. concluded that another mechanism for carbon deposition, previously not stated, was the precipitation of carbon, from solution in the metal during the cooling stage of the experiment. Since graphite flakes and crystallites grew from the metal-deposit interface which had not been exposed to methane,

Baker et al. beleived this to be support for their mechanism where carbon fibers are formed from the precipitation of dissolved carbon in nickel. It was pointed out that the failure to produce filamints can be attributed to the use of research grade methane. It would be both interesting and informative to carry this experiment out using hydrocarbons which are know to decompose exothermally and produce filaments.

A similar study was carried out by Derbyshire et al. (1972) which looked at the dissolution-precipitation process of carbon in 0.0125 cm thick polycrystalline nickel foils. The procedure was begun by coating the nickel foil with a 500A thick layer of amorphous carbon within a vacuum evaporation unit. At this point the foil was heated in vacuum to 1223K upon which the deposit was seen to disappear. This procedure, one sided carbon coating followed by dissolution, was repeated until heating to 1223K failed to remove the deposit. At that point the specimen was raised to 1323K, upon which the deposit disappeared. Upon lowering the temperature back to 1223K, a visable growth of a dark grey, reflective coating appeared almost instantaneously on both sides of the foil.

The carbon film was examined with an electron microscope after the nickel foil was dissolved away with HCl. The carbonaceous film was described as a polygonal structure which covered the nickel grain boundaries Selected area diffraction yielded a graphitic pattern. Upon reheating and cooling, the graphitic film would disappear and reappear with no change in the structure of the amorphous deposit. This observation seemed consistant with Baker et al.'s (1972) mechanism.

Baker and Waite (1975) studied filamentary growth over Pt-Fe particles using controlled atmosphere electron microscopy. This technique was used to study the decomposition of acetylene on iron particles which gave rise

to filamentary growth. A mechanism was given which explains the tendency of the iron particle to remain incontact with its support as filamentory growth occurred.

This mechanism is based on the diffusion of carbon through iron as is that of Baker et al. (1972), however, the latter observed that the catalytic particle became detached from its support.

In the study, Pt-46% Fe wire was evaporated onto either graphite or silica supports. These catalytic specimens were then heated to 920K in H_2 or Ar, at which point 30-120nm particles nucleated as shown in part (a) of Figure 2-20. As acetylene was decomposed upon the hypothesized Fe-rich crystallite, a carbon filament was observed to grow out from the crystallite as the latter remained fixed to its support. Figure 2-20 illustrates how the catalyst consisted of a particle or a dense embryo and an apron which lay upon the support. The relative size of the apron to the embryo was observed to be about 7/1. The carbon filaments formed seemed to take on the diameter of the embryo. These carbon fibers grew up to a point at which it was observed that the apron surface became covered with amorphous carbon. As indicated in other systems (Baker et al., 1972) reactivation occurred upon exposure to hydrogen. During the final stages of growth, some of the filament ends tapered. As this occurred the dense embryo disappeared, suggesting the removal of iron during fiber growth. When filament growth did cease, a ring of a lighter carbonaceous material remained where the iron crystal had rested. When subjected to oxygen the fiber was shown to be composed of a reactive inner core and relatively inert outer one. Upon removal of the inner core, 2-20 nm diameter metal particles were observed to be embeded within the outer core.

In their mechanism, Baker and Waite assumed that the crystal which was

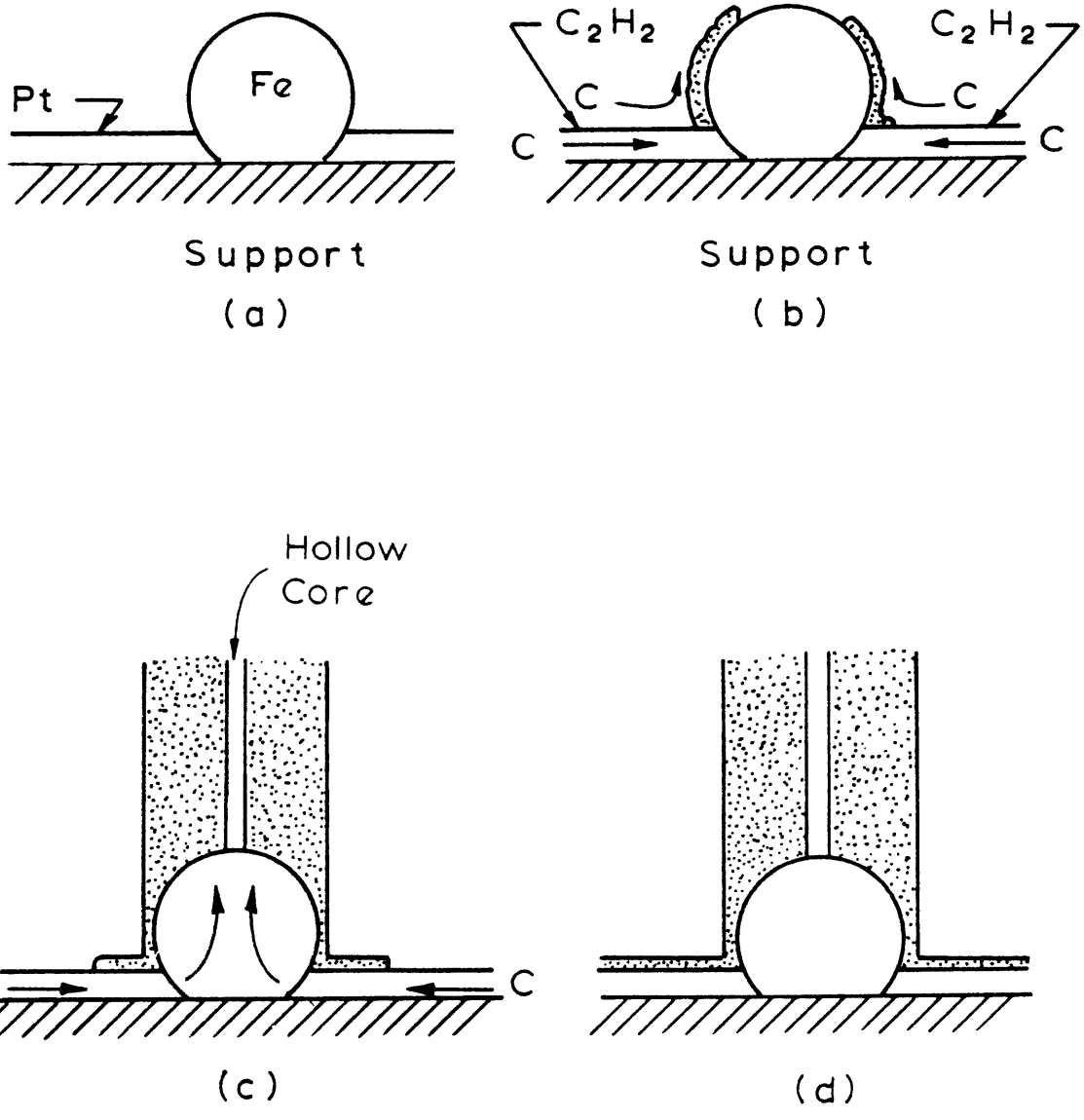

Fig. 2-20 EXTRUSION MECHANISM OF FIBER GROWTH (BAKER AND WHITE , 1975)

formed upon the apron was relatively rich in Fe in comparison with the apron. At the start, fiber formation began with the catalytic decomposition of acetylene upon the Pt-rich apron, followed by dissolution of the carbon within the Pt. From this point on the mechanism follows that of Baker et al. (1972) with carbon diffusion being driven by a temperature gradient induced by the exothermic decomposition of acetylene. As reasoned previously, carbon will diffuse to the cooler regions, i.e. the Pt-Fe interface, and finally precipitate from the iron crystal, from which point fiber growth occurs. Baker and Waite point out that although solubility of carbon in Pt is low, its diffusion rate is quite high (Selman et al, 1970). However, review of Selman et al.'s publication reveals that no quantitative diffusion experiments were performed. An observation which gives support to this mechanism is that the rate of linear filament growth over the Fe-Pt catalyst was 100x the rate over an iron particle of similar size (Baker et al., 1973). The authors believed that the rate increase was due to the apron serving to give a large catalytic area for acetylene decomposition and the collection of carbon which was fed to the iron particle and fiber.

Baker et al. (1972) and Baker and Waite (1975) both proposed filament growth mechanisms which were based on the disolution-diffusion-precipitation of carbon within a catalyst. This process was believed to be dependent upon the exothermicity of the decomposition reaction which served to heat-up the catalyst particle. Many experiments were run (Baker et al., 1975a) to show the importance of this. All of them showed the relative yield of carbon filaments as a function of the heats of formation of different gases. The results appeared to give support to his mechanism. Other experiments showed that carbon could be readily dissolved and precipitated in nickel as the temperature was raised and lowered (Derbyshire et al., 1972). In another experi-

ment, Baker et al. (1975b) showed that carbon could be precipitated from one side of a piece of nickel foil which had only been exposed to inert gas.

There has been much work done to prove this mechanism in the past years. There is, however, one major question which is raised. Can the kinetic process of diffusion account for the rates of carbon filament growth which have been observed. Baker et al. (1972) claim to have calculated a heat balance on the nickel particles and found that radiation losses balance the heat input at 900K for their system which was at 870K. They further claimed that at this temperature the calculated rate of diffusion of carbon through nickel could explain the rate of filamentary growth.

To calculate the rate of diffusion, it can be assumed that the nickel crystallite can be modeled as a cube, with cross sectional area d^2 and diffusion length d of 9×10^{-12} cm^2 and 3×10^{-6} cm, respectively. Decomposition of acetylene and dissolution of carbon is assumed to occur on only one side of the cube, while the precipitation occurs on the opposite wall. The other four sides are considered to be inert. Diffusion occurs from the catalytic face to the fiber-crystallite interface. At steady-state, the rate of diffusion can be expressed as

$$R_D = - D\, d^2\, \frac{\Delta c}{d} = - D\, d\, \Delta c$$

Expressions for the diffusion coefficient have been reported by Diamond and Wert (1967) as

$$D = 0.05 \exp (-34{,}800/RT)\ cm^2/s$$

and

$$D = 0.13 \exp (-34{,}500/RT)\ cm^2/s$$

by Shovensin et al. (1965). The maximum concentration gradient that could exist is one where a side of the cube is saturated with carbon and the other side is pure nickel. For nickel, the solubility of carbon in nickel at 900K is 0.0026 mole fraction (Dunn et al., 1968). Given the density and molecular weight of both carbon and nickel, ΔC is equal to 0.004 g/cm^3. For the diffusion coefficient of Diamond and Wert,

$$R_D = 2.7 \times 10^{-18} \text{ g/s}$$

and for that of Shovensin et al.,

$$R_D = 8.2 \times 10^{-18} \text{ g/s}$$

The rate of carbon filament growth for which Baker et al. made their calculations was 9×10^{-6} cm/s. Considering that the diameter of the fiber was 2×10^{-6} cm, and the density of carbon is 2.3 g/cm^3, the mass rate of filament growth is

$$R_M = 1.9\ 10^{-16} \text{ g/s}$$

Even for the high diffusion coefficient reported by Shovension et al, the rate of filament growth observed is 23 times faster than that predicted by diffusion. This indicates that either the fiber growth occurs via a different mechanism or the particle temperature predicted by Baker et al. is too low. For the rates to be equal, the particle temperature would have to equal 1030K, for $R_D = 0.5\ R_M$ the temperature would have to be 1000K.

Baker et al. made another claim that there existed a temperature gradient across the nickel particle. This can easily be checked by considering the heat of reaction and solution which must be transfered across the particle. If heat losses are neglected, the answer will be a maximum possible gradient

since heat losses, which would primarily occur from the hot side, will tend to lessen the gradient. The difference between the heat input between the hot and cold side of the particle is

$$- \Delta H_{f ACETYLENE} / \left(\frac{0.7 gC}{g ACETYLENE}\right) (70 g/mole) + \Delta H_{SOLN} / (12 g/mole)$$

$$= - 7.9 \text{ kJ/gC}$$

this will equal the heat transfered from one side to another

$$- k \, (3 \times 10^{-6} cm) \, \Delta T = - 7.9 \text{ kJ/gC} \, (1.9 \times 10^{-16} g/s)$$

k for Ni is reported to be 5.5×10^{-4} kJ/scmK, at 870K (Rohsenow and Choi, 1961). Thus ΔT equals 9×10^{-7} K and the particle is determined to be isothermal. From these two calculations, two things become clear. First, the thermal conductivity of nickel is too high to expect a temperature gradient to exist. Secondly, the particle temperature increase, due to hydrocarbon decomposition, must be greater than that predicted by Baker et al. (1972) if their mechanism which includes diffusion is to be shown to be valid. Since fiber growth on nickel cyrstallites has been shown to occur at much lower temperatures (773K) (Rostrup-Nielsen, 1972), it is unlikely that these large temperature differences really exist.

2.2.4.2 Filamentary Growth through a Carbide Intermediate

Boehm (1973) studied the termal decompositoion of $Ni(CO)_4$ and $Fe(CO)_5$ in CO and CO-20%H_2 mixtures at temperatures between 823 and 1043K and atmospheric pressure. The carbonyl was added to the feed stream by diverting about 20% through a saturator containing pure $Ni(CO)_4$ or $Fe(CO)_5$ which was maintained at 273K. The vapor pressure at 273K of $Ni(CO)_4$ is 0.166 atm and of $Fe(CO)_5$ is 0.020 atm. The combined gas feed was fed to a reaction tube after which

the products were collected in a large flask. Reaction products were then refluxed in 6M HCl for several days until none other than the carbon lines could be seen in the X-ray powder diffractograms.

Morphological studies of the carbonaceous formations from $Ni(CO)_4$ in a stream of carbon monoxide revealed thin foils which appeared as cylindircal and spherical skins. The skins were thin-walled and were not to be confused with tubular growth. Decomposition of carbon monoxide over Raney nickel gave the typical fine tubes. Experiments where $Fe(CO)_5$ in CO-20%H_2 was reacted, yielded the usual fibrous growth with twisted strands. However, when the carbonyl in pure carbon monoxide was reacted empty skins and densely agglomerated material was prevalent. Also, Friz, in a private communication with Boehm, reported that upon pyrolysis of dilute $Fe(CO)_5$ vapor, formations similar to those found in the nickel carbonly system were observed.

An explanation of the observed morphology of carbon formed from nickel carbonyl in carbon monoxide was that the nickel carbonyl decomposed to form globular particles and chains of fused particles analogous to carbon blacks. The hollow thin-walled tubes were formed when carbon films precipitated on the nickel particles, the nickel finally being removed by the acid wash.

A mechanism for the growth of carbon fibers, both straight and helical, was based upon the iron carbide catalytic recrystallization of disorganized carbon, a schamatic is shown in Figure 2-21. The first step in the mechanism is the disproportionation of carbon monoxide on the iron carbide surface. The carbon formed here is disorganized and is more soluable in the carbide than graphite. The carbon filament begins to grow when graphite precipitates from the iron carbide. As shown in Figure 2-21 helical filamentary growth is caused by particles with two active faces at angles to one another.

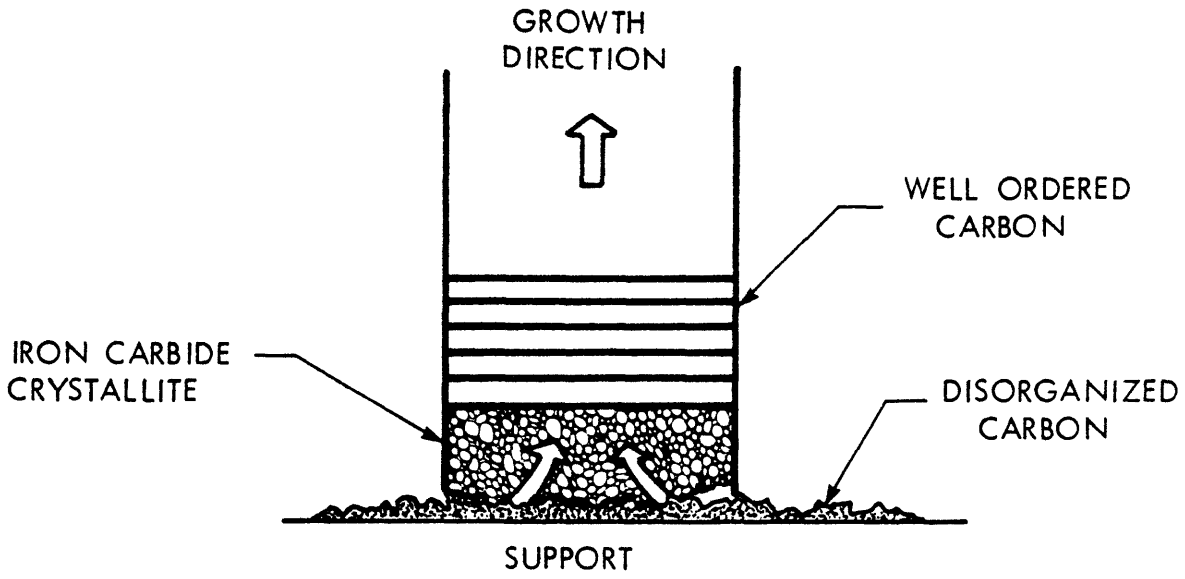

GROWTH OF RIBBON-LIKE FIBERS

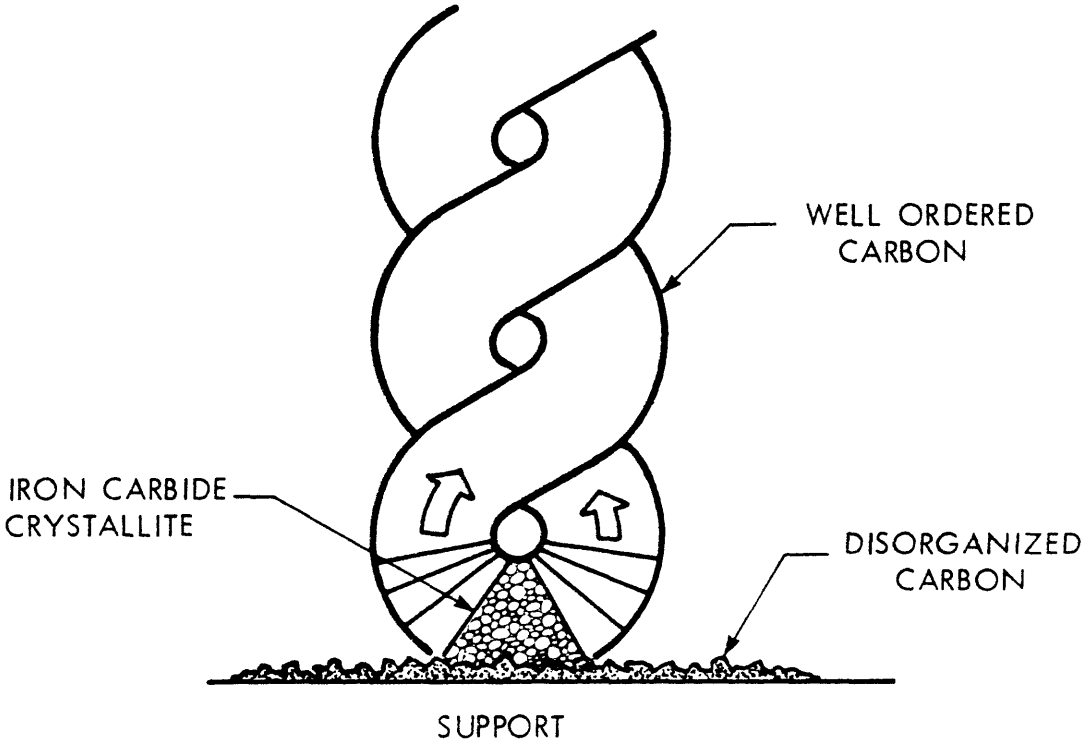

GROWTH OF TWISTED FIBERS

FIGURE 2-21

FIBER GROWTH MECHANISMS INVOLVING IRON CARBIDE
(BOEHM, 1973)

2.2.4.3 The Importance of Surface Diffusion in Filamentary Growth

Baird et al. (1974) developed a mechanism which they believed could explain both hollow carbon fiber growth and platelet formation. This mechanism was put in schematic form by Oberlin et al. (1976) and is shown in Figure 2-22. As is shown, carbon formation results from the thermal decomposition of a hydrocarbon upon an iron or nickel crystallite. By surface diffusion this carbon may end up as flake carbon on the substrate surface or as part of a wall of a filament. Filamentary growth occurs when the catalytic crystallite is lifted from the surface.

By studying the decomposition of methane, propane, propylene, butadiene, and acetone over polycrystalline nickel and iron foils at temperatures of 900-1000K, Baird et al. (1974) made some interesting observations. In their system they observed three forms of carbon, first, a flake graphite, which were single crystals that were aligned with the metal substrate, secondly, a less well defined graphite which was randomly oriented, and was poly crystalline, third filamentous carbon.

It was reported that the gas purity had little, if any effect on the nature of the carbon growth. However, the unsaturated gases decomposed faster than the saturated gases forming longer, structureless filaments similar to those described by Baker et al. (1972). The saturated gases formed more graphitic filaments which had a well defined outer sheath. When butadiene, propylene, and acetone were reacted at low pressure (below 1 torr) they gave similar results.

Some very interesting observations were made on the nature of carbon fiber growth. It was observed that carbon filaments grew out of deposits of carbon platelets which generally formed over grain boundaries. Holes were observed within deposits of single crystal graphite which were believed

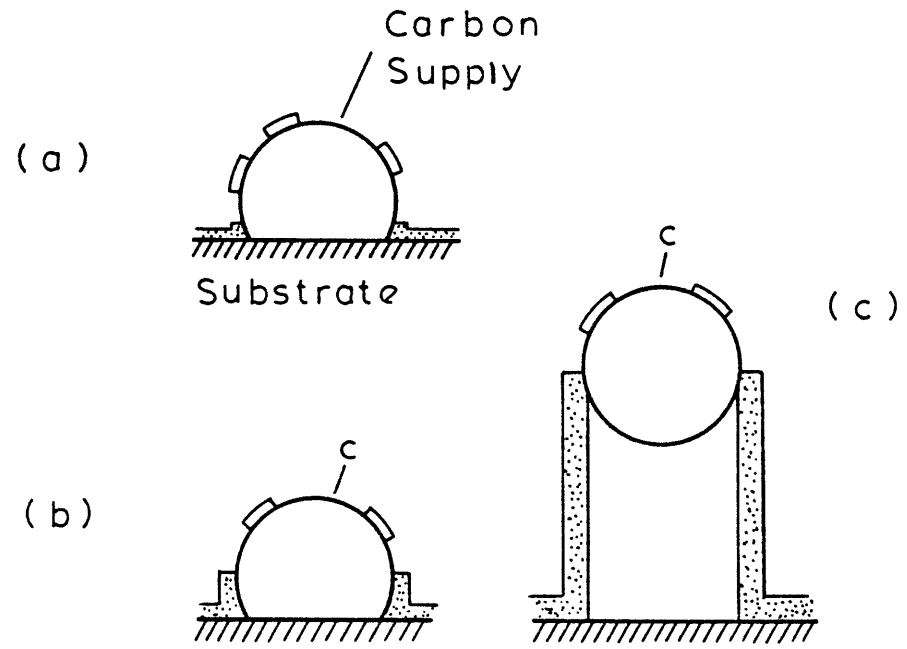

Figure 2-22 Fiber Growth Mechanism Involving Surface Diffusion (Oberlin et al.,1976)

to be growth sites for fibers. Regions of light contrast were observed about the holes which were hypothesized to be the bending of the crystal lattice out of the plane. Electron diffraction patterns from holes showed strong (0001) reflections indicating that the graphite basal planes around the hole were vertical with respect to the foil surface. Adjacent areas showed no such reflections.

Oxidation studies revealed that both filaments and platelets contained metal particles within the carbon matrix. Chemical analysis showed that the carbon was composed of 2% wt. nickel. Electron microscopy showed that finely divided nickel accounted for 0.1%. The typical inner, oxidizable core and outer, more stable section of the filament were not observed. Instead, oxidation appeared to occur from the outermost layers of the fiber and was caused by the catalytic activity of the nickel within the filaments. The nickel particles tended to aggolmerate and caused channeling through the carbon during oxidation.

The most important contribution of Baird et al.'s mechanism is that they can explain many of the previously observed phenomena without the pathway where carbon diffuses through the catalyst particle. The idea of surface diffusion alone can explain the observation of the nickel crystallite moving with the carbon fiber as it grows. It also clearly explains the existance of hollow fibers. The importance of the exothermicity of the decomposition of hydrocarbons (Baker et al., 1975a) in fiber formation could be due simply to a kinetic phenomena. The observation that a large fraction of fibrous material is formed in these systems can alternately be explained by the increased rates which would result from a hotter particle than would have been in the decomposition of methane (endothermic).

3. Apparatus and Procedure

3.1 Experimental Apparatus

A block diagram of the experimental system is shown in Figure 3-1. The primary elements are the feed-gas delivery system, a thermogravimetric reactor, and a gas sampling system.

3.1.1 Feed-Gas Delivery System

The feed-gas delivery system was designed to provide mixtures of dry reactant gases and superheated steam feed. The dry-gas feed is shown in Figure 3-2. Cylinders of carbon monoxide, carbon dioxide, methane, and hydrogen were used as sources of reactant gases, while a cylinder of helium served for an inert. Their analyses are shown in Table 3-1. Figure 3-2 also shows the components which permitted the metering of gas flow rates. They included mass flow regulators, capillary tubes, and u-tube manometers. The system used two-stage regulators, which maintained the upstream pressure

Table 3-1

Feed-Gas Analysis

	Supplier	CO_2	O_2	N_2	Dewpoint
Hydrogen Purified Grade	(Airco)		< 20 ppm		213.6 K
Methane CP Grade	(Matheson)	0.2 mole %	0.005 mole %	0.6 mole %	
Carbon Dioxide Bone Dry Grade	(Matheson)	99.95 mole %	0.05 mole %		238.6 K
Carbon Monoxide CP Grade	(Matheson)	50 ppm	600 ppm	1500 ppm	
Helium High Purity Grade	(Airco)	1 ppm	1 ppm	14 ppm	

at 3.5×10^5 N/m^2 (50 psig), the gas was fed to Brooks Model 8944 mass flow

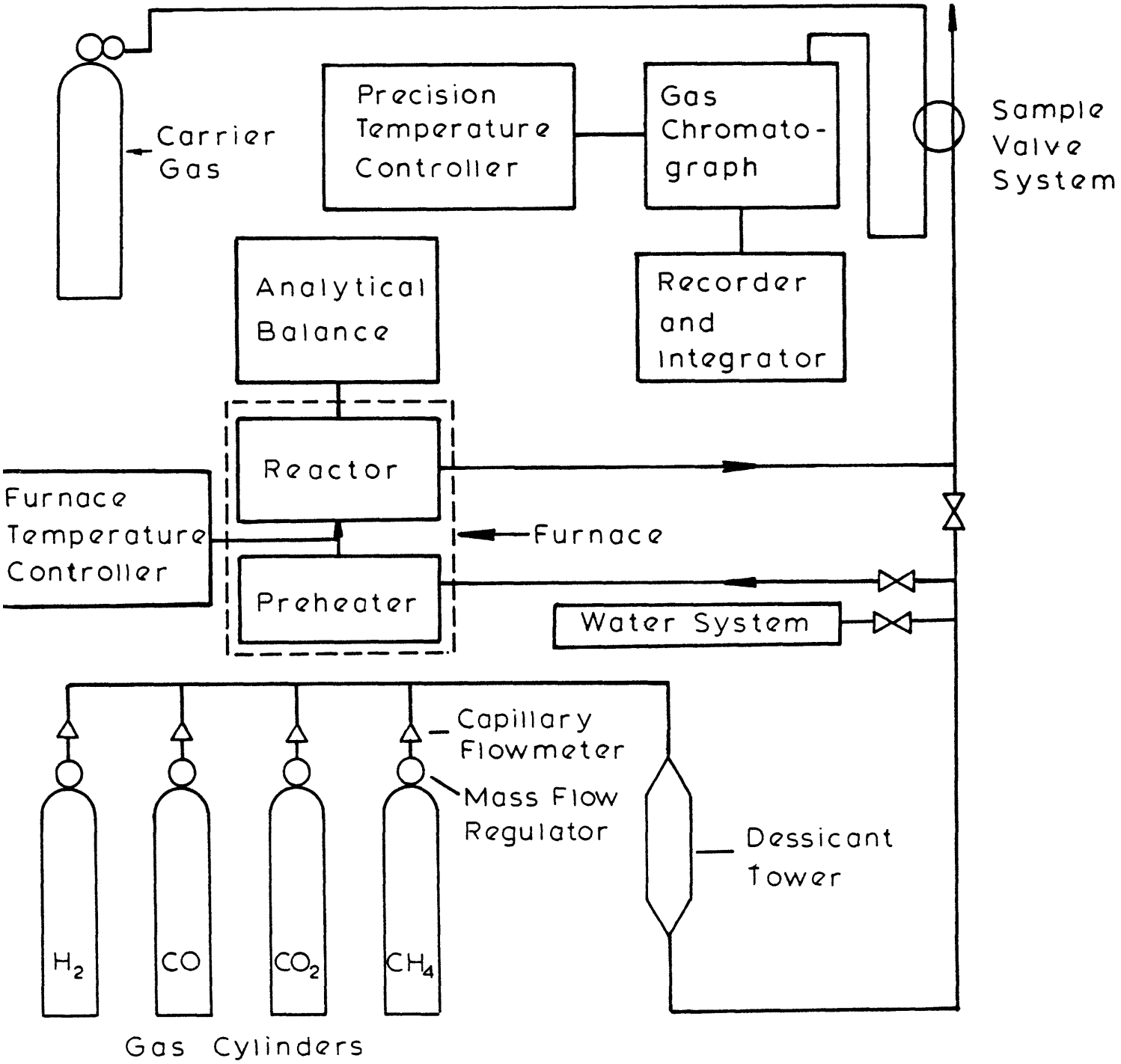

Figure 3-1 Schematic Diagram of Experimental System

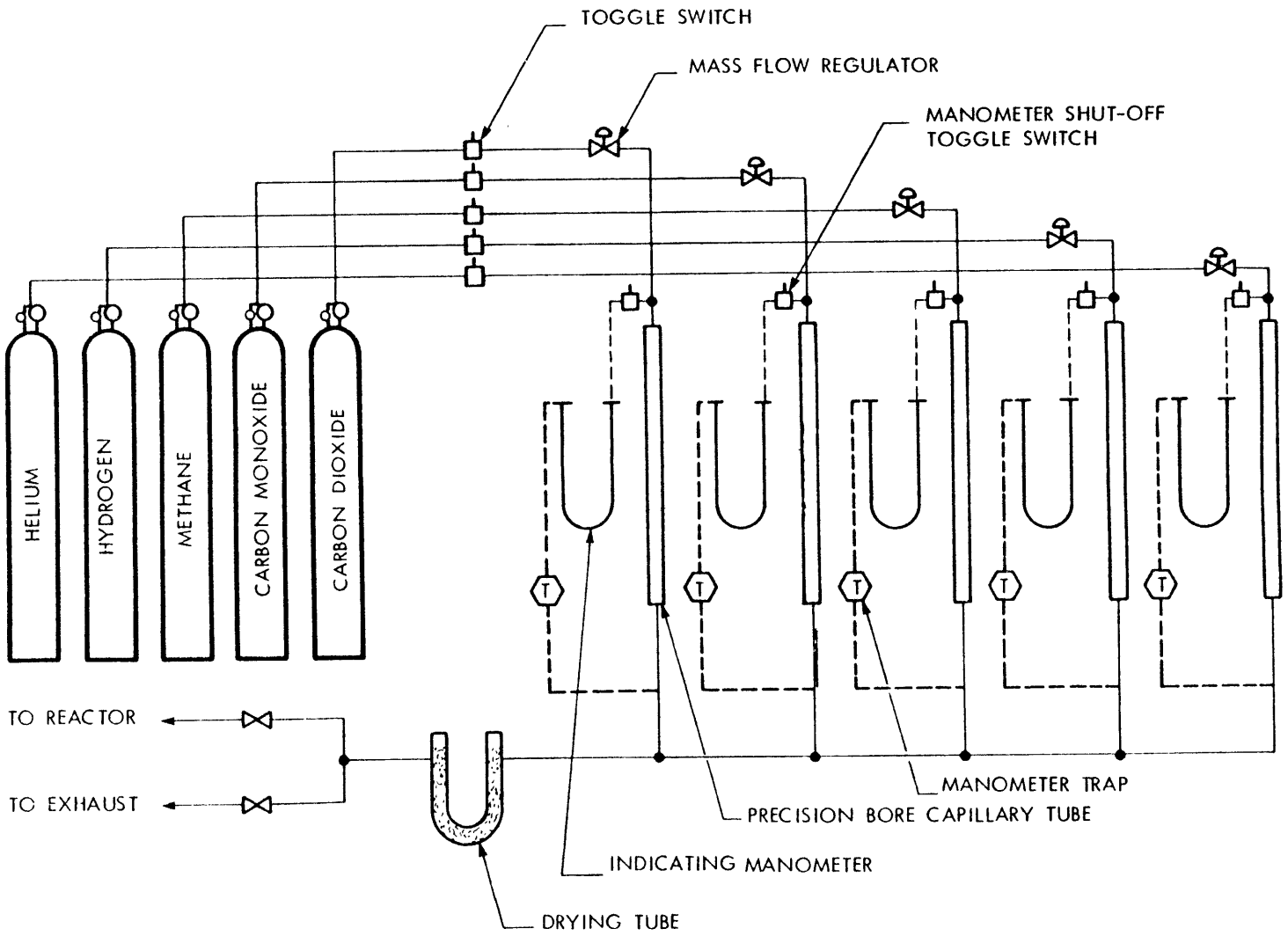

Fig. 3-2 FEED GAS DELIVERY SYSTEM

regulators fitted with inline filters capable of trapping particles greater than 2μm. The gases individually passed through precision bore capillary tubes (diameter tolerance ± 0.007mm). Since the flow rate through a capillary is proportional to pressure drop, by fitting u-tube manometers across them, flow rates could be determined. The manometers were filled with Meriam high vacuum manometer fluid (ρ = 1.04 g/cm^3). The capillary tubes were calibrated for gas flow rates using a wet-test meter at high flow rates and a soap film flow meter at low flow rates. Since flow through the capillary tubes was laminar, plots of flow rate versus pressure drop were linear. Calculations revealed that end effects were negligible. The gases which exited the capillary tubes were joined and then dried over dessicant. At this point the mixture could be fed to the reactor or exhausted to a hood.

To add water to the feed-gas, liquid water was pressurized, metered, and vaporized before it was mixed with the remainder of the feed-gas. Figure 3-3 shows the water feed system. A 1ℓ cylindrical water resevoir was pressurized using a cylinder of helium. The water was then fed to a precision bore capillary with an I.D. of 0.2mm. A 15μm filter prevented the blocking of the fine capillary. A mecury manometer allowed the calibration of the system. A metering valve used in conjunction with the helium regulator, permitted an accurate and reliable control of the liquid flowrate. At this point the water was fed to the vaporizer which was constructed out of a section of 0.64cm (1/4 in.) stainless-steel tubing which had a thin cement coating on the outer surface. A winding of nichrome wire, about the cement, served as a heating element. The tubing was packed with 0.5mm borosilicate beads to facilitate heat transfer. The tubing assembly was then encased in a cylinder of cement, around which Kaowool blanket and asbestos stripping was wrapped. The nichrome wire was controlled by a Variac. The exit of the

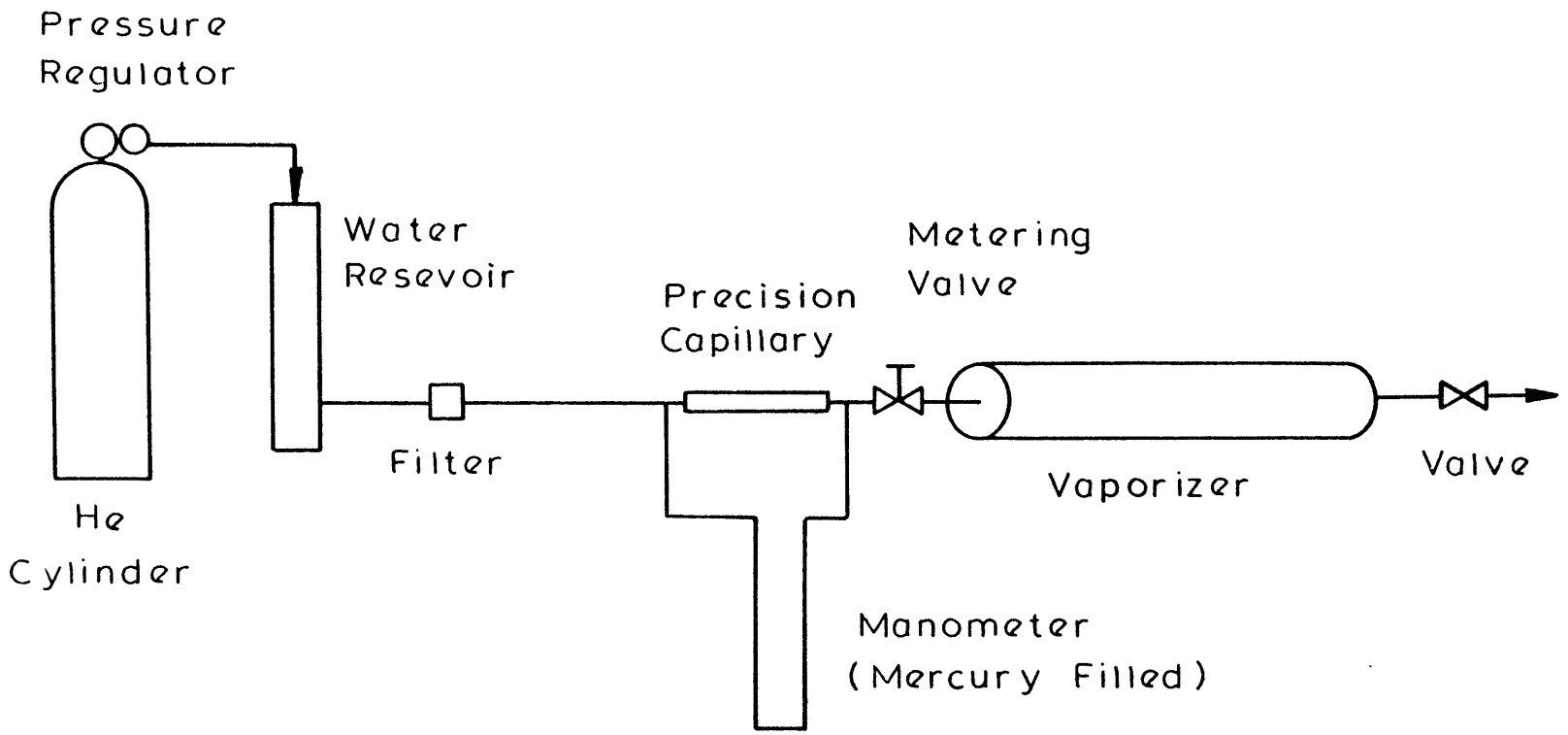

Figure 3-3 Water Vapor Delivery System

vaporizer was fed to a 1m length of 0.64cm (1/4 in.) stainless steel tubing heated with Briskeat heating tapes and insulated with a Kaowool blanket. An inline filter and the tubing served to eliminate any surges in the gas stream. Two valves at the end of the tubing allowed the steam to be by-passed to the atmosphere or mixed with the gas stream which was finally fed to the reactor. The steam exiting the vaporizer was at approximately 423K and 1 atm.

3.1.2 Thermogravimetric Reactor

The thermogravimetric reactor consisted of the preheater and lower reactor support tube, the top section reactor support tube, the catalyst assembly, and the furnace. Figure 3-4 illustrates the top and lower reactor sections including the preheater.

3.1.2.1 Preheater and Lower Reactor Support Tube

The preheater and lower reactor support tube served as the base of the quartz reactor. The preheater coil was formed from 6m of 7mm I.D. quartz tubing which was wound into a helical coil 32cm high and 6cm in diameter. This coil was mounted concentrically about the reactor support tube which was 2.8cm in diameter and 28cm in height. A 34/45 tapered inner ground-glass joint was fitted to the top of the reactor support tube, to which the top section reactor support tube was positioned. Mounted from the bottom of the reactor support tube, an 11cm quartz thermocouple well extended upward. In this, a two hole Alundum thermocouple sheath was provided to hold the two thermocouples. A 19/38 inner ground-glass joint was mounted upward, 2cm from the base of the reactor support tube, to support the catalyst assembly.

3.1.2.2 Top Section Reactor Support Tube

The top reactor section was designed to support the reactor within the furnace, to allow the sampling and exhausting of outlet gases, and the weighing

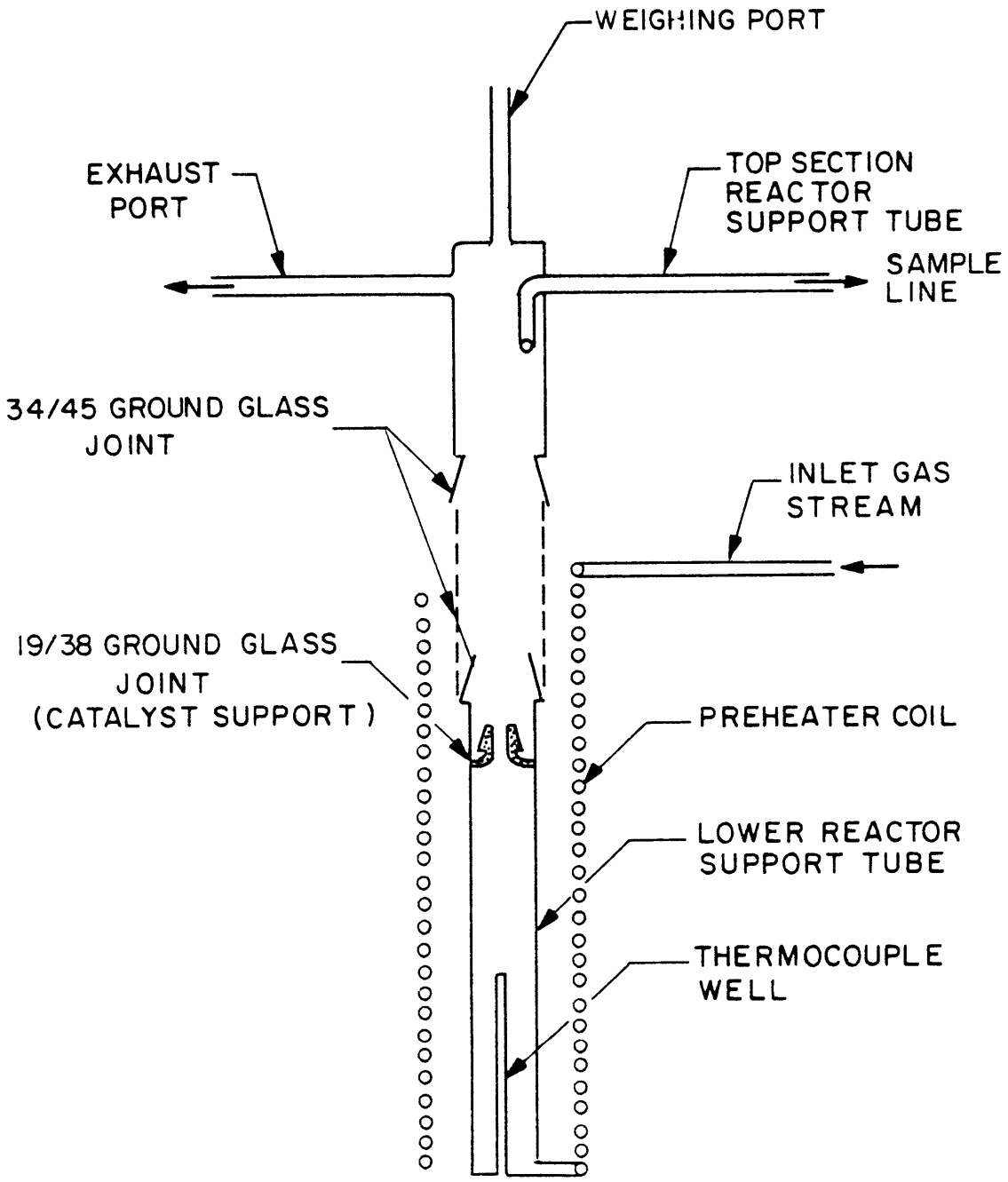

Fig. 3-4 REACTOR TOP AND LOWER SECTIONS WITH PREHEATER

of the catalyst mass. It was constructed out of a 2.8cm I.D. quartz tube, 15.2cm in height, with a 34/45 ground-glass joint mounted on its lower end which joined with the lower reactor support tube. The upper end was fitted with an 8mm I.D. quartz tube mounted concentrically. This tube was used as a weighing port. Connected at right angles to the support tube centerline were two additional 8mm I.D. quartz tubes. One of these tubes was sealed and was used only to hold the top section in place, while the other served as a support and an outlet used for taking reactor outlet gas samples.

3.1.2.3 Catalyst Assembly

Figure 3-5 shows the assembly used to contain the catalyst. It was constructed out of a 2cm I.D. quartz tube which was 12cm in length. A 19/38 outer tapered ground-glass joint allowed the assembly to be sealed to the lower reactor. At the top, a 2mm diameter quartz rod, 25cm long, was mounted concentrically with the tube and permitted weight measurements to be taken. This was done by periodically supporting the quartz rod from an overhead Sartorius balance, sensitive to ± 1mg.

3.1.2.4 Furnace

The entire three-piece reactor assembly was housed in an electrically heated furnace. The furnace consisted of two Thermeraft Model RH 254 semi-cylindrical ceramic heating elements, which were 7.5cm in diameter and 30.5cm in length. The two elements were wired in parallel to a 220 volt line. The power to the elements and thus the reactor temperature was controlled by a Thermolyne Dubuque III solid state controller. The controller kept the reactor temperature to within ± 2K, and had a maximum temperature of 1450K. The maximum power output of the heaters was 2300 watts. Two Omega stainless steel sheathed type K thermocouples were located in the thermocouple well, directly below the catalyst assembly. One was connected to the controller, while the

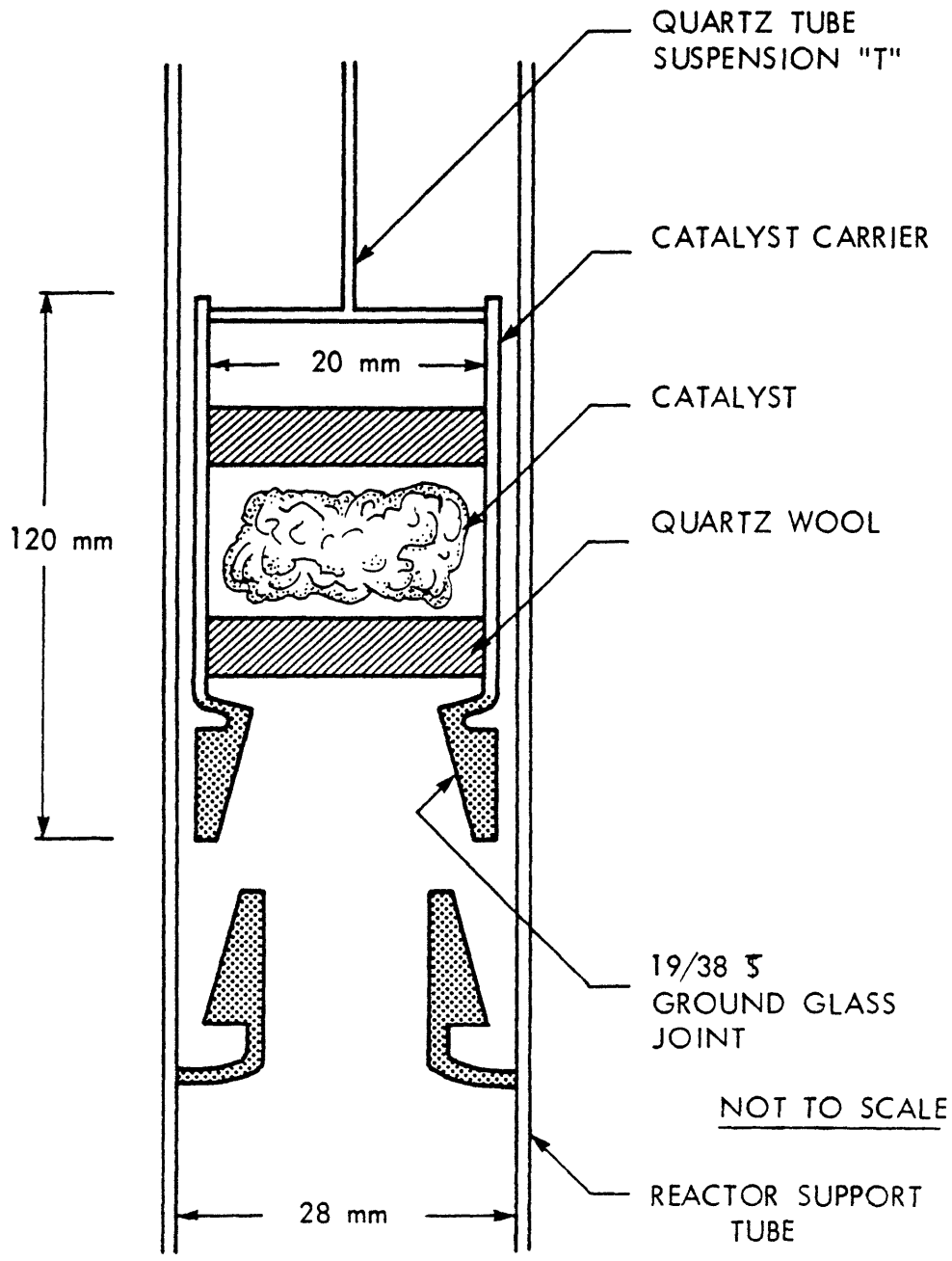

FIGURE 3-5

CATALYST CARRIER IN SUPPORT TUBE

other was connected to an Omega Engineering 200 digital pyrometer.

The structural part of the furnace which supported the heating elements and served as insulation was constructed as follows. The heating elements were surrounded by 11cm of Babcock and Wilcox type K-30 insulating fire-brick. This formed a square structure about the cylinderical heaters. The outside of the brick was covered with a 6.5mm layer of asbestos board, and then a 6.5mm layer of transite, an asbestos-concrete composite.

3.1.3 Gas Sampling System

To determine both reactor inlet and outlet gas compositions, a gas sampling system was constructed. It consisted of a heated gas sample valve, gas chromatograph, and a digital integrator.

A Carle, model 2014, Micro Volume valve, fitted with 0.25 cm^3 Teflon sample loops, was used to inject gas samples into the gas chromatograph. It was mounted in an insulated aluminium box which was heated by three 200 ohm, 75 watt tubular resistors, controlled by a model 220 Hewlett Packard temperature controller, utilizing an iron-constantan thermocouple. The sample box was maintained at 373K to prevent the condensation of water. A small fan, mounted within the box, kept the box isothermal. A series of toggle operated shut-off valves allowed the sampling of inlet or outlet gases, a special calibration mixture, or air. Inlet and outlet gas sample lines were heated above 373K to prevent the condensation of water. A vacuum system, equipped with a U-tube manometer and a McLoed guage, allowed the evacuation of the sample loop for the injection of a given sample of gas. Figure 3-6 shows the sample loop with sample lines, toggle values, and vacuum system. The sampling procedure consisted of flushing the sample loop several times using the toggle value of the desired gas sample and the vacuum system, followed by sample injection.

A Hewlett Packard Series 700 gas chromatograph was used in conjunction

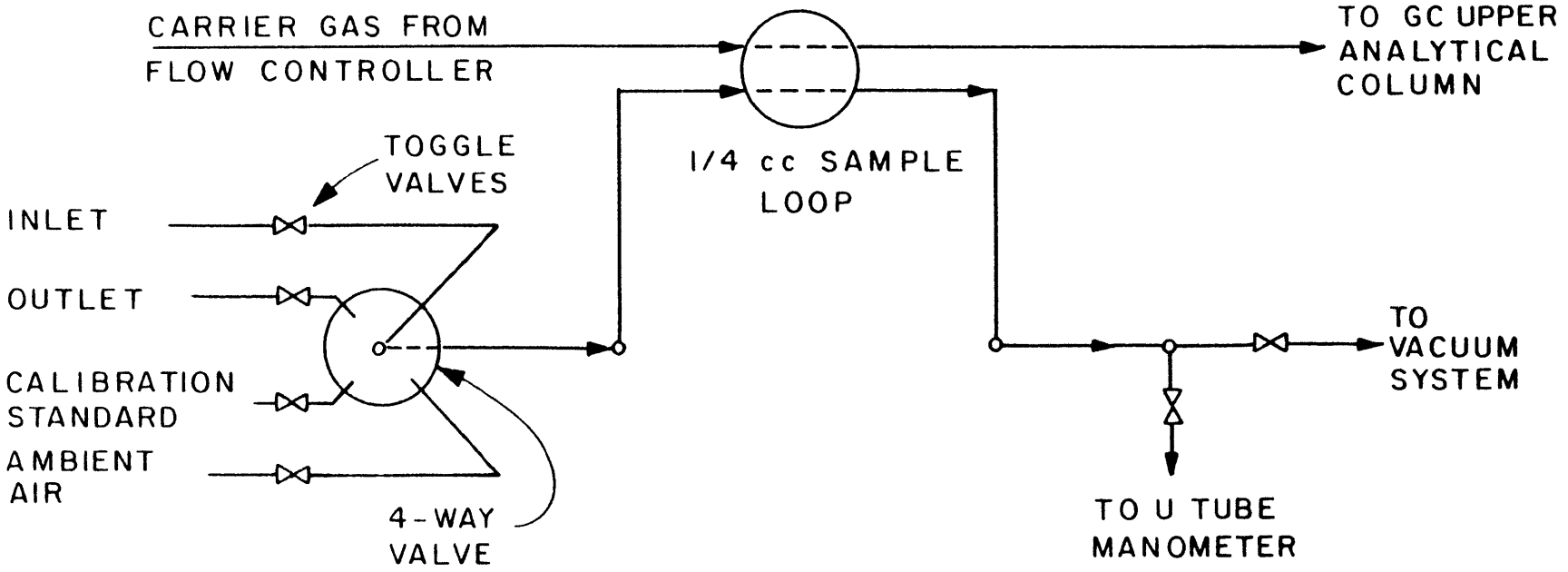

Fig. 3-6 GAS SAMPLING VALVE SYSTEM

with an Autolab 6300 digital integrator for gas analysis. The critical gas chromatograph parameters are given in Table 3-2. The columns used in the chromatograph were constructed of 6.1m of 3.2m O.D., 2.4mm I.D., Teflon

Table 3-2 Critical Gas Chromatograph Parameters

Filaments	GOW-MAC Rhenium Tungsten Code 13.002 (wx)
Sample Size	$0.25cm^3$
Carrier Gas Flowrate	$30cm^3$
Column Operating Temperature	358K
Detector Operating Temperature	473K
Detector Filament Current	200mA

columns filled with Porapak QS manufactured by Waters Associates. This packing allowed the separation of hydrogen, carbon monoxide, methane, carbon dioxide,and water in less than thirteen minutes. A special carrier gas of 91.5% He and 8.5% H_2 supplied by Matheson Gas Products allowed the direct measurement of hydrogen by the method of Purcell and Etre (1965). Response factors for the five gases, determined by the method of Dal Nogare and Juvet (1962), allowed the calibration of the thermal conductivity detector by an external standard. The three standards typically used were (1) hydrogen, (2) and equimolar mixture of hydrogen, carbon monoxide, methane, and carbon dioxide, and (3) a gas mixture of a given compostion of carbon dioxide and water. This mixture was made up using the feed-gas delivery system. A Honeywell chromatographic chart recorded allowed the visual observation of the chromotographic peaks. Through the repeated sampling of a gas standard, it was found that through the use of the digital integrator and gas chromatograph, gas compositions calcualted were accurate to with ± 1%.

3.2 Experimental Procedure

The experimental procedures for the determination of run conditions, equipment start-up, operation, and shut-down were as follows.

3.2.1 Determination of Run Conditions

A detailed technique for determining carbon-gas equilibrium compositions as a function of ΔG_c has been described in section 2.2.2. The technique involves varying the Gibbs energy of the reactions which involve the deposition of carbon by an amount ΔG_c. This was done to account for the possibility of a different form of carbon which might exist in a given system. At the beginning of a run, equilibrium calculations were made for a range of values of ΔG_c. For instance, if the experimental run was at 750K, calculations were made for values of ΔG_c from-5.0 to 5.0kcal/mole, every 0.5kcal/mole. During the run these different mixtures were passed over a nickel or cobalt catalyst, which had been covered with a layer of carbon deposited from an equimolar mixture of hydrogen and carbon monoxide at the given reaction temperature. Rates of carbon deposition were followed to determine if carbon would be deposited, removed, or if no net reaction would occur. From this, the equilibrium point could be determined. Studies were conducted at a given temperature, atmospheric pressure, and a given O/H ratio of the gas-feed between 0 and ∞.

3.2.2 Equipment Start-Up

All electronic equipment was turned on one hour before run time. The water flow to the vaporizer was turned on and the flow rate was ajusted for the first run condition. Power was turned on to all heated gas lines to prevent water condensation. The catalyst assembly was filled with a known mass of the appropriate catalyst, which was held in place by quartz wool. Three catalysts which were typically used were as follows: Cobalt powder, supplied by Bram Metalluagical Chemical Co., 1-5μm in diameter, which was re-

ported to be 99.9% pure. The surface area was measured by the B.E.T. method and shown to be $0.7m^2/g$. A Ni/Al_2O_3 catalyst, supplied by the Alfa division of Ventron Corporation, was reported to be 60-65% Ni, reduced and stabilized, and have a surface area of $200m^2/g$. A third catalyst used was prepared by drying a 5% wt solution of cobalt nitrate, supplied by Fisher Scientific Company, on 1g of quartz wool, at 423K over a copper screen.

The catalyst assembly was then placed in the reactor, where it rested on the lower reactor support tube's 19/38 ground-glass joint. The top section of the reactor support tube was put in place and the reactor was closed with the top section of insulating firebrick. The catalyst assembly was attached to the analytical balance to assure proper alignment and that reliable weight measurments could be made. The furnace was then turned on, heated up to the desired operating temperature, and allowed to stabilize for 1 hour. During the heat-up period hydrogen was passed over the catalyst at $20cm^3/s$. The gas sample valve box was heated to 373K and the vacuum of the system checked to make sure it was below $400N/m^2$. Calibration gases were then run through the gas chromatograph to calibrate the thermal conductivity detector. At this point, an experimental run could be made.

3.2.3 Run Procedure

The run procedure consisted of setting the gas flow rates to a given gas mixture. During this process, periodic weight measurements were made to determine whether carbon deposition or removal occurred. Gas samples were run through the gas chromatograph to determine inlet and outlet compositions.

3.2.4 Shut-Down Procedure

At the end of an experimental run, the reactant gases were shut-off and a stream of He at $20cm^3/s$ was passed over the catalyst. The power to the furnace was then shut off. All gas line heaters were turned off. After the

reactor had cooled down, the spent catalyst was removed, inspected, bottled, and labeled.

4.0 Results and Discussion

4.1 Preliminary Experiments

Two of the catalysts which were used in the experimental study were examined for their catalytic activity along with 0.25mm cobalt wire. The cobalt wire was of interest because of its similarity to the steel wool which was used previously. The form of wire or wool allows the catalyst to be well distributed in a large volume, utilizing a small fraction of that volume, so that a large proportion of carbon, relative to metal, may fillup the space. The difficulty with powdered catalysts is that they tend to agglomerate and plug the reactor.

In Figures 4-1, 4-2 and 4-3 the carbon deposition is shown as a function of time for the reaction of an equimolar mixture of hydrogen and carbon monoxide over the different catalysts at 800K. For all three experiments, a linear rate is obtained after a period of roughly five minutes. For the total reaction times studied these rates remained linear.

The ultimate yield from the catalyst used in the Bosch process is critical (g C/g catalyst). Certainly no weight savings is made if one must transport more mass of catalyst than the mass of oxygen which it eventually regenerates. To estimate the ultimate yield, carbon was deposited upon cobalt powder from a 1:1 mixture of hydrogen and carbon monoxide at 800K. Figure 4-4 shows the results. As can be seen, the rate of carbon deposition remains constant up to 100g C/gCo. Certainly, this shows that the Bosch process would allow very large weight savings.

4.2 Equilibrium Studies

In this section, the results of the equilibrium studies over nickel and cobalt are presented and discussed. The experiments were run at temperatures of 700, 750, 800 and 900K and a pressure of 1.0 atm. Measurements were made

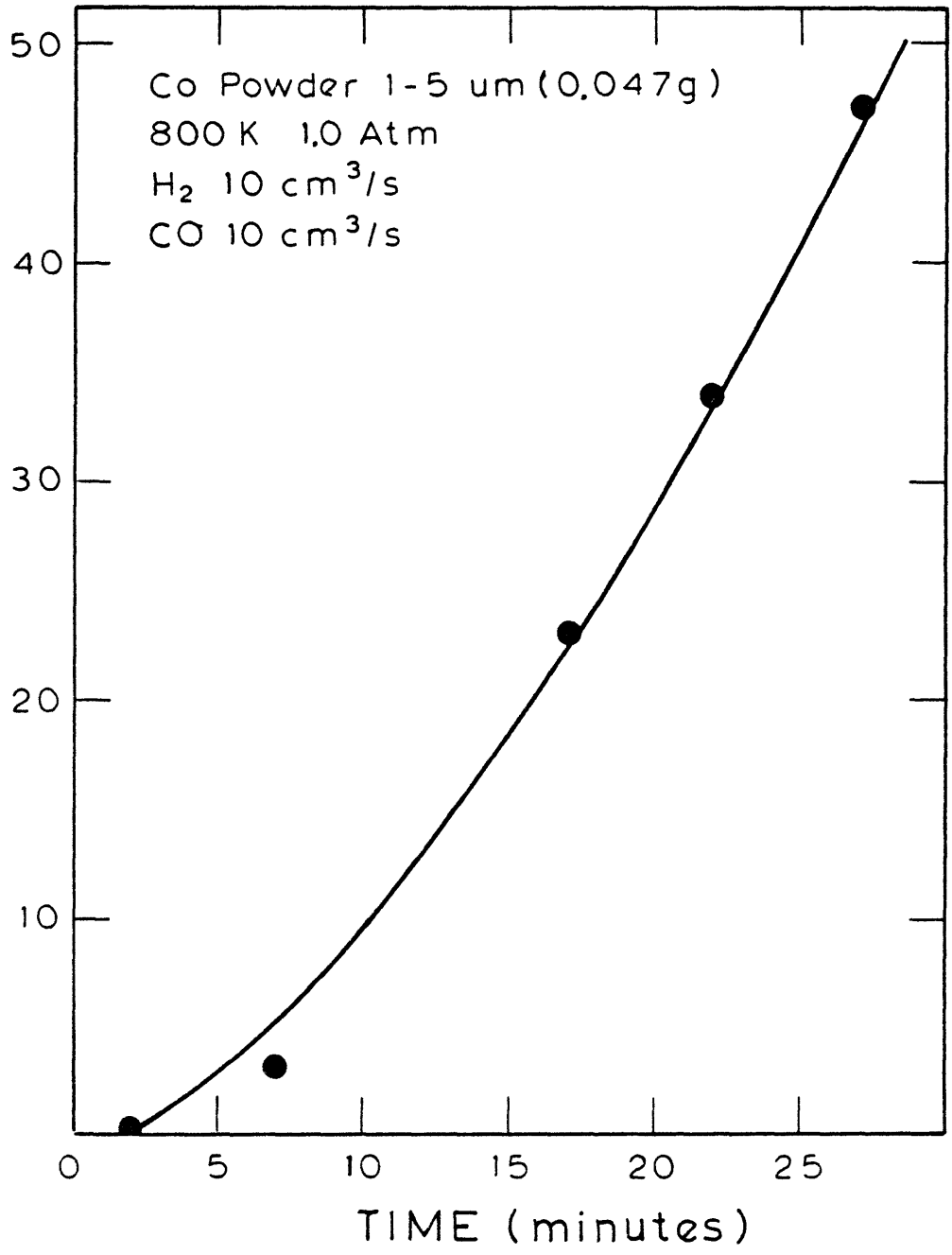

Figure 4-1 Carbon Deposition on Cobalt Powder From a H_2: CO (1:1) Mixture

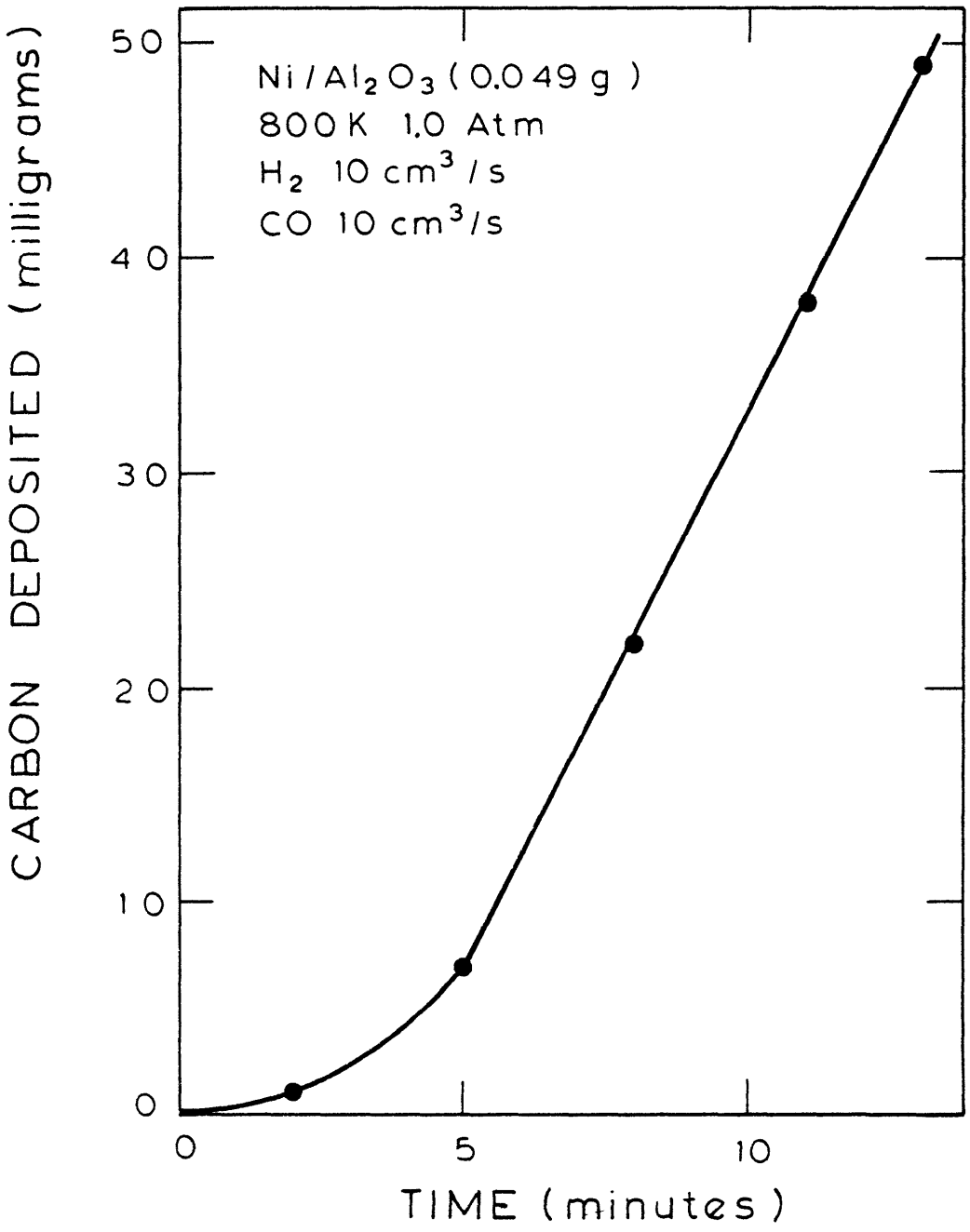

Figure 4-2 Carbon Deposition on a Ni/Al_2O_3 Catalyst from a $H_2:CO$ (1:1) Mixture

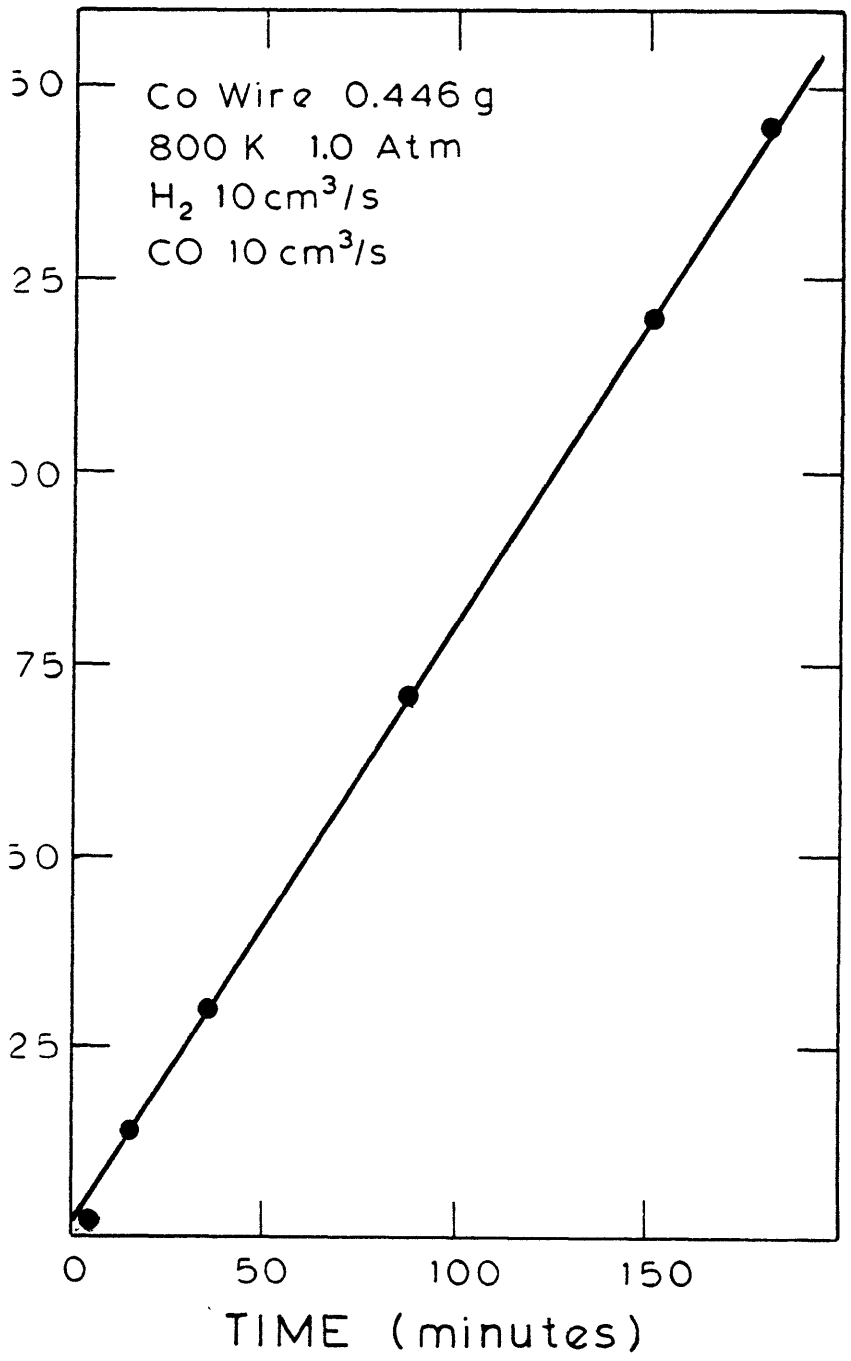

igure 4-3 Carbon Deposition on Cobalt
Vire from a H_2 : CO (1:1) Mixture

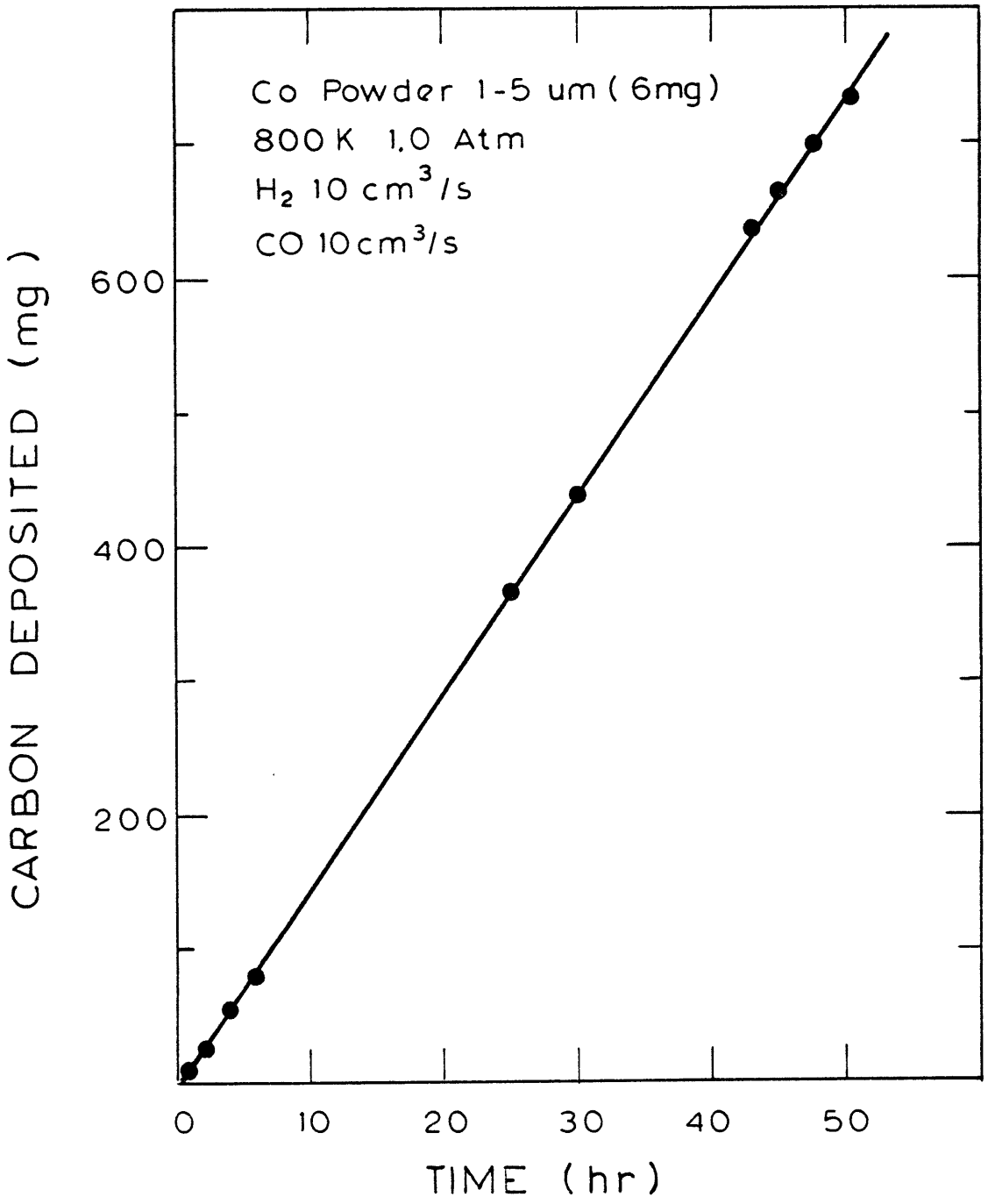

Figure 4-4 Carbon Deposition on Cobalt Powder from a H_2:CO (1:1) Mixture

for the binary-gas systems of CO-CO_2 over carbon and CH_4-H_2 over carbon. Multi-component experiments with H_2, CO, CH_4, CO_2, H_2O and C were also carried out at O/H ratios of 0.17, 0.5 and 1.5.

Prior to an experiment the gas phase compositions to which the carbon-catalyst mass would be exposed were calculated at the desired temperature, pressure, and O/H ratio. Then, equilibrium gas phase compositions were calcalated at various hypothetical Gibbs energies for the solid carbon phase as discussed in Section 2.2.2 and 7.1. These calculations extended beyond the values of ΔG_c reported by Dent (1945), Rostrup-Nielsen (1972), and Schenck (1927), for their studies of different non-graphitic equilibria. This procedure insured that at the extreme values of ΔG_c carbon deposition would occur. For instance at 750K, Dent, Rostrup-Nielsen, and Schenck reported values of ΔG_c (extrapolated from Figures 2-10, 2-11 and 2-13b) of 2.2, 2.1 and 3.2 kcal/mole, respectively. Equilibrium calculations were then made, at a given temperature, atmospheric pressure, and O/H ratio, for Gibbs energies of carbon from 5.0 to -5.0 kcal/mole, every 0.5 kcal/mole.

During an experimental run mixtures of the calculated composition, which consisted of either CO and CO_2, CH_4 and H_2, or H_2, CO, CH_4 CO_2 and H_2O, were passed over nickel or cobalt to determine the rate at which carbon deposition or removal occurred. At the equilibrium point in this system, the rate of carbon deposition or removal should become zero. Hopefully, the slope of the rate versus ΔG_c curve, about the equilibrium point would be non zero so no uncertainty would be introduced into the value of ΔG_c at equilibrium. The different experimental conditions were run in order from mixtures rich in carbon depositing gases to ones rich in carbon removing gases. At each condition, a rate of carbon deposition was determined by the intermittent weighing of the catalyst carrier. Both time and weight were recorded. For fast rates,

> 1 mg/min, four weight measurements were taken, one every ten minutes. For slow rates, ∿0.05 mg/min, four measurements were taken, one everythirty minutes. The rate was then determined by the slope of the linear section of a plot of weight versus time. If no linear section existed, more weighings, at the same experimental condition, were taken.

The experimental study of the Bosch process is important since the assumption of a solid phase of graphite in equilibrium calculations could lead to errors in predicted results. This follows from the fact that calculations assuming Dent carbon (1945) as the solid phase reveal very different results. Table 4-1 shows the discrepancy between the two systems at an O/H ratio of 0.5 and temperatures of 700, 800 and 900K. In terms of the water concentration, the equilibrium values fall from 18% to 13%, from 32% to 17%, and from 45% to 11% at temperatures of 900, 800 and 700K, respectively, for the system based on graphite versus those of Dent.

4.2.1 Bosch Equilibrium Studies

Typically, a Bosch reactor feed is a 2:1 mixture of hydrogen and carbon dioxide. Such a feed has an O/H ratio of 0.5 and since neither elemental oxygen nor hydrogen are consumed in the process, at steady state the O/H ratio of the equilibrium gas mixture exiting the reactor equals 0.5. Considering the direct application of studies of the equilibrium of this five-component system, the first experiments run were chosen to be at an O/H ratio of 0.5.

Results from the first set of experiments are shown in Figures 4-5 through 4-8 and are for the experiments at 900, 800, 750 and 700K and 1.0 atm over cobalt. In each figure the experimentally obtained rates of carbon deposition (mg/min) are plotted as a function of the parameter ΔG_c (kcal/mole), which is characteristic of the corresponding gas phase composition. Simultaneously drawn against ΔG_c are curves which represent the gas compositions which

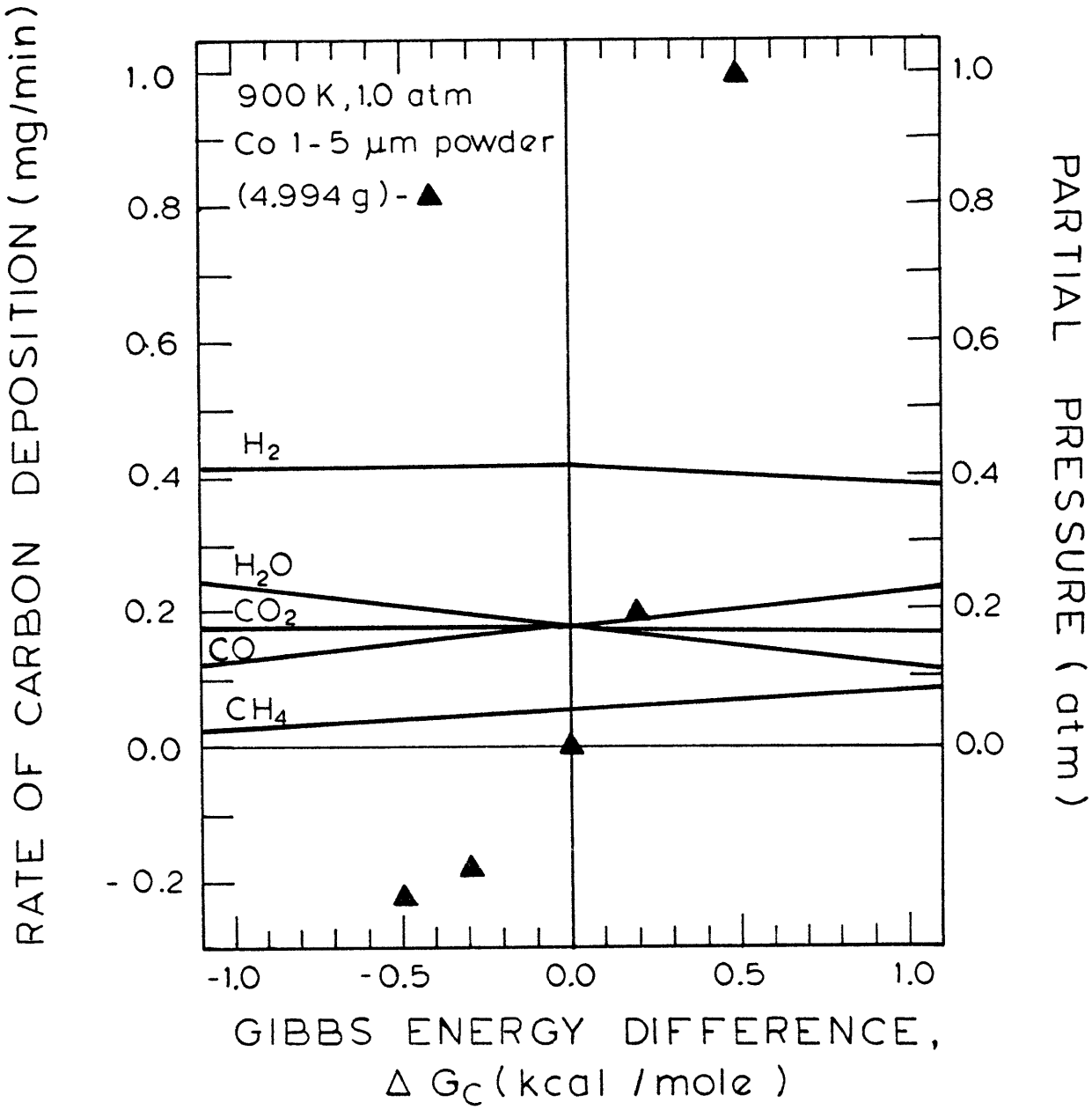

Figure 4-5 Rate of Carbon Deposition as a Function of ΔG_C for an O/H = 0.5

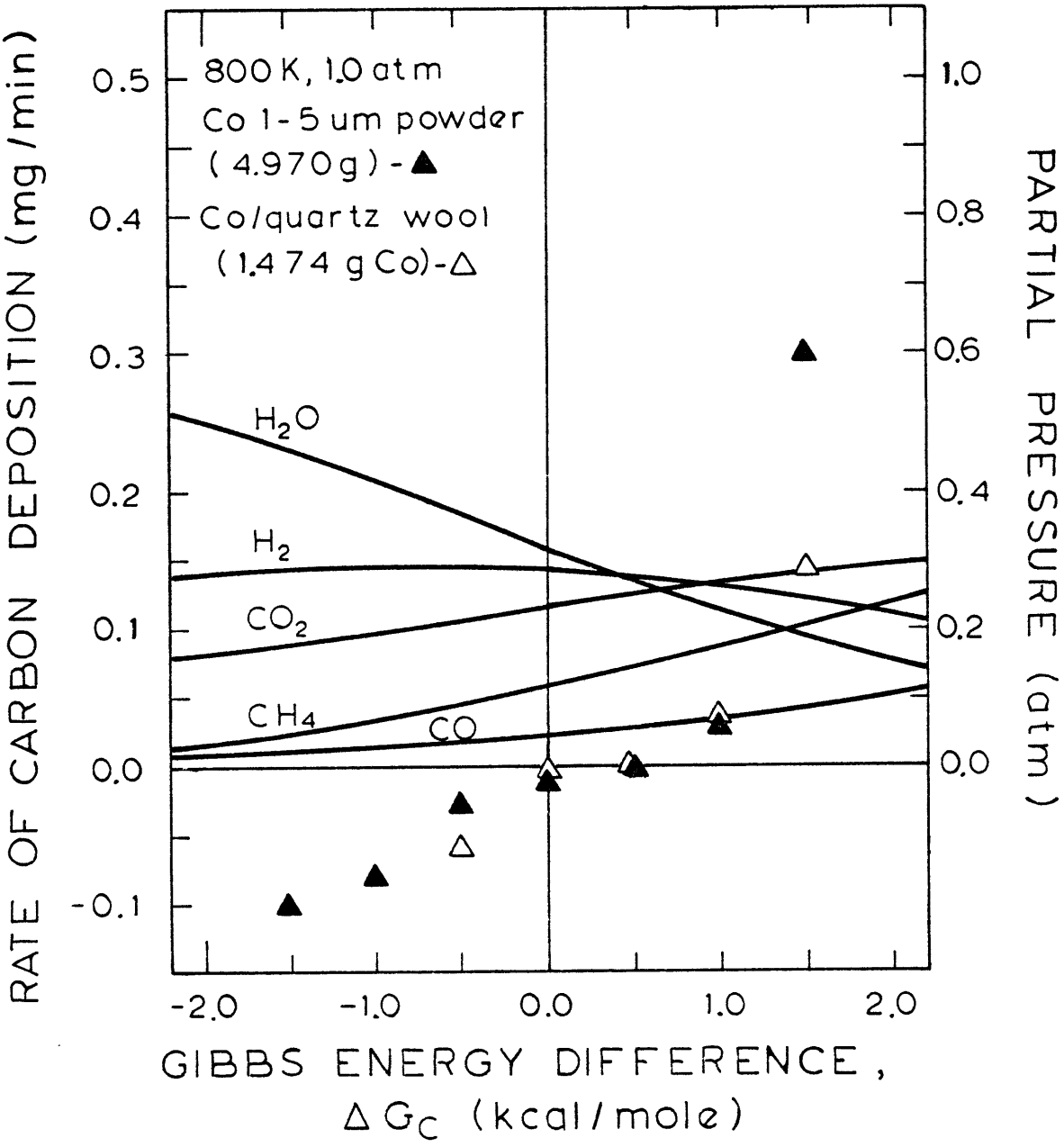

Figure 4-6 Rate of Carbon Deposition as a Function of ΔG_C for an O/H = 0.5

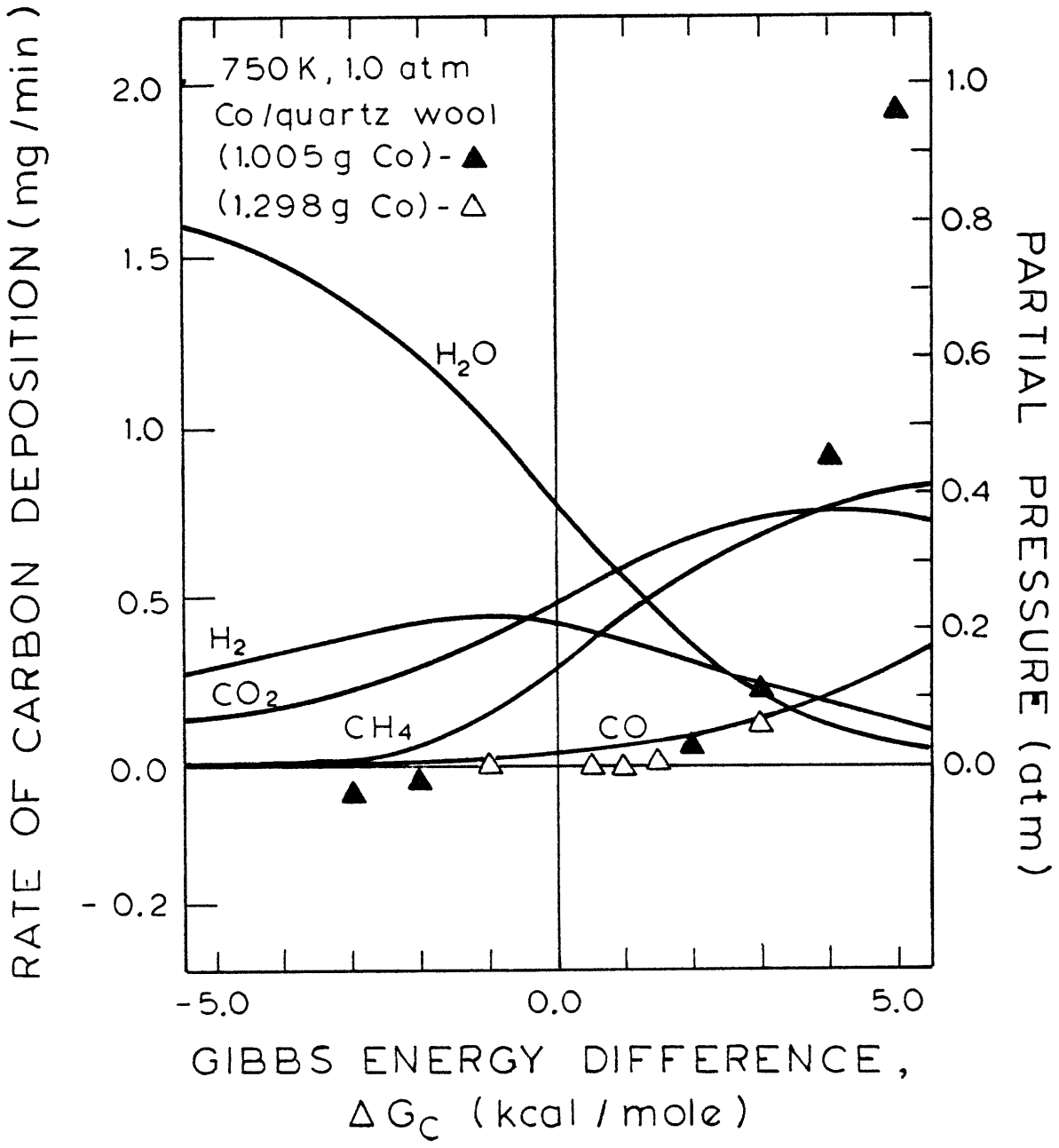

Figure 4-7 Rate of Carbon Deposition as a Function of ΔG_C for an O/H = 0.5

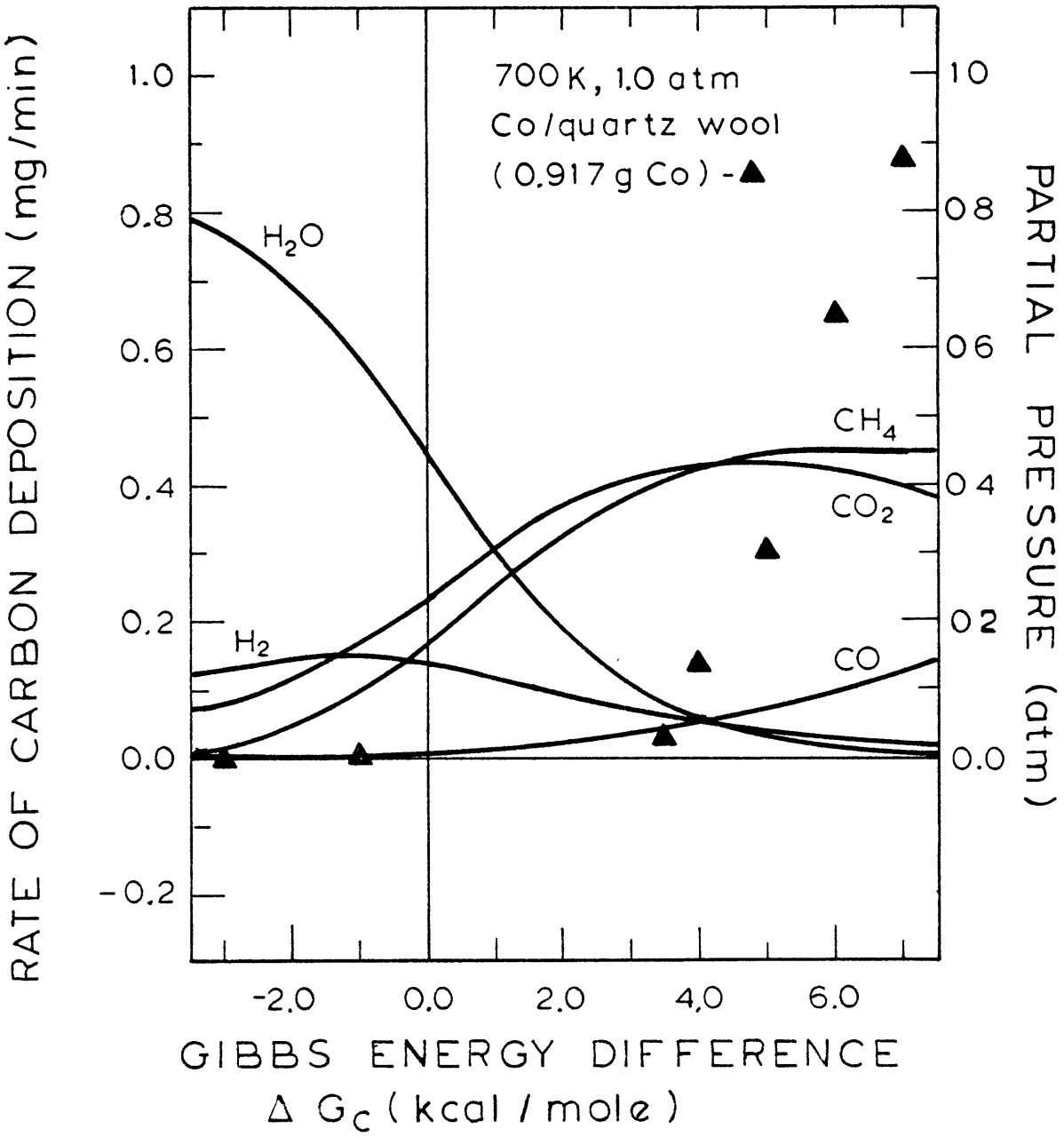

Figure 4-8 Rate of Carbon Deposition as a Function of ΔG_C for an O/H=0.5

Table 4-1

Effect of ΔG_C on the Equilibrium Gas Compositions in the Bosch Process

O/H = 0.5, Pressure = 1.0 Atm

Equilibrium Solid		Partial Pressure (Atm) P_{H_2}	P_{H_2O}	P_{CO}	P_{CO_2}	P_{CH_4}	ΔG_C(kcal/mole)
Graphite	900K	0.41	0.18	0.18	0.18	0.05	0.0
Dent	900K	0.40	0.13	0.22	0.17	0.08	0.85
Graphite	800K	0.28	0.32	0.05	0.23	0.11	0.0
Dent	800K	0.23	0.17	0.09	0.29	0.22	1.69
Graphite	700K	0.14	0.45	0.01	0.23	0.17	0.0
Dent	700K	0.08	0.11	0.03	0.40	0.38	2.86

yielded the experimental data. These compositions were calculated to be in equilibrium with a carbon of the corresponding ΔG_c.

Preceeding every equilibrium run where fresh catalyst was put into the reactor and reduced, carbon was deposited from a 1:1 mixture of hydrogen and carbon monoxide. This was done at the reaction temperature of the equilibrium run. In each case about 0.2g C/g catalyst was deposited.

As indicated in the experimental section the experimental gas mixture composition fixed by setting the flow rates of each component. The inlet compositions were confirmed by gas chromatography. Also, the outlet gases were analyzed to insure that the reactor was operating differentially.

There are some interesting trends which are observed in the four figures which present the results for the temperatures of 900, 800, 750 and 700K. First, when going from high to low temperature, carbon deposition is observed to cease at a larger and larger value of ΔG_c. For instance, carbon deposition stops at 0.0, 0.5, 1.5 and 3.0 kcal/mole at temperatures of 900, 800, 750 and 700K, respectively. Also, since the slope of the rate versus ΔG_c curve goes to zero, there exists a gap between the point at which carbon deposition and removal become zero. It is observed that at 900 and 800K, carbon removal begins at ΔG_c less than 0.0 kcal/mole. However, at 750, this occurs at -1.0 kcal/mole. At 700K, even for the lowest value of ΔG_c (-3.0kcal/mole), no carbon removal was observed. These results are shown in Figure 4-9 where ΔG_c of either the carbon deposition and removal boundary are plotted versus temperature. Note that the distance between the two points becomes larger at low temperature.

The results for the study of the equilibrium over the nickel catalyst is presented in a similar fashion as was for the cobalt. Figures 4-10 through 4-13 present the data from the studies at 900, 800, 750, and 700K and 1.0 atm

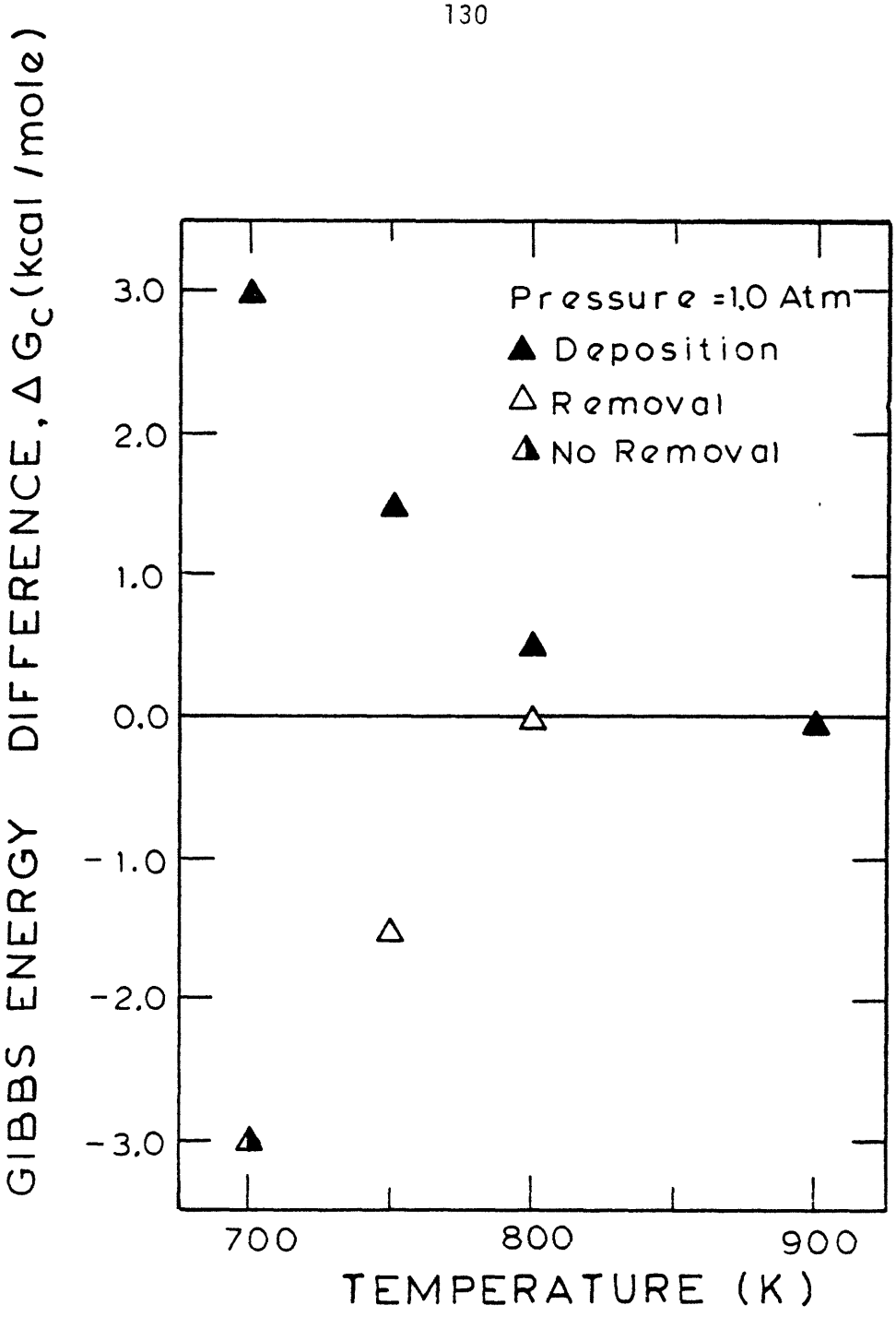

Figure 4-9 Carbon Deposition and Removal Boundary for an O/H = 0.5 Over Cobalt

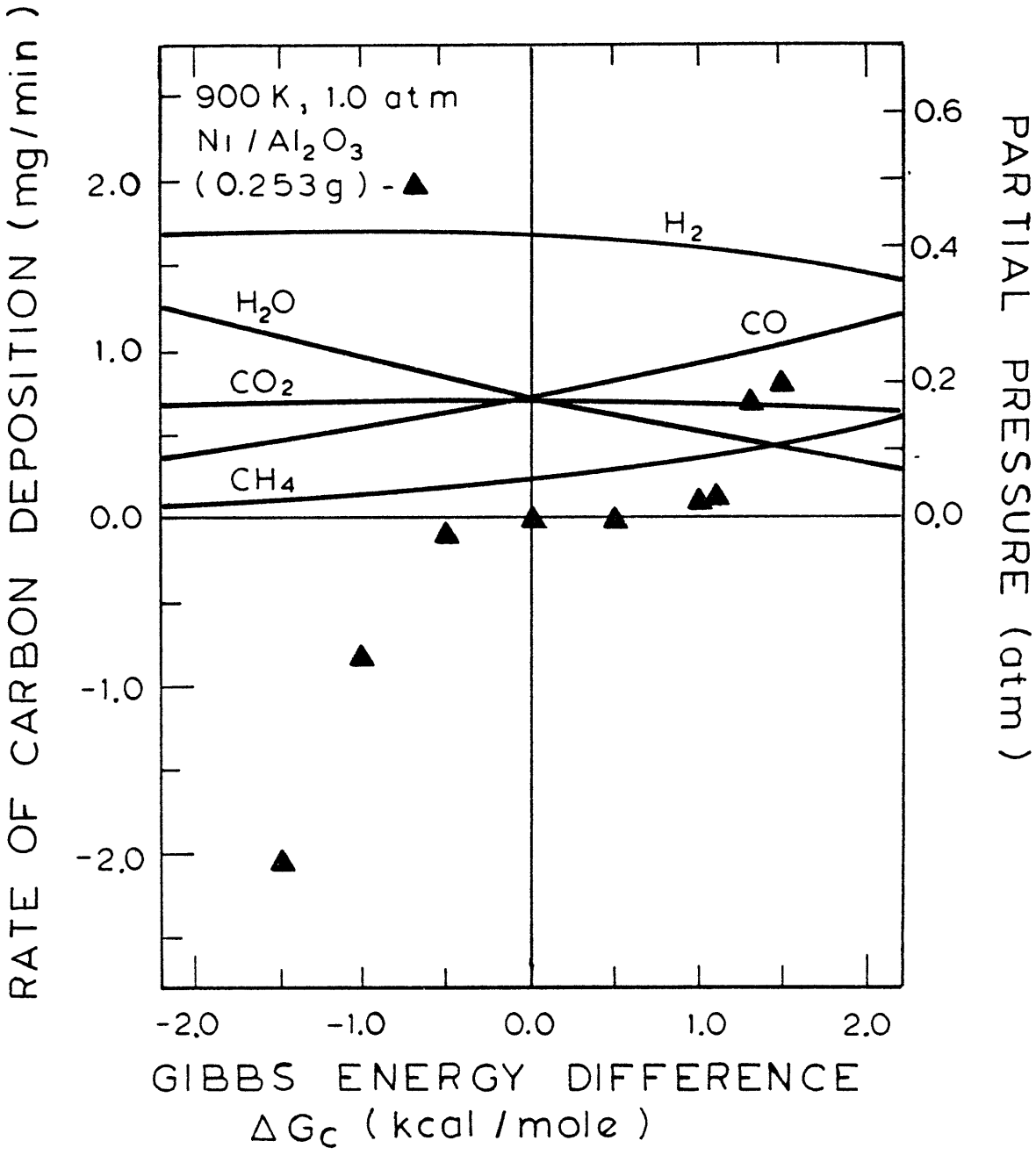

Figure 4-10 Rate of Carbon Deposition as a Function of ΔG_c for an O/H = 0.5

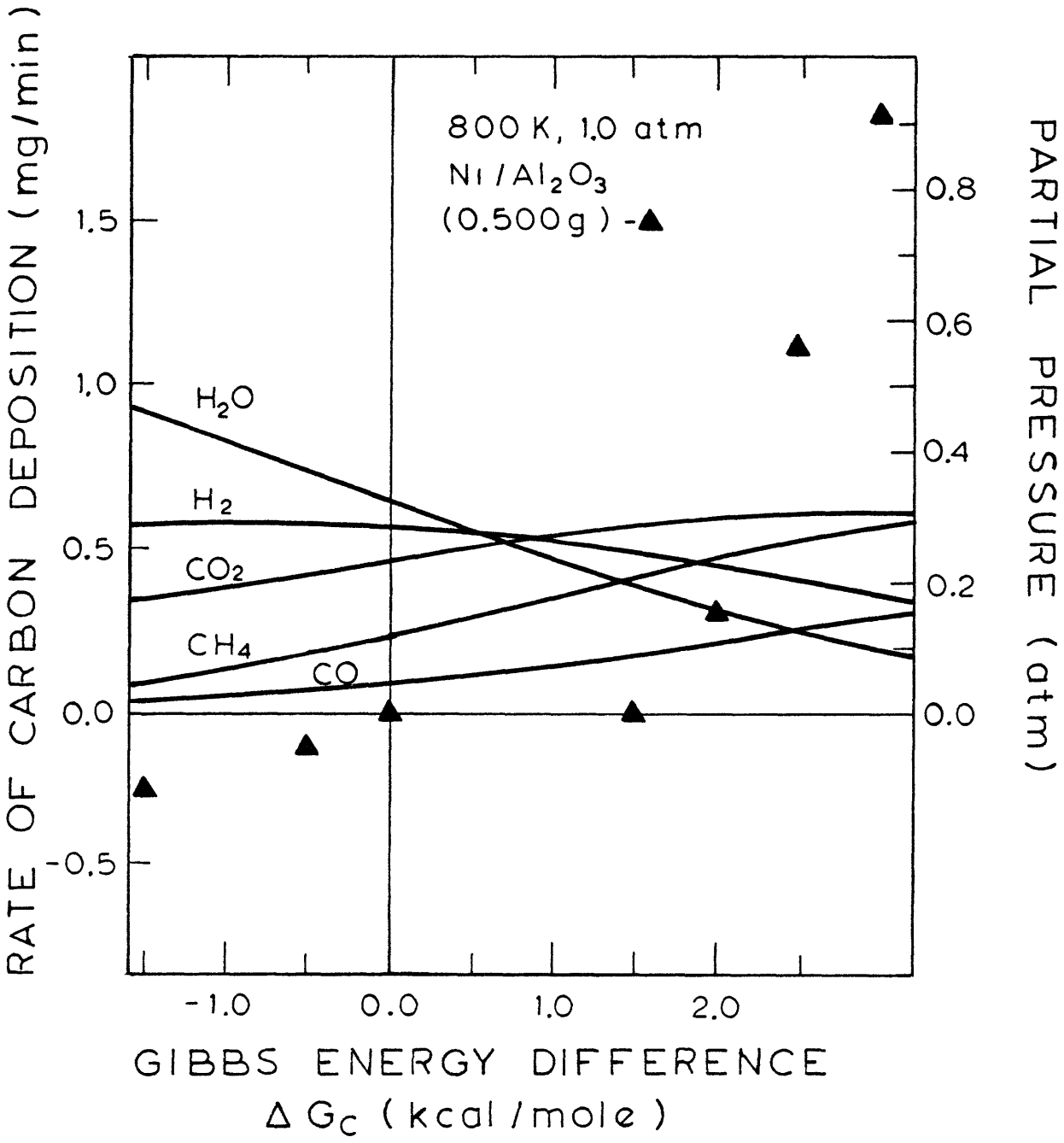

Figure 4-11 Rate of Carbon Deposition as a Function of ΔG_c for an O/H=0.5

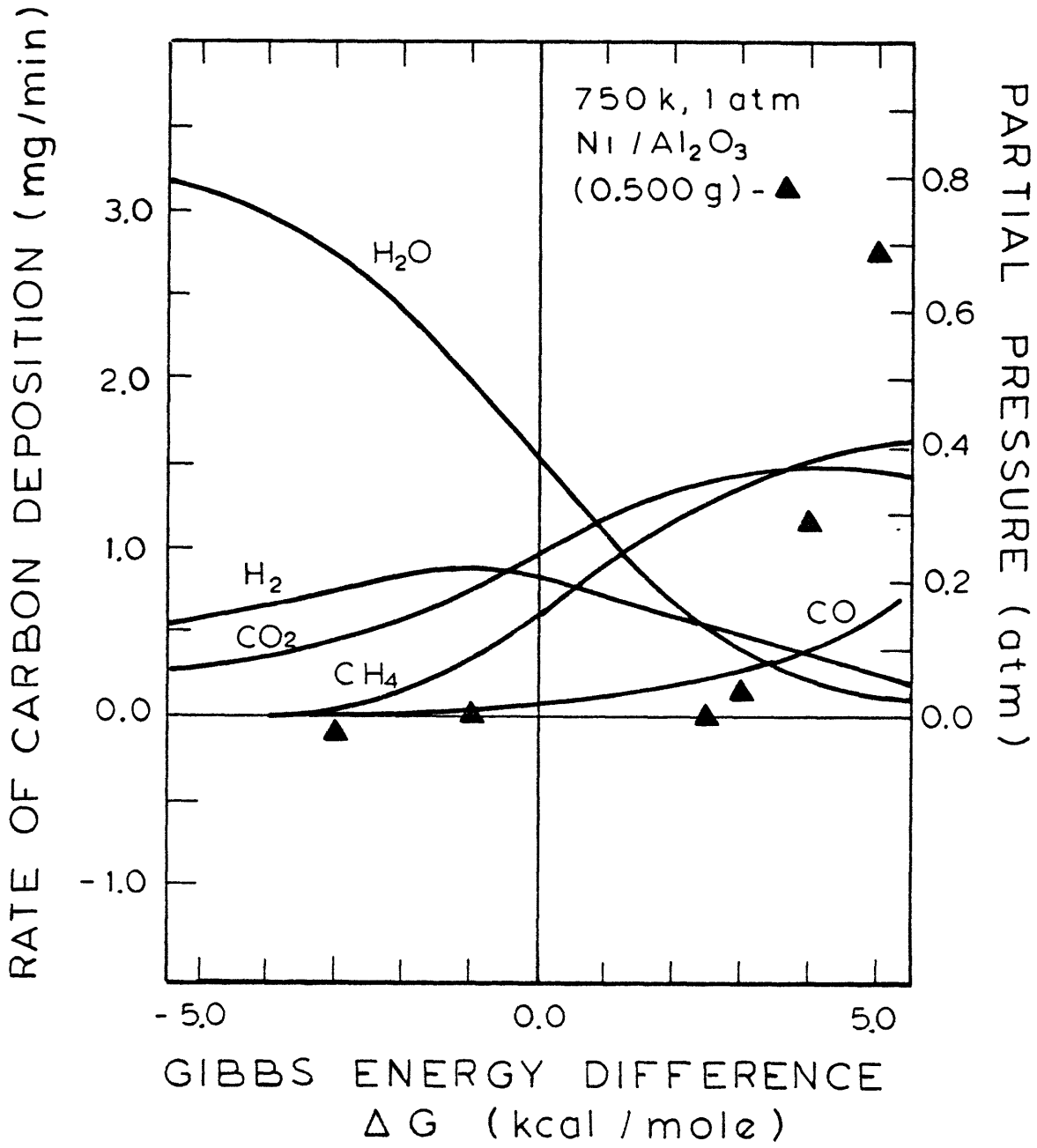

Figure 4-12 Rate of Carbon Deposition as a Function of ΔG_c for an O/H = 0.5

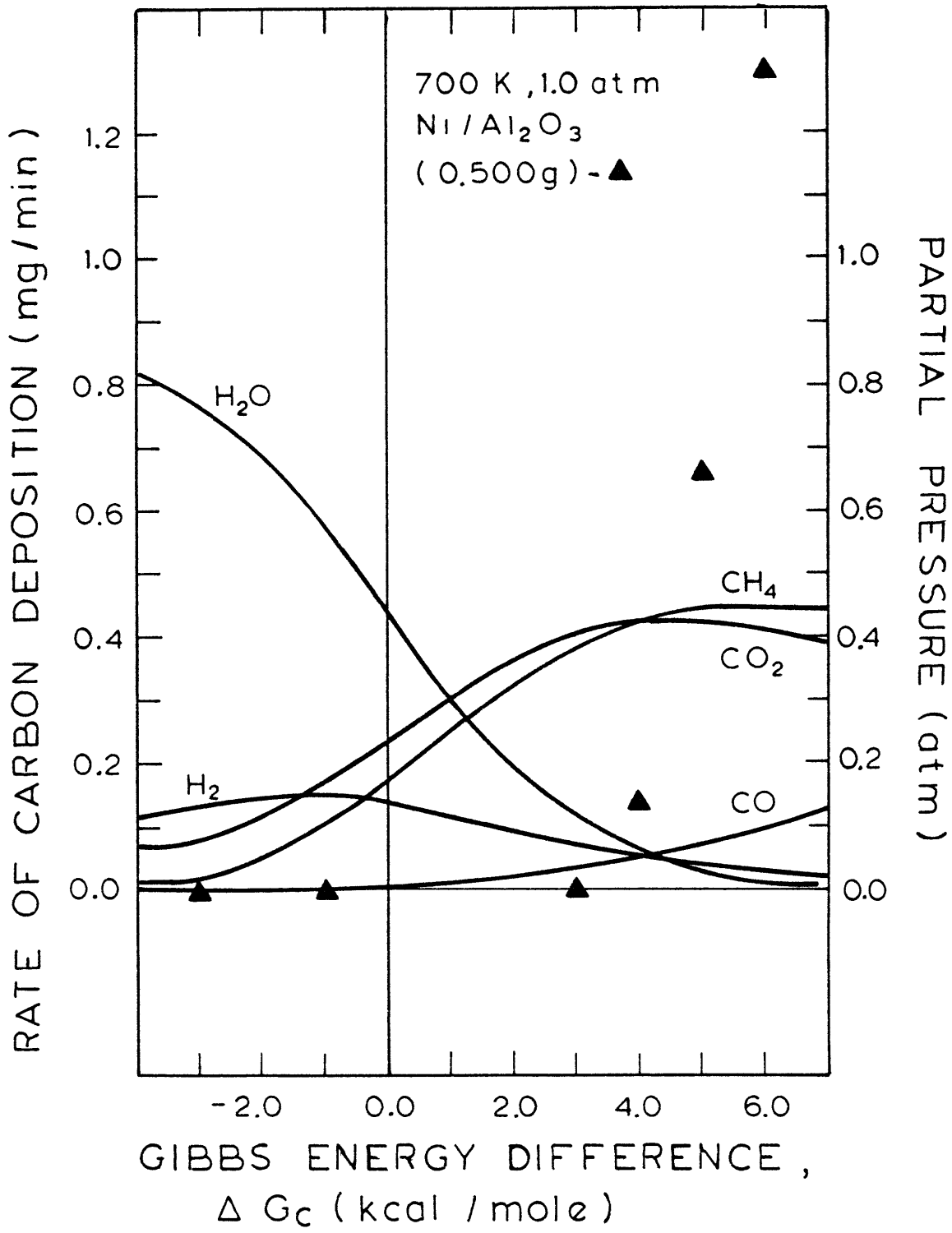

Figure 4-13 Rate of Carbon Deposition as a Function of ΔG_c for an O/H = 0.5

for the O/H ratio of 0.5. The results are similar to those found over cobalt, but the ΔG_c at which carbon deposition ceased is somewhat different, i.e., it is 0.5, 1.5, 2.5, and 3.0 kcal/mole at temperatures of 900, 800, 750, and 700K, respectively. Carbon removal is observed to begin at -0.3, 0.0, about -2.0 kcal/mole, at temperatures of 800, 900, and 750K, respectively. At a temperature of 700K, carbon removal was not observed even at a low ΔG_c of -3.0 kcal/mole. These results are shown in Figure 4-14

The results presented show that the rate of carbon deposition became zero prior to the graphite equilibrium. As can be seen, these results follow the general trend of Dent (1945) (Figure 2-10), and Rostrup-Nielsen (1972) (Figure 2-11). Both these studies employed nickel catalysts. It is observed that, at high temperature, the assumption that there is equilibrium with graphite is reasonable, at low temperature, the carbon appears to have a higher Gibbs energy. The interesting thing to note is that although the slope of the rate versus ΔG_c curve about the equilibrium point would be expected to be non-zero, in many of the experiments carbon removal was not observed until gas mixtures with ΔG_c values much less than zero were passed over the catalyst. This is similar to results which Manning (1976) and Sacco (1977) observed. In their experiments, carbon deposition was observed only on the iron side of the iron-iron oxide-gas phase boundary. On the oxide side, no removal of solid carbon was observed. Although oxidation of cobalt or nickel was shown not to occur from gas mixtures in the vicinity of the graphite-gas phase boundary. (Section 2.2.1), the existence of carbides has been shown quite conclusively (Section 2.2.3). Since the carbide-metal-gas phase boundary separates the regions of carbide and metal, the carbide region being richer in carbon depositing gases, it is possible that the active catalyst for carbon deposition is a carbide.

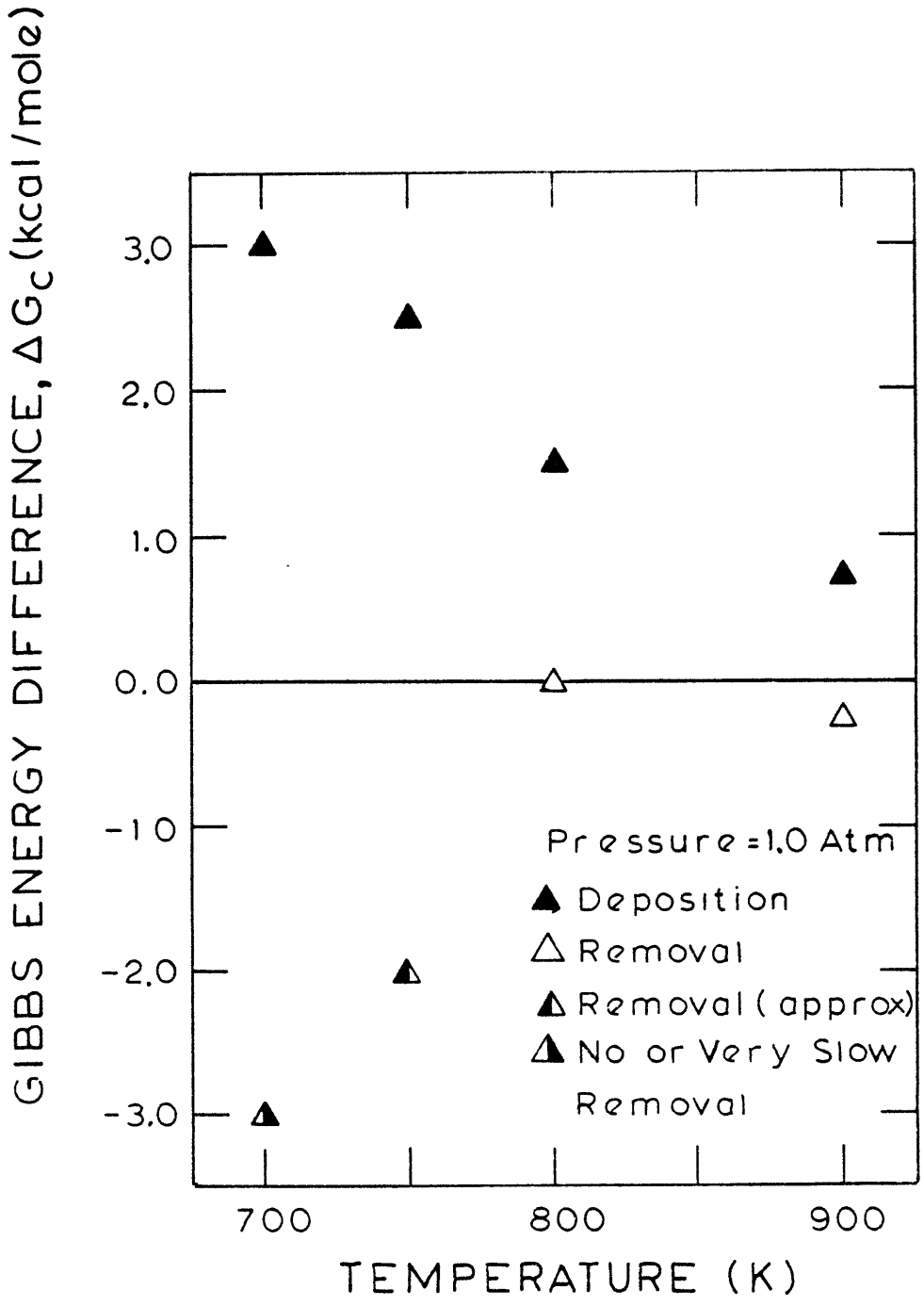

Figure 4 -14 Carbon Deposition and Removal Boundary for an O/H = 0.5 Over Nickel

4.2.2 Equilibrium Studies at Various Compositions and Temperatures

Equilibrium studies were run at O/H ratios other than 0.5 over cobalt and nickel. Specifically, those of 0.0 (CH_4-H_2-C), 0.17, 1.5 and ∞ (CO-CO_2-C) were studied. The temperatures again were 900, 800, 750 and 700K. The results with cobalt are presented in Figures 4-15 through 4-26 and are similar to those at an O/H ratio of 0.5. In Figure 4-27, the value of ΔG_c where carbon begins to deposit (or remove) is plotted versus temperature. For the methane-hydrogen mixtures (O/H=0.0), the % CH_4 is labled on the upper abscissa, for carbon monoxide-carbon dioxide (O/H=∞), % CO.

Two important features can be observed in Figure 4-27. First, the carbon deposition boundary is essentially independent of the gas species O/H ratio studied. This indicates that the Gibbs energy of the carbon (or carbide), at a given temperature, is independent of the gas phase composition. The figures which have been presented showing the experimentally observed rate of carbon deposition as a function of the parameter ΔG_c, indicate that bulk carbon is being formed. This follows from the fact that the amount of carbon present in carbide is about 5 wt %. Although the carbon actually formed experimentally could have a different Gibbs energy than graphite, the carbon deposition boundary could coincide with the carbide-metal-gas equilibrium as discussed at the end of the previous section.

Also plotted in Figure 4-27 is the point at which carbon removal begins. Since more experiments were made on the carbon deposition side, the point at which carbon removal begins is not as well determined. In some cases the point has been found by extrapolation of a few points. Figure 4-27 also indicates the temperatures and O/H ratios for systems where no carbon removal was observed even for the lowest value of ΔG_c studied.

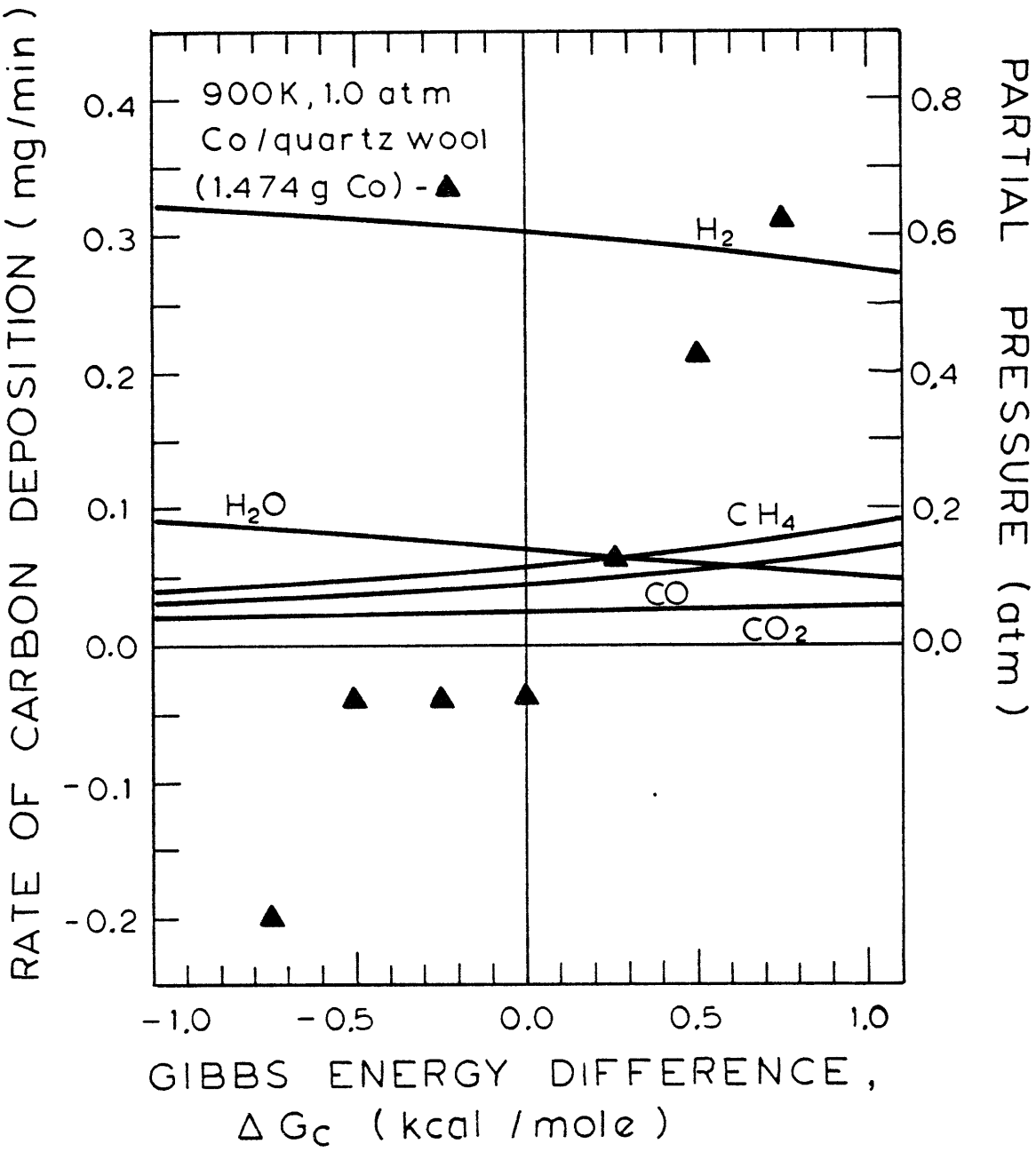

Figure 4-15 Rate of Carbon Deposition as a Function of ΔG_c for an O/H = 0.17

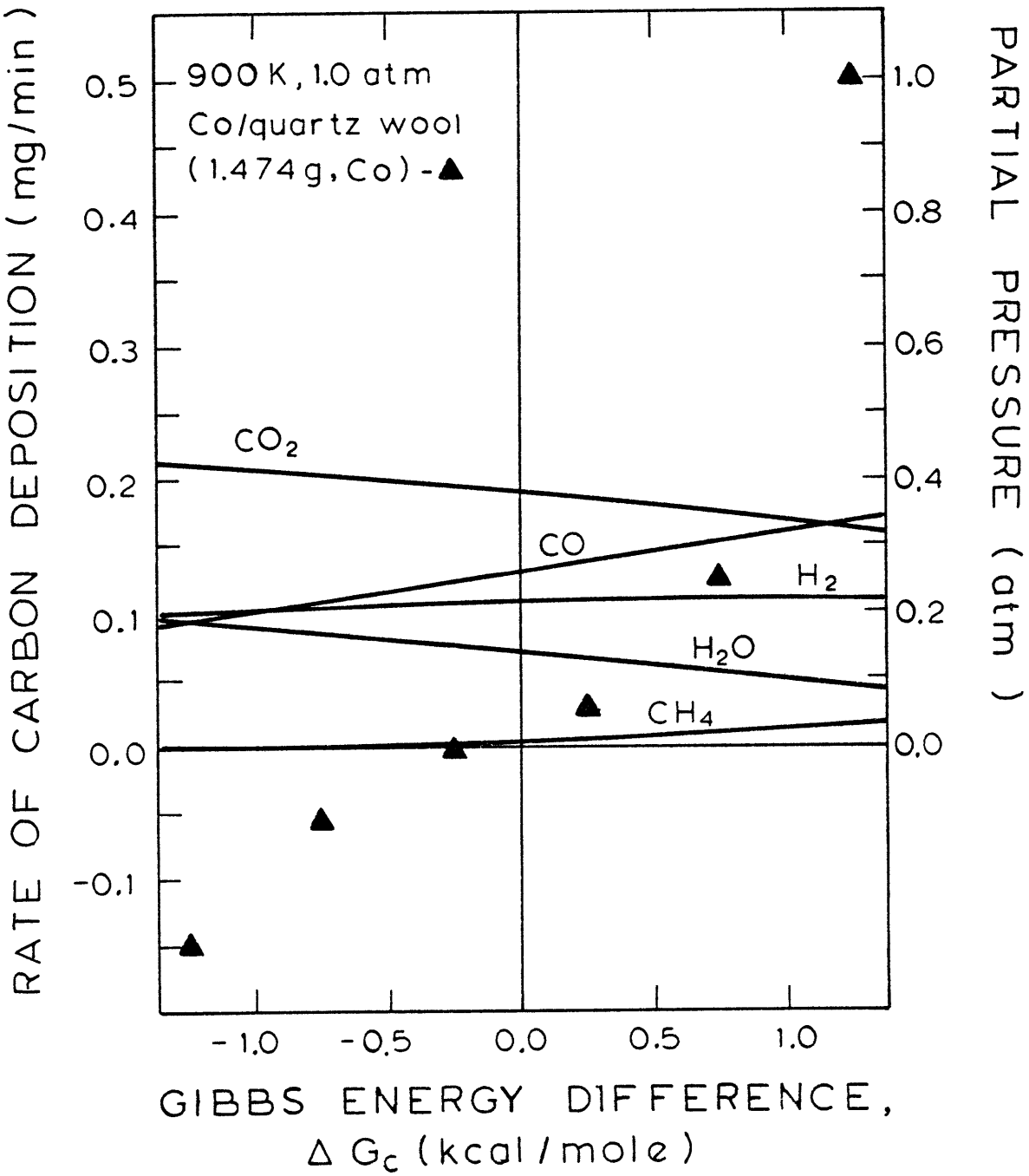

Figure 4-16 Rate of Carbon Deposition as a Function of ΔG_c for an O/H = 1.5

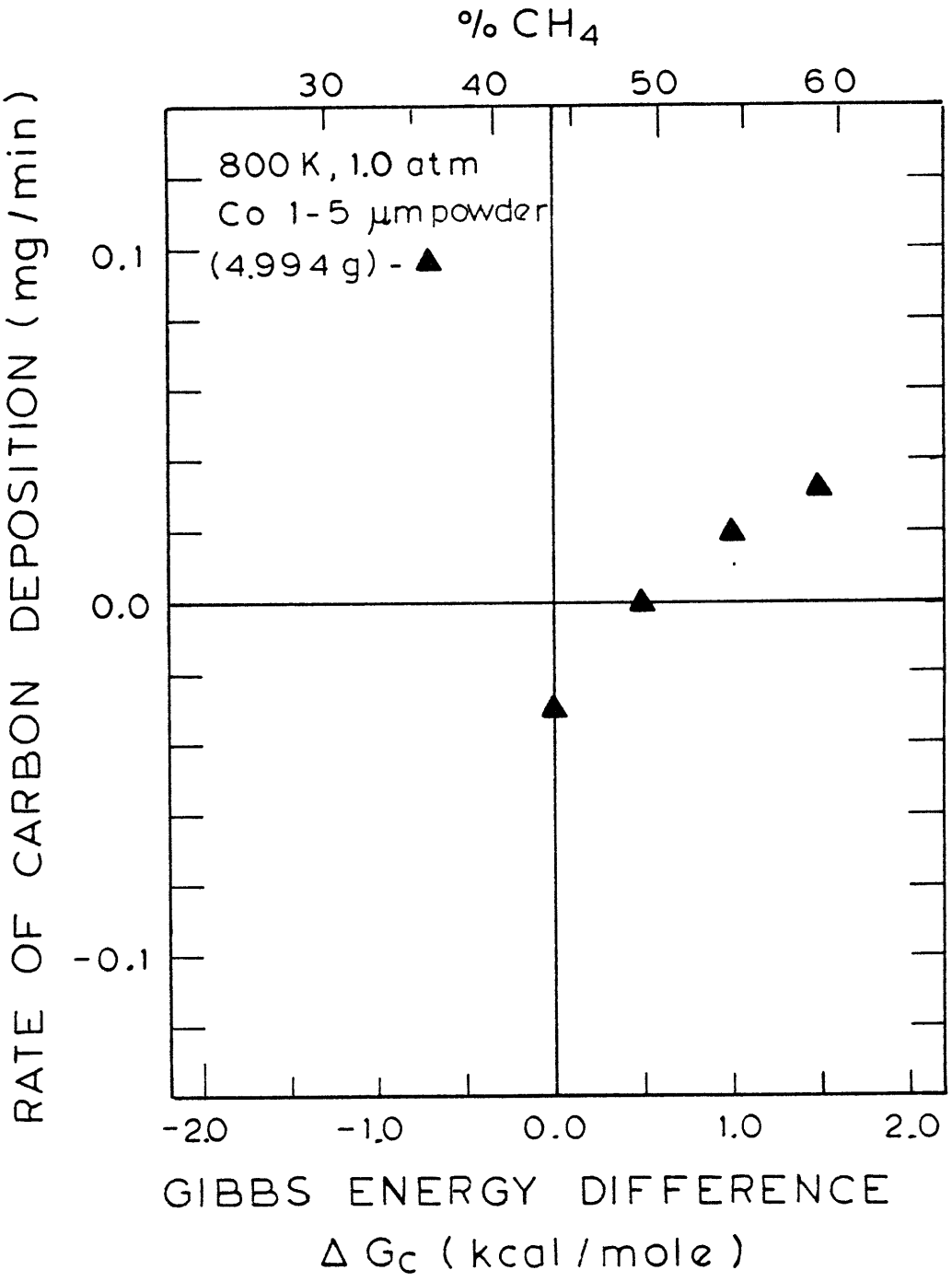

Figure 4-17 Rate of Carbon Deposition as a Function of ΔG_C for CH_4-H_2 Mixtures

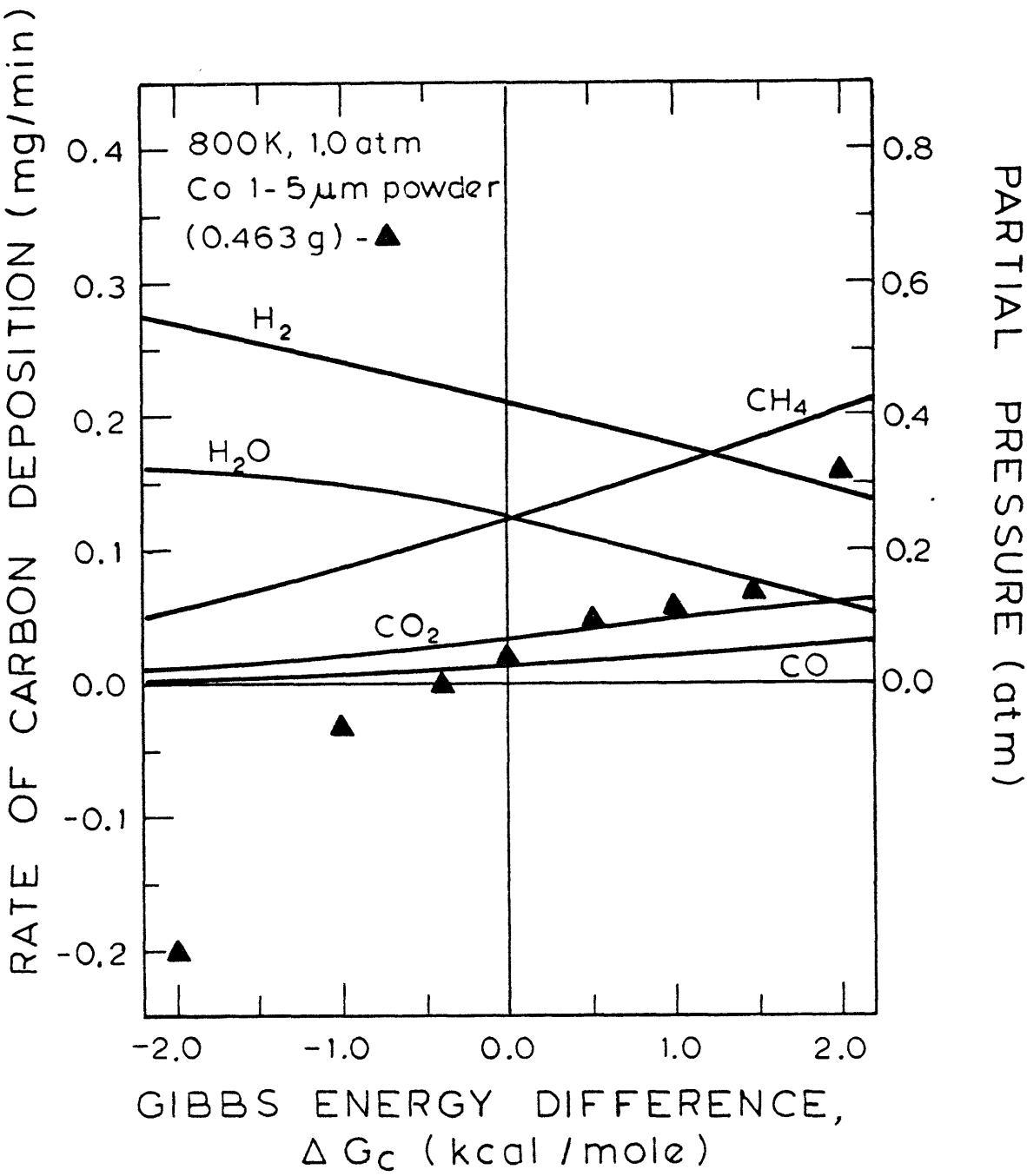

Figure 4-18 Rate of Carbon Deposition as a Funtion of ΔG_C for an O/H = 0.17

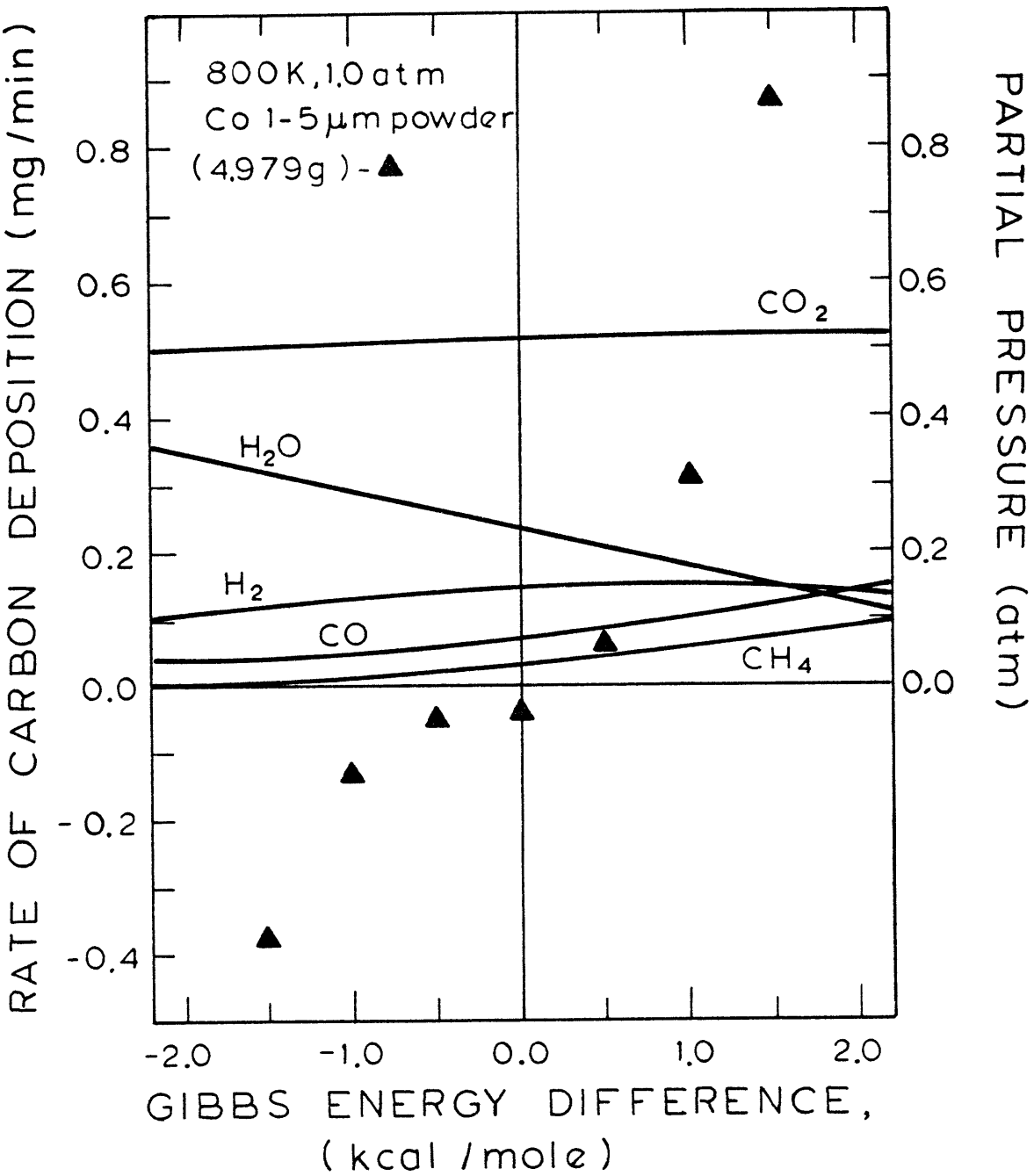

Figure 4-19 Rate of Carbon Deposition as a Function of ΔG_C for an O/H = 1.5

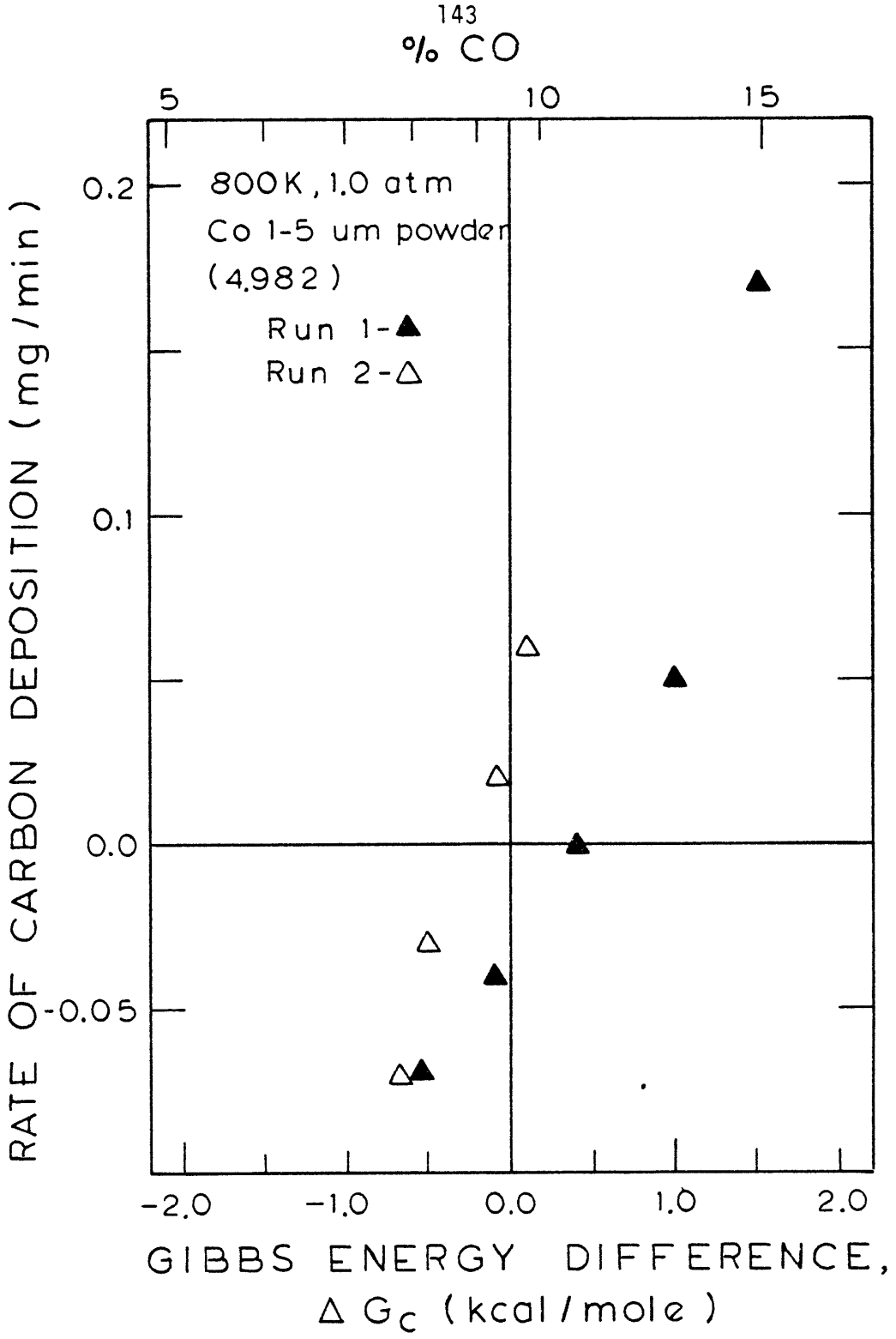

Figure 4-20 Rate of Carbon Deposition as a Function of ΔG_C for $CO-CO_2$ Mixtures

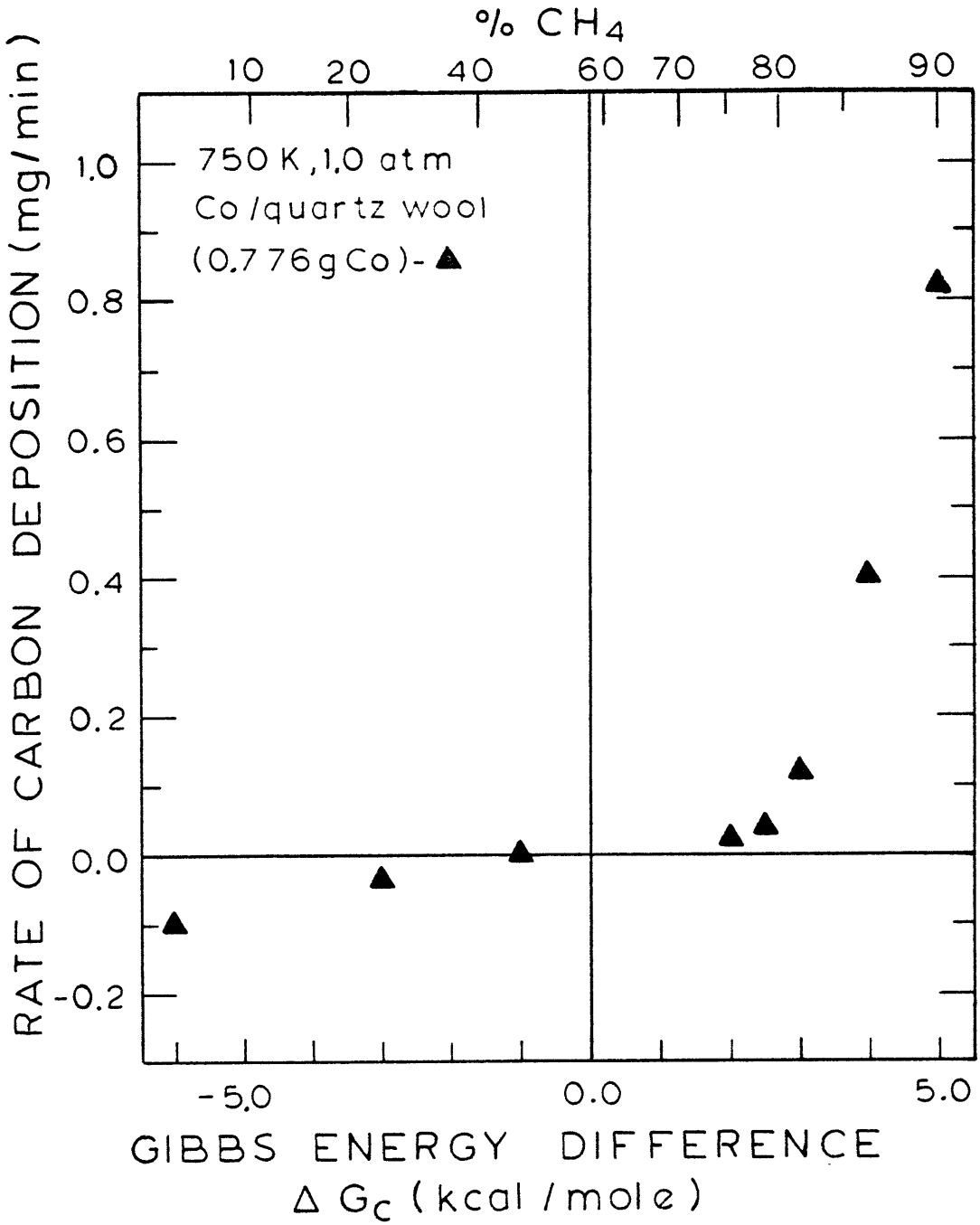

Figure 4-21 Rate of Carbon Deposition as a Function of ΔG_C for $CH_4 - H_2$ Mixtures

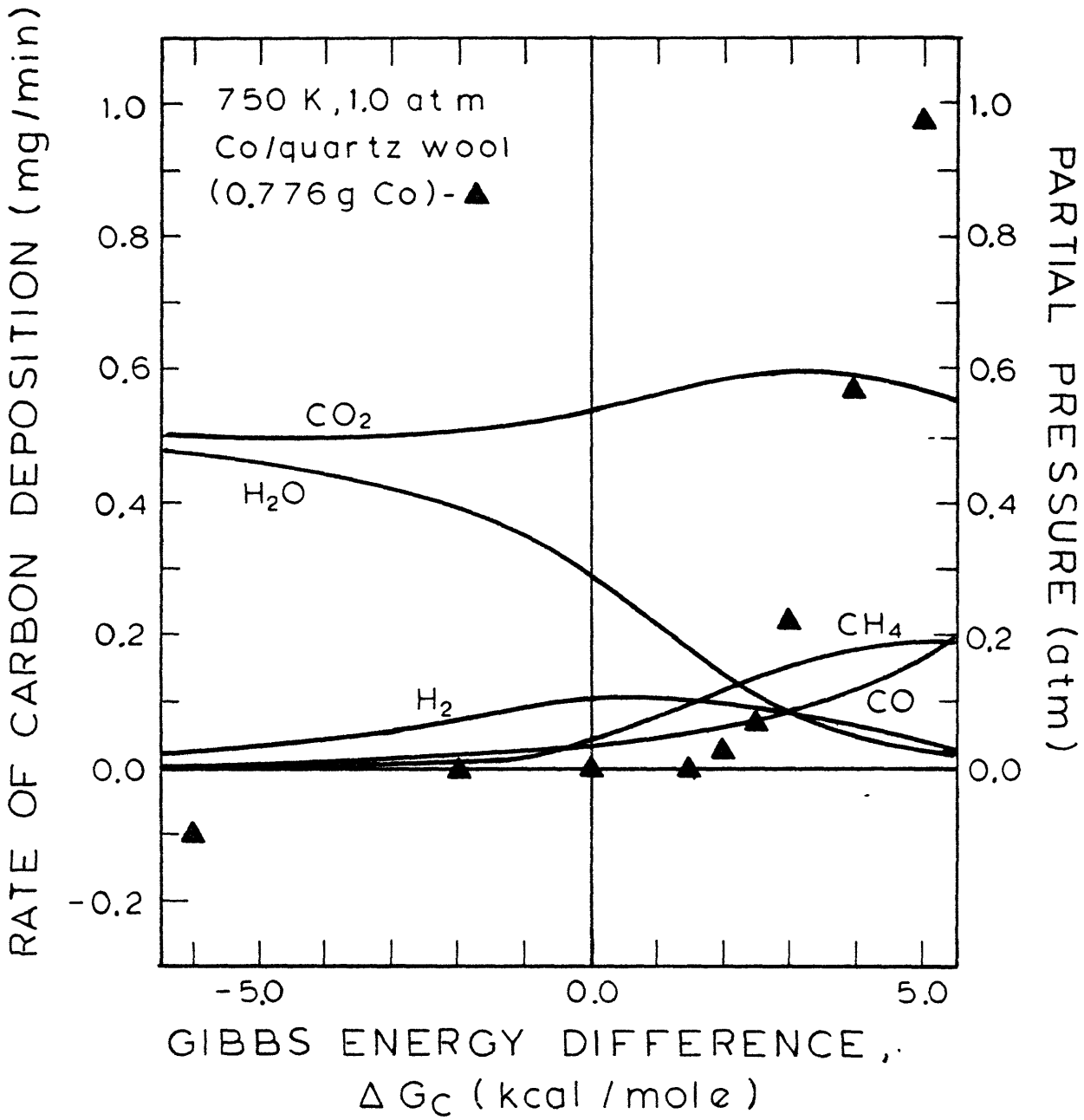

Figure 4-22 Rate of Carbon Deposition as a Function of ΔG_C for an O/H = 1.5

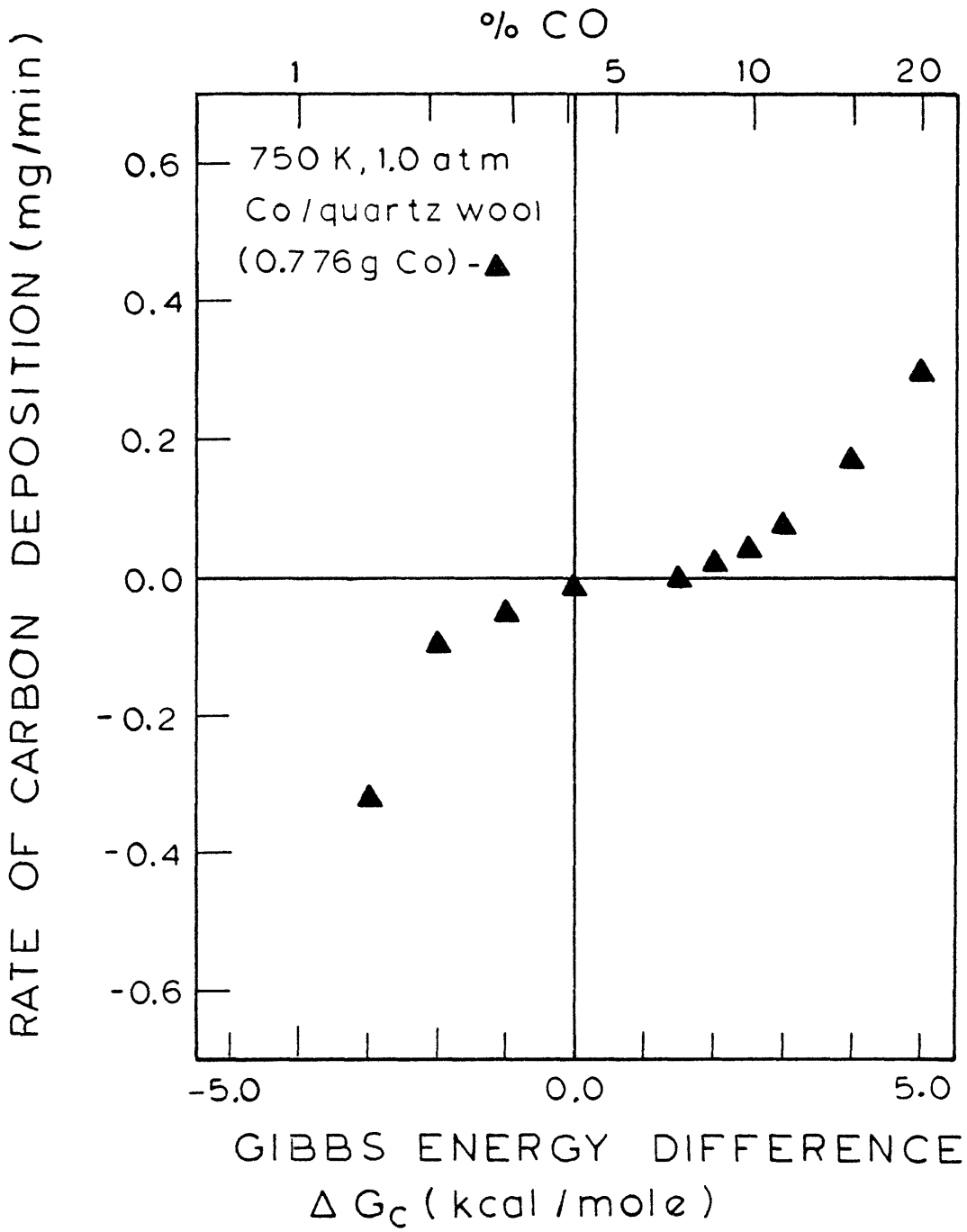

Figure 4-23 Rate of Carbon Deposition as a Function of ΔG_C for $CO-CO_2$ Mixtures

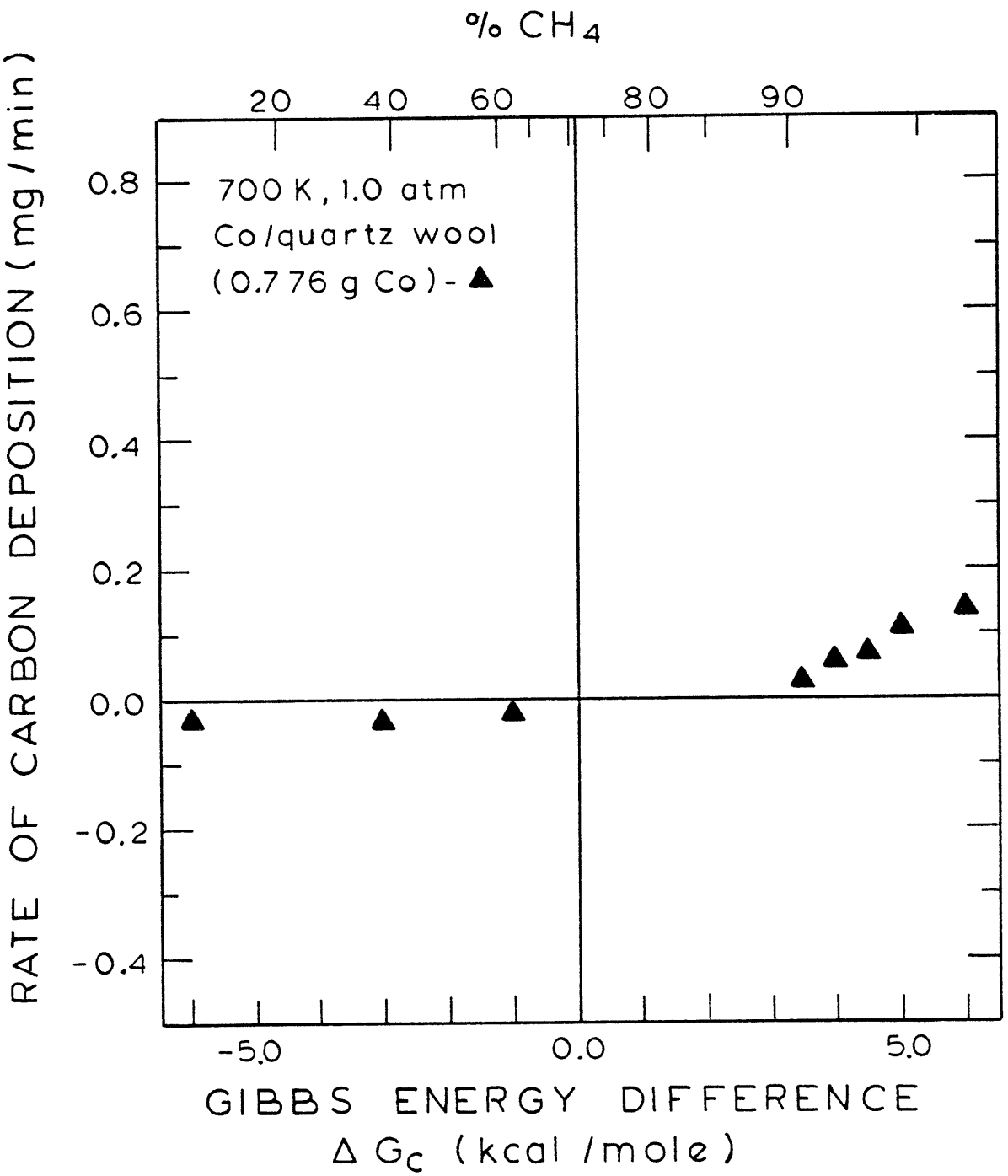

Figure 4-24 Rate of Carbon Deposition as a Function of ΔG_C for CH_4-H_2 Mixtures

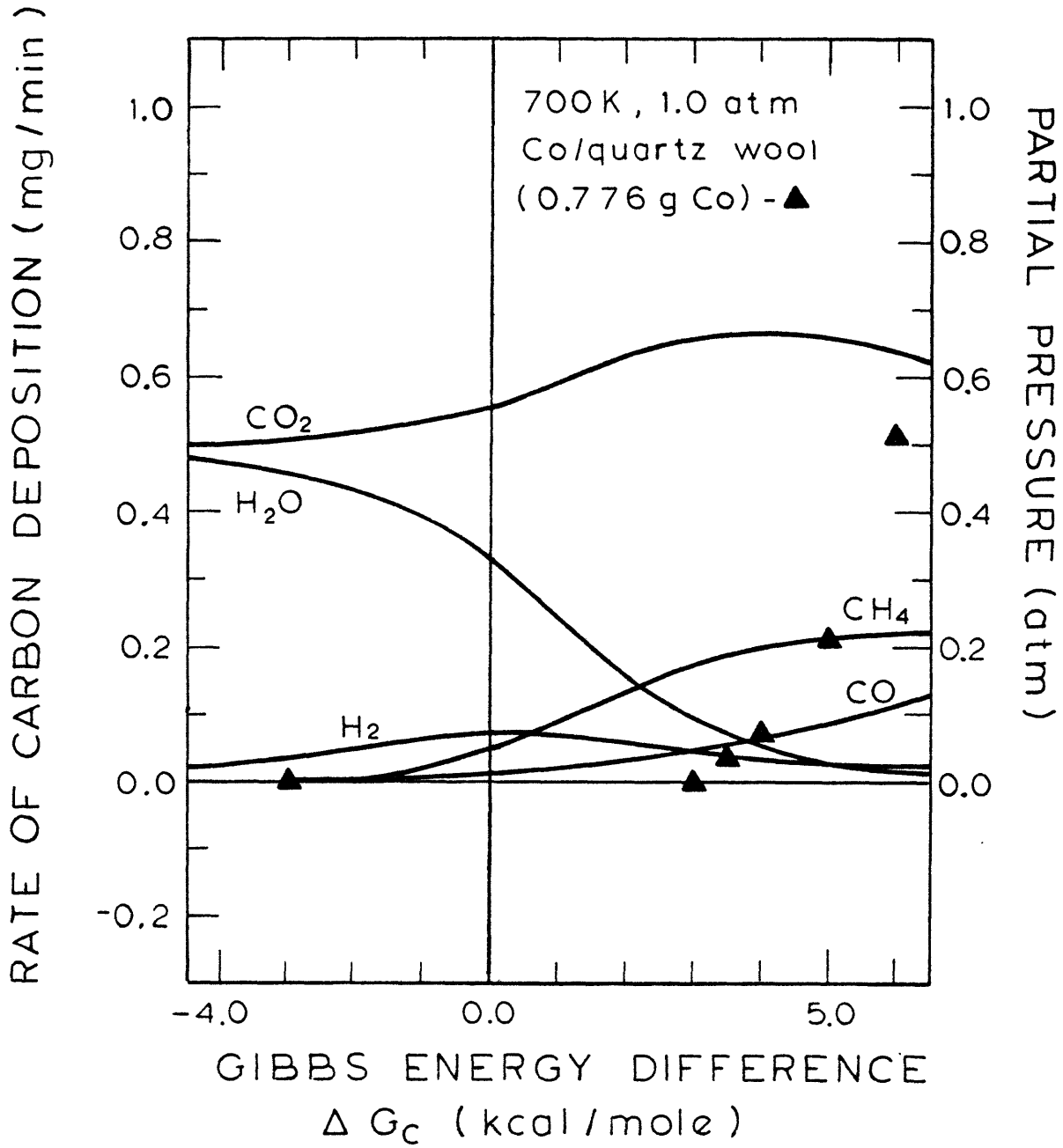

Figure 4-25 Rate of Carbon Deposition as a Function of ΔG_c for an O/H = 1.5

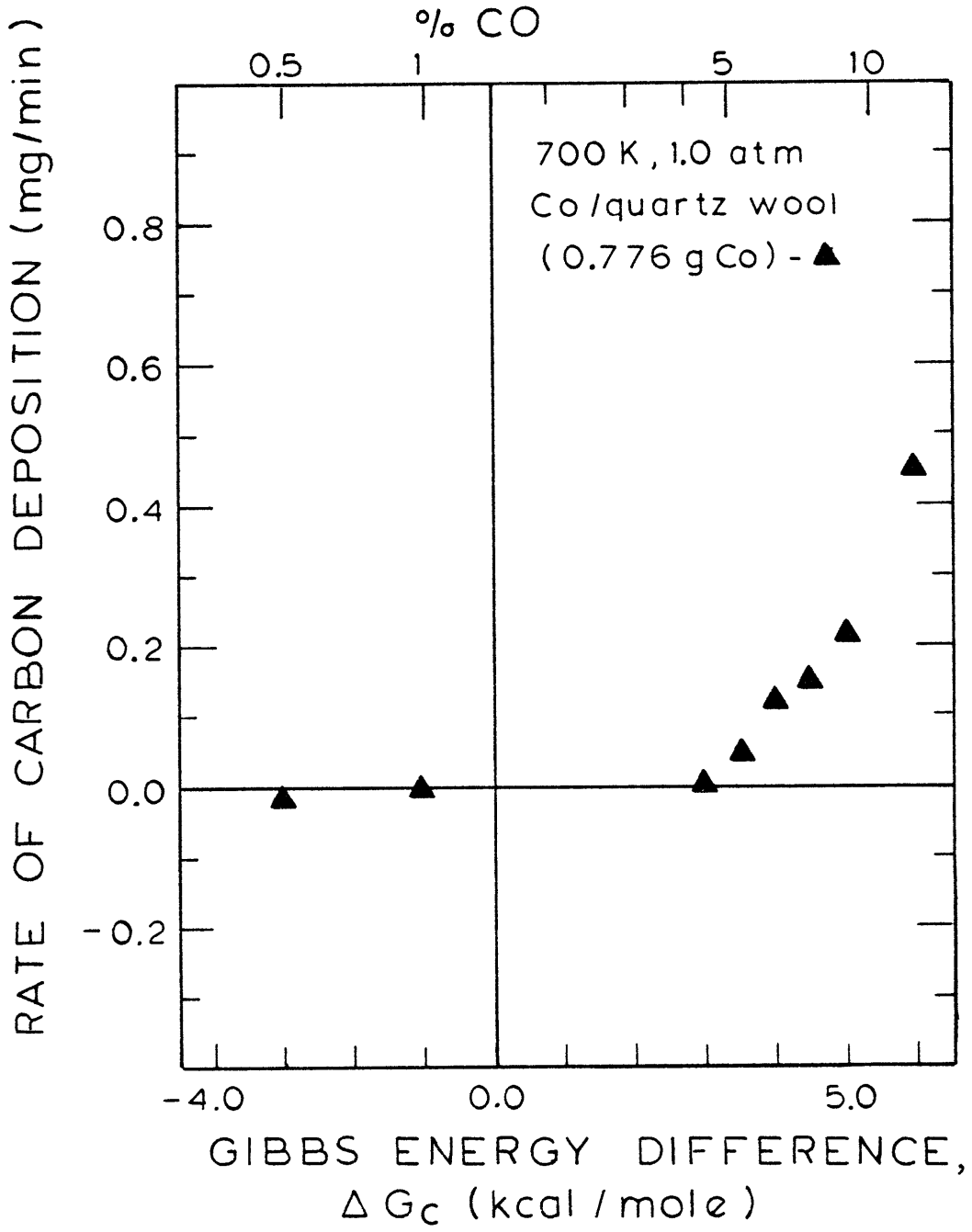

Figure 4-26 Rate of Carbon Deposition as a Function of ΔG_C for $CO-CO_2$ Mixtures

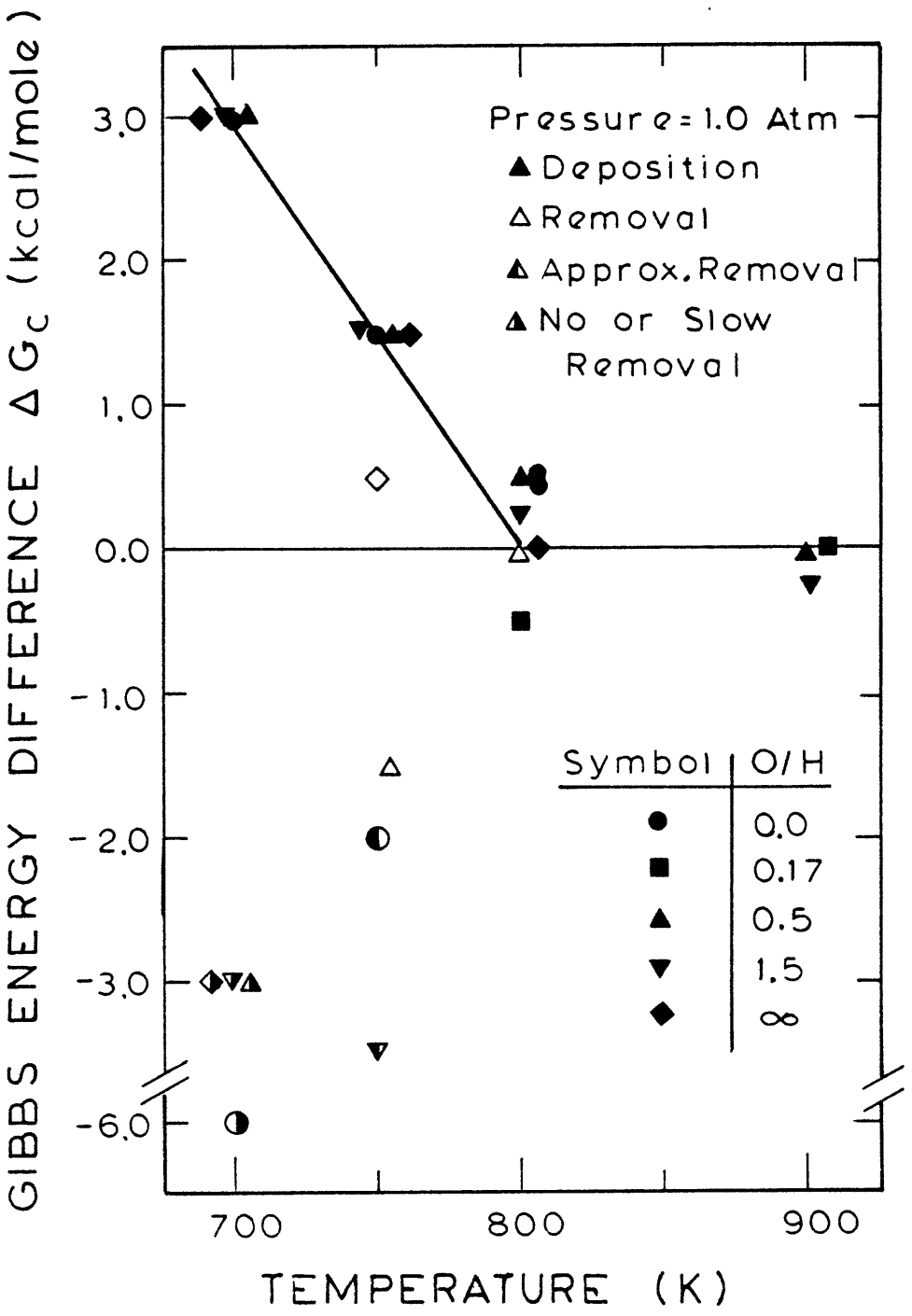

Figure 4-27 Carbon Deposition and Removal Boundary for Various O/H Ratios Over Cobalt

Figure 4-27 reveals that although there is no correlation of the ΔG_c, values are normally less than 0.0 kcal/mole. This would be expected for carbon removal in a system where graphite was the stable solid phase and the rates of the reaction of the gas phase with the solid were measurable.

Similar experiments were run over a nickel catalyst. The result are presented in Figures 4-28 through 4-38. ΔG_c at the carbon deposition and removal boundary, is graphed versus temperature in Figure 4-39. Although the data are not as consistant as in the cobalt system, it is observed that at a given temperature the carbon deposition boundary is still independent of the gas mixture studied. Again it is seen that carbon removal will only occur for gas mixtures with a ΔG_c less than 0.0 kcal/mole. It is also noted that carbon removal did not occur in any case at 700K except in the $CO-CO_2-C$ experiment. The lowest values of ΔG_c studied in this system are shown in the figure. Observation of the experimental data, such as in Figures 4-13, 4-36, 4-37,4-38 shows that at the lowest ΔG_c of each experiment, the gas mixture is composed mostly of carbon removing gases. To go to lower values of ΔG_c would not be expected to increase the rate of carbon removal.

4.2.3 A Discussion of the Equilibrium Results

In the iron-catalyzed Bosch process studied by both Manning (1976) and Sacco (1977), the iron-iron oxide-gas phase boundary was shown to correspond with the carbon deposition boundary and hence would determine the water concentration in that system. The inactivity of the iron oxide prevented the attainment of the higher water-concentration expected at the graphite-gas equilibrium. In other words, if iron oxide were active for the various carbon deposition reactions, the graphite-gas equilibrium should be reached. This has been discussed in detail in Section 2.1.

The experimental results presented in Section 4.2 clearly show that the

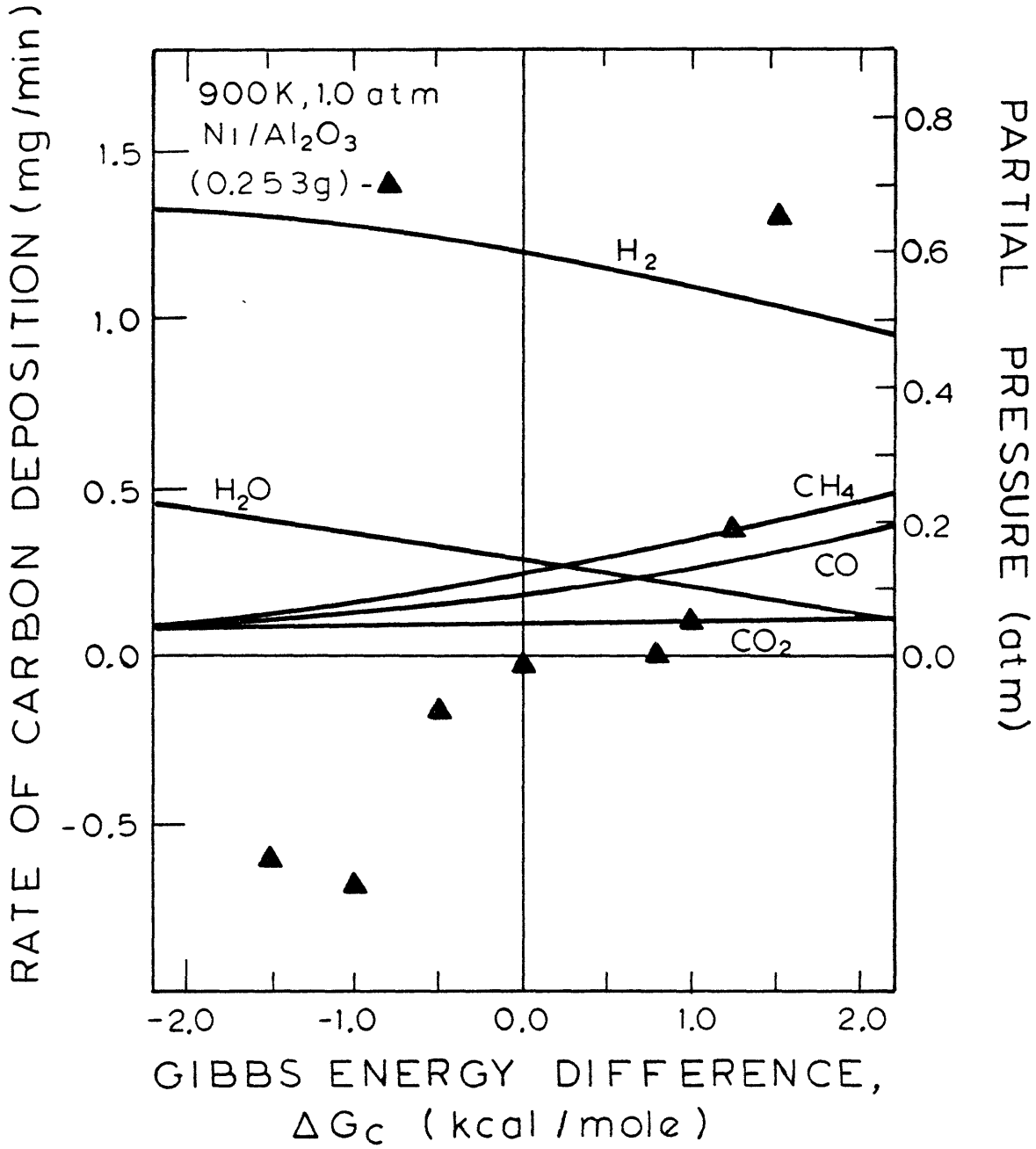

Figure 4-28 Rate of Carbon Deposition as a Function of ΔG_c for an O/H = 0.17

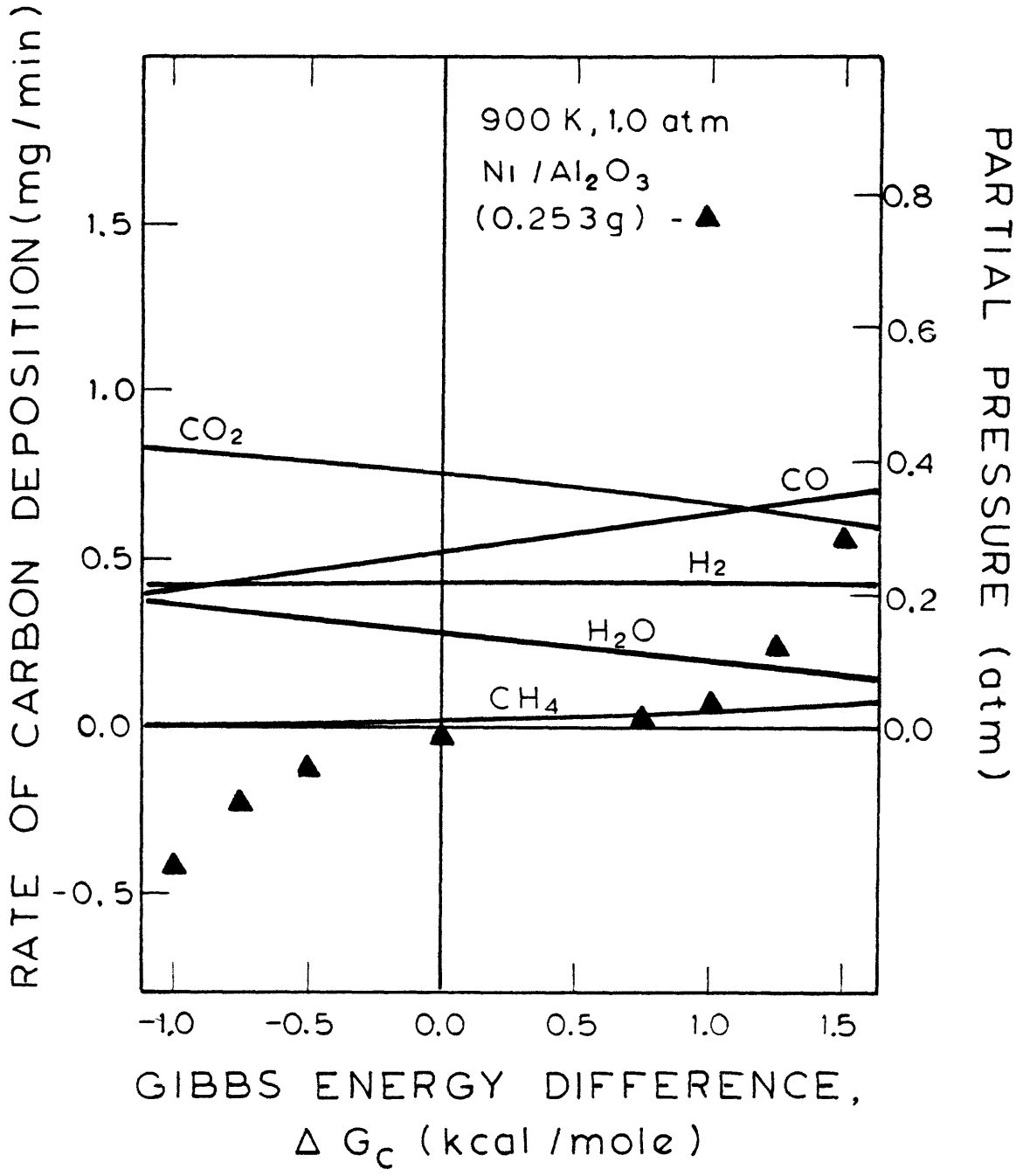

Figure 4-29 Rate of Carbon Deposition as a Function of ΔG_C for an O/H = 1.5

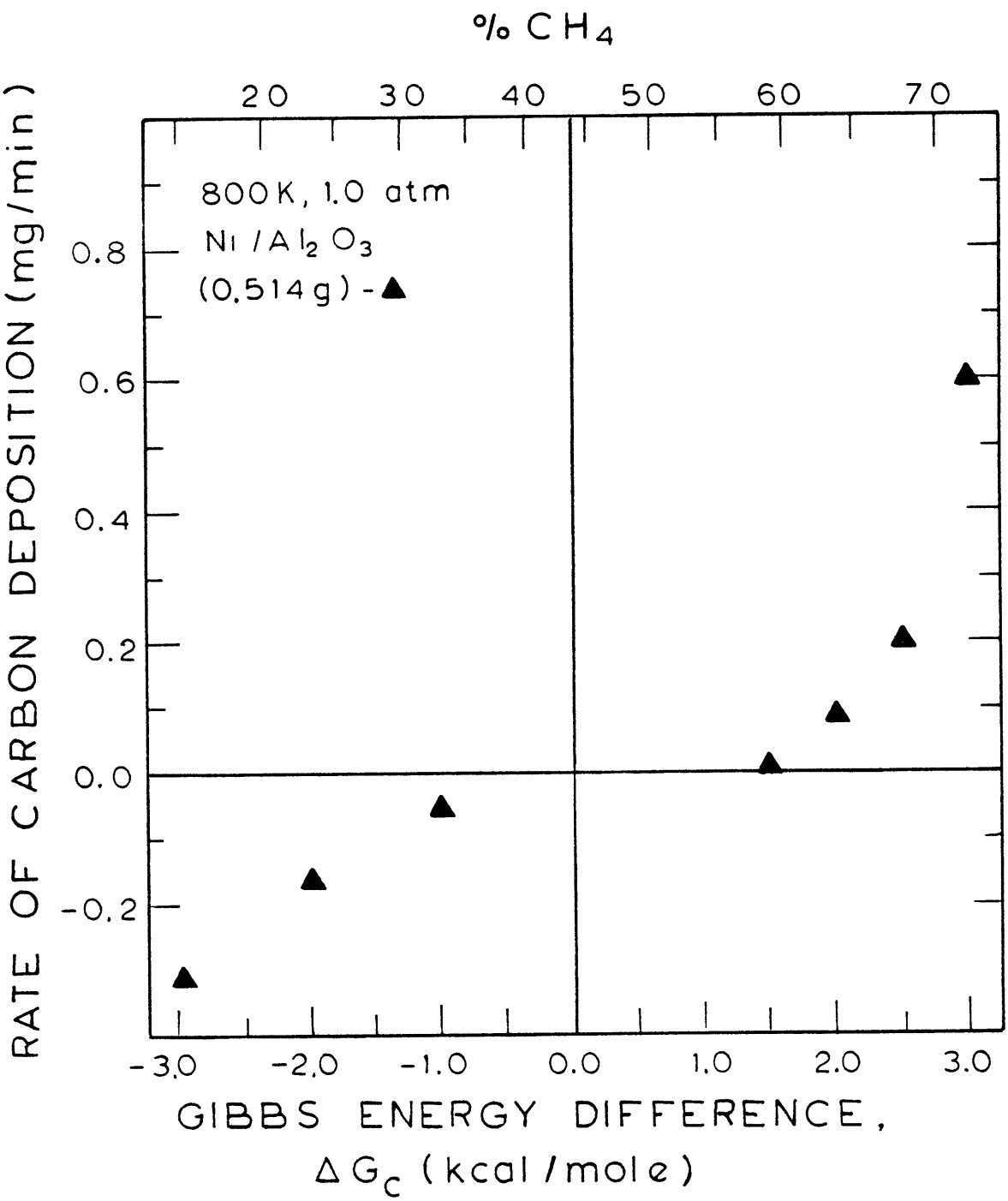

Figure 4-30 Rate of Carbon Deposition as a Function of ΔG_C for CH_4 - H_2 Mixtures

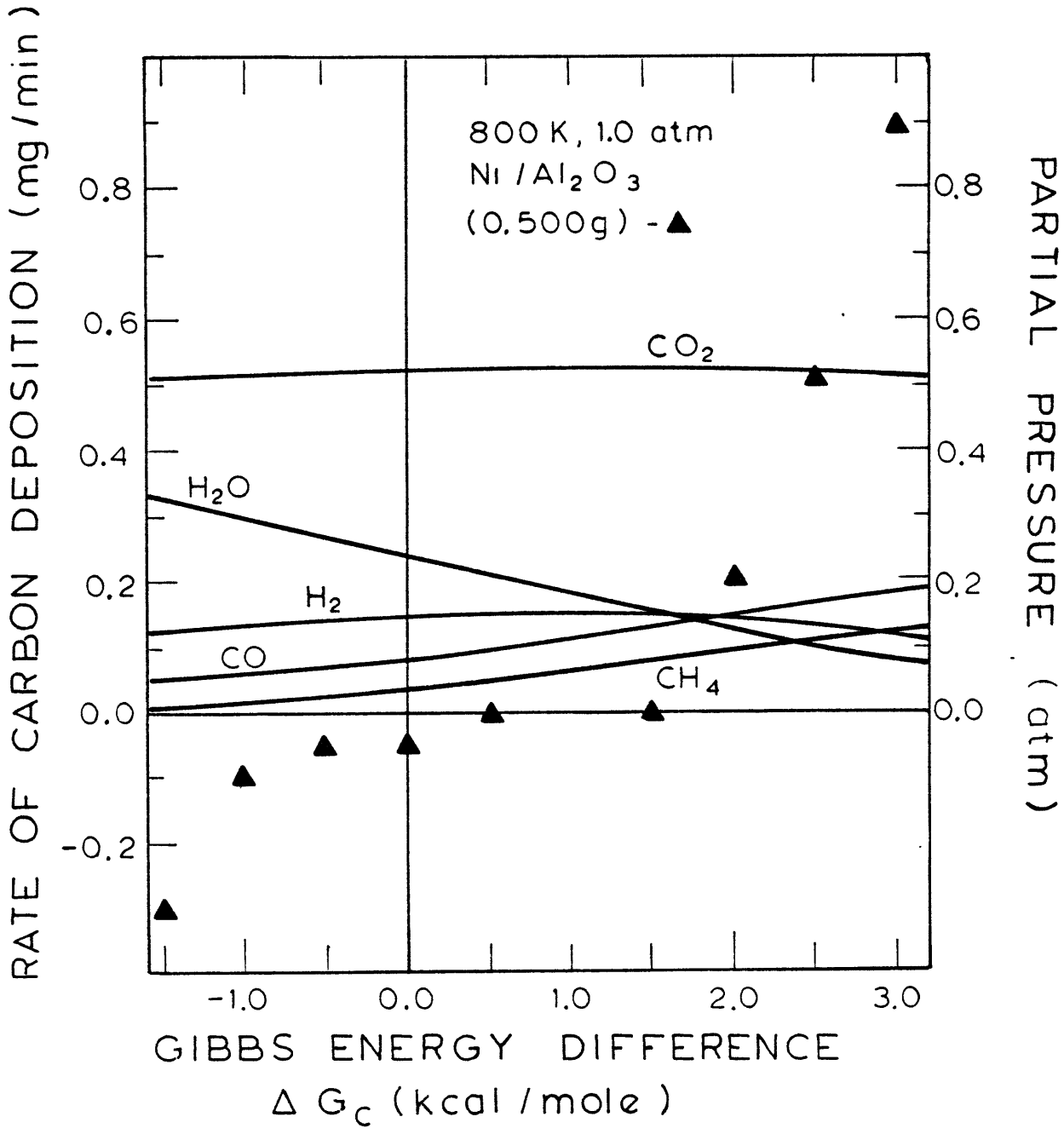

Figure 4-31 Rate of Carbon Deposition as a Function of ΔG_C for an O/H = 1.5

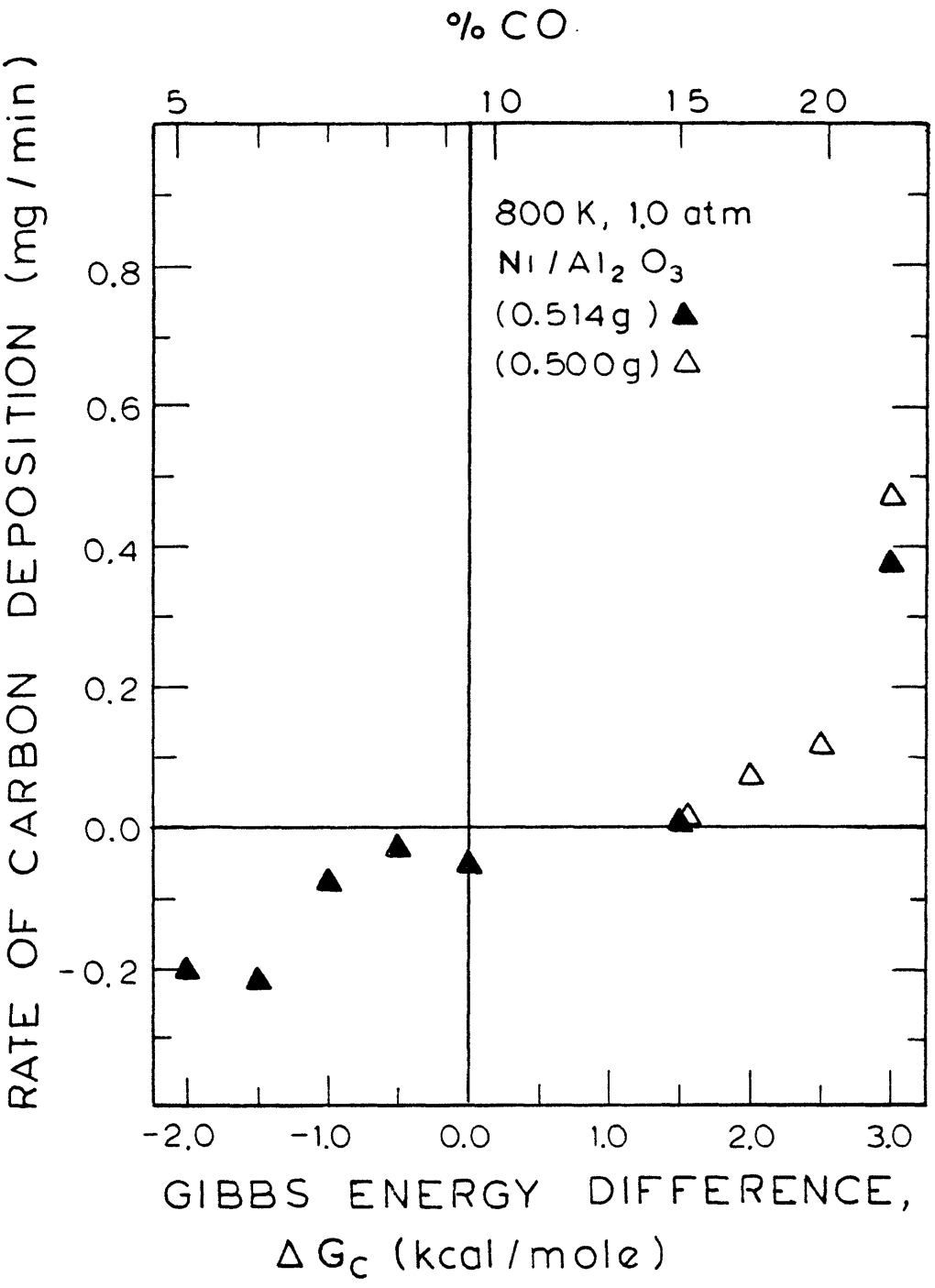

Figure 4-32 Rate of Carbon Deposition as a Function of ΔG_C for $CO - CO_2$ Mixtures

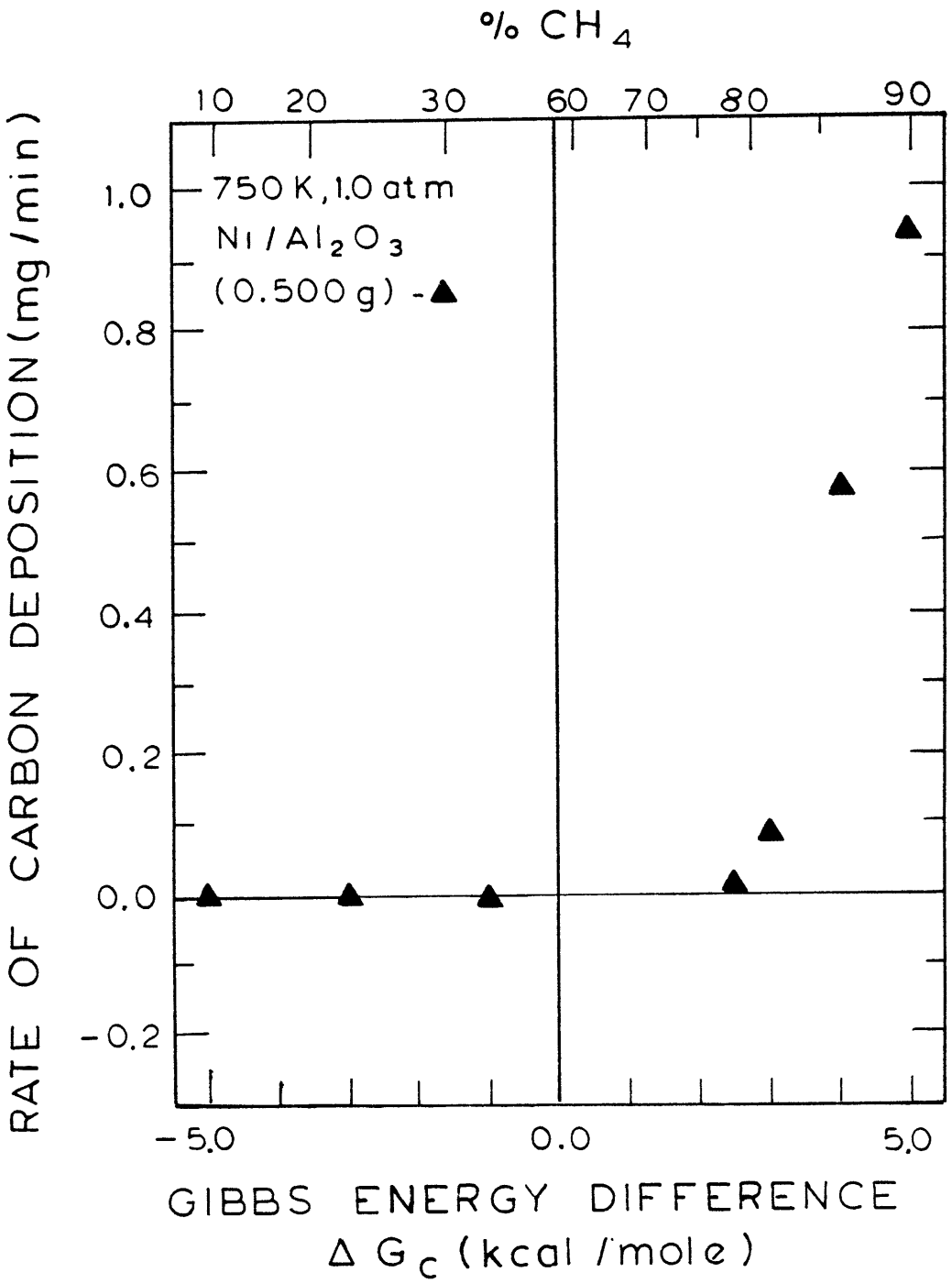

Figure 4-33 Rate of Carbon Deposition as a Function of ΔG_C for $CH_4 - H_2$ Mixtures

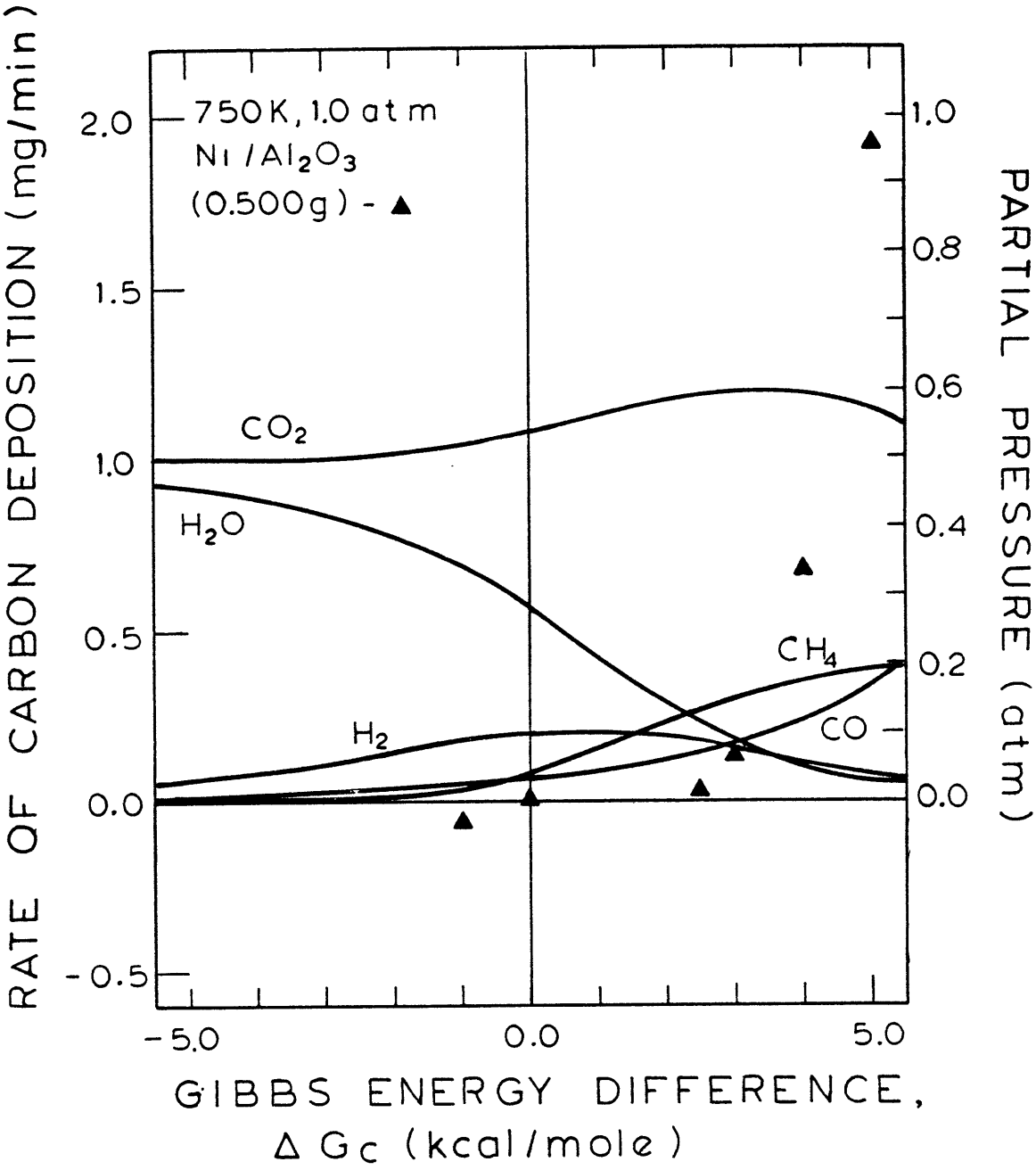

Figure 4-34 Rate of Carbon Deposition as a Function of ΔG_C for an O/H = 1.5

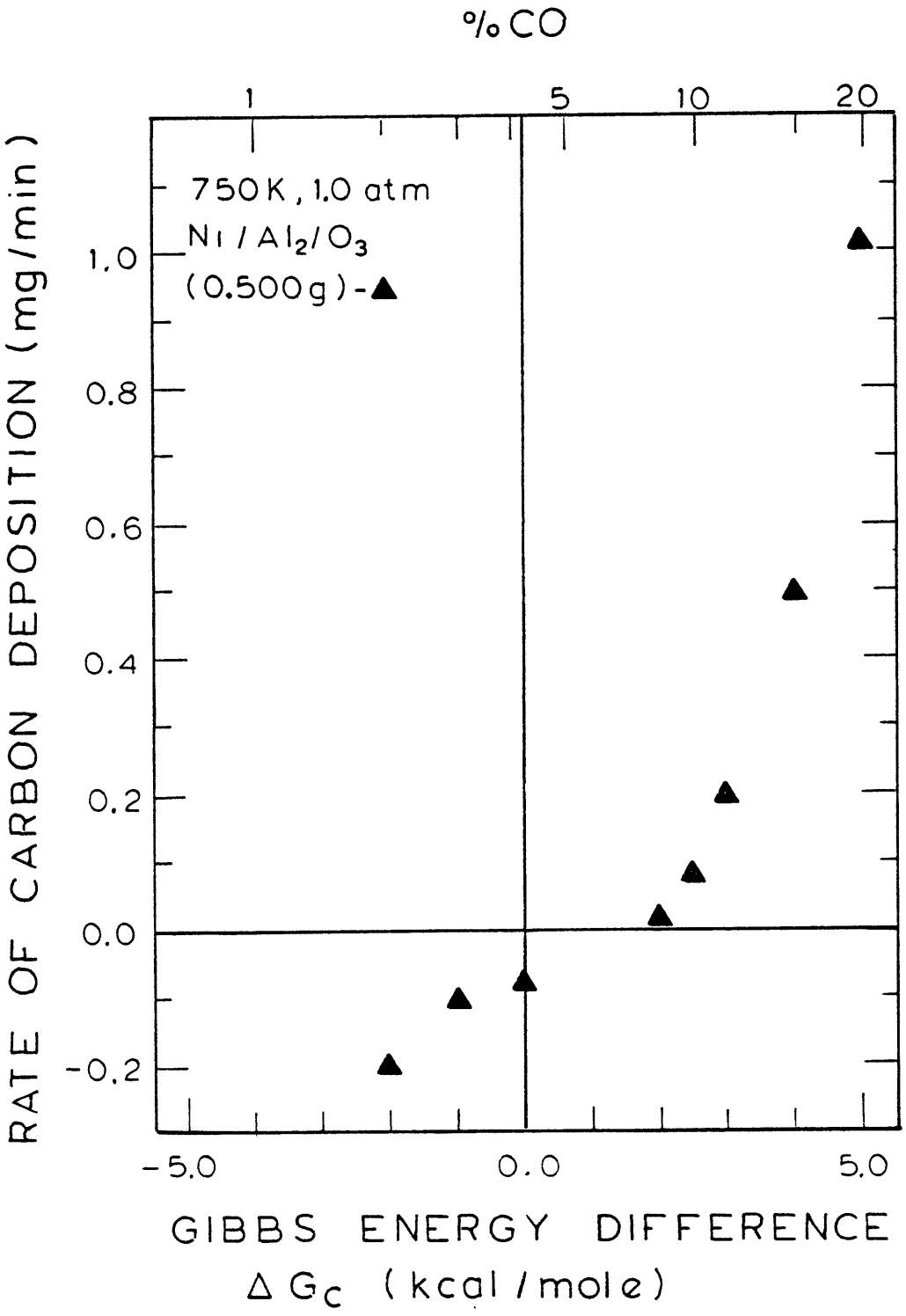

Figure 4-35 Rate of Carbon Deposition as a Function of ΔG_C for CO - CO_2 Mixtures

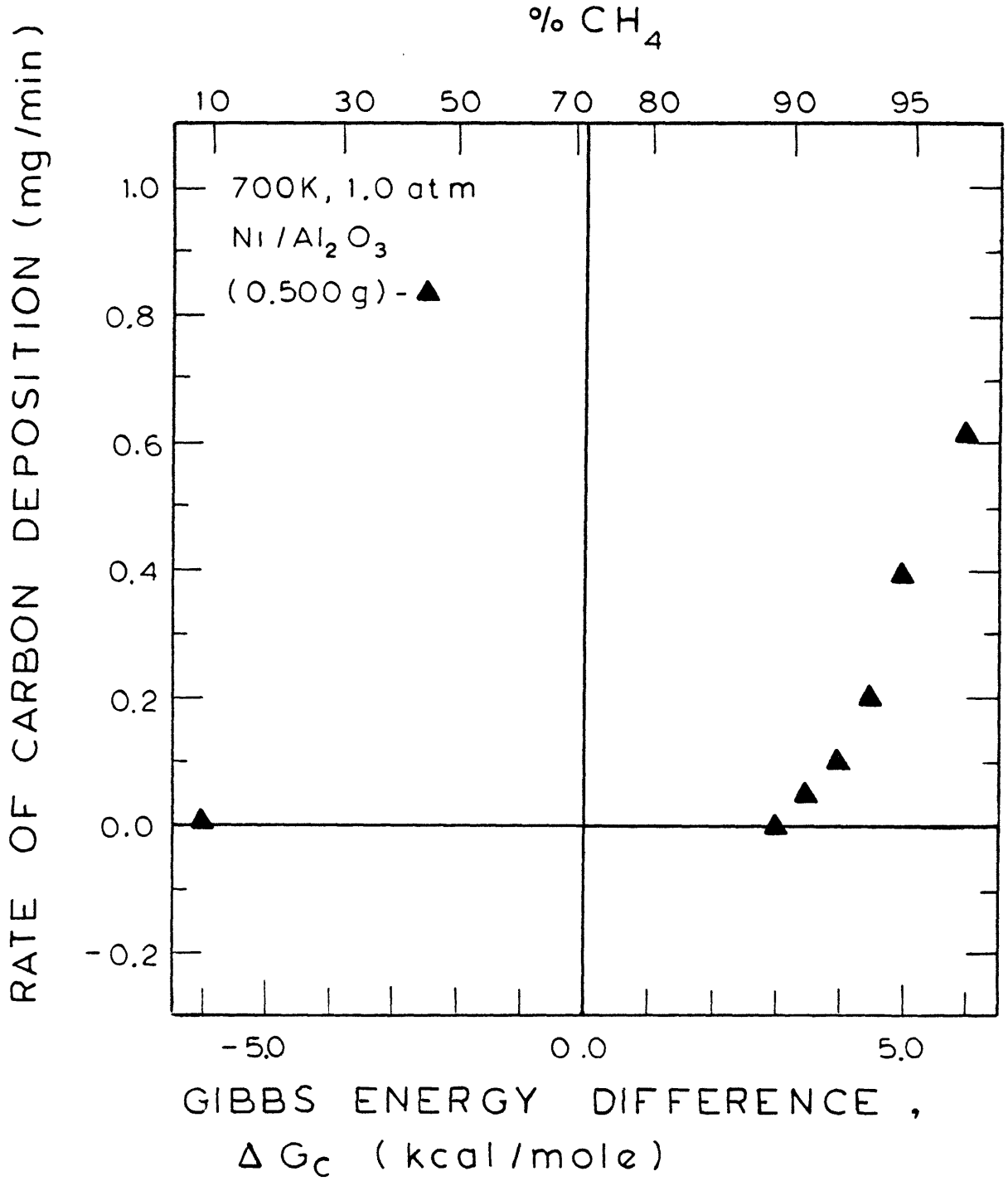

Figure 4-36 Rate of Carbon Deposition as a Function of ΔG_c for CH_4-H_2 Mixtures

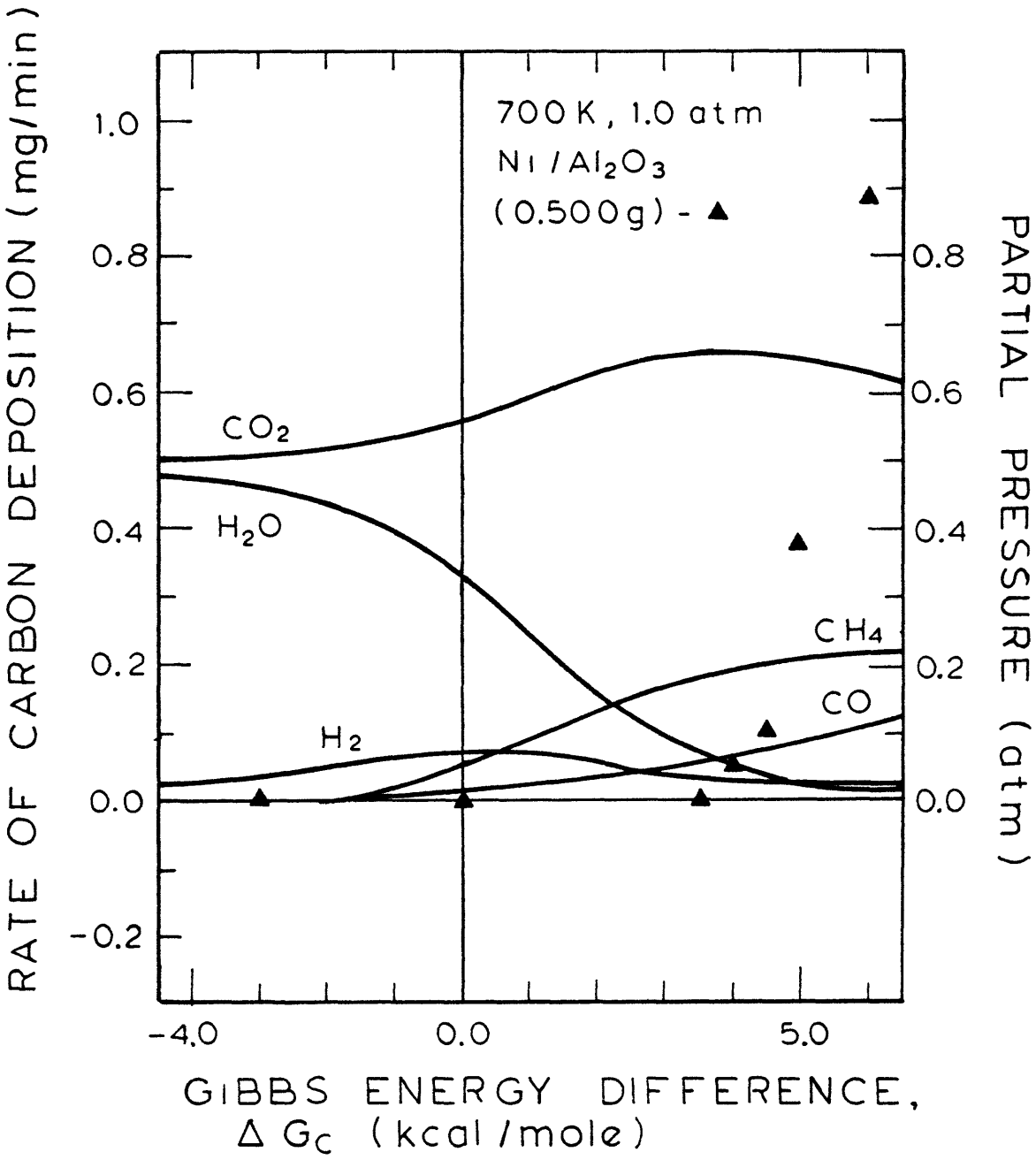

Figure 4-37 Rate of Carbon Deposition as a Function of ΔG_C for an O/H = 1.5

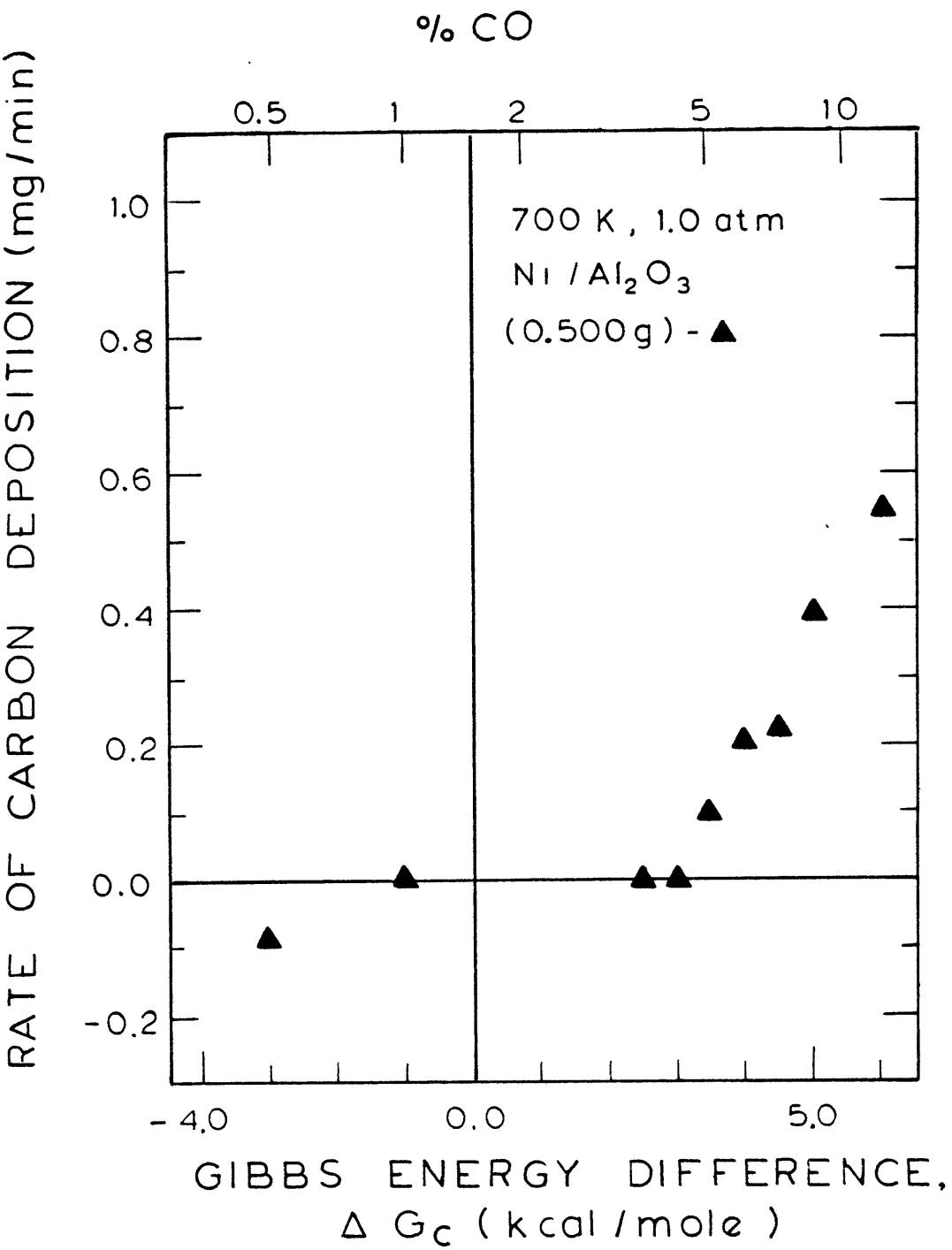

Figure 4-38 Rate of Carbon Deposition as a Function of ΔG_C for $CO - CO_2$ Mixtures

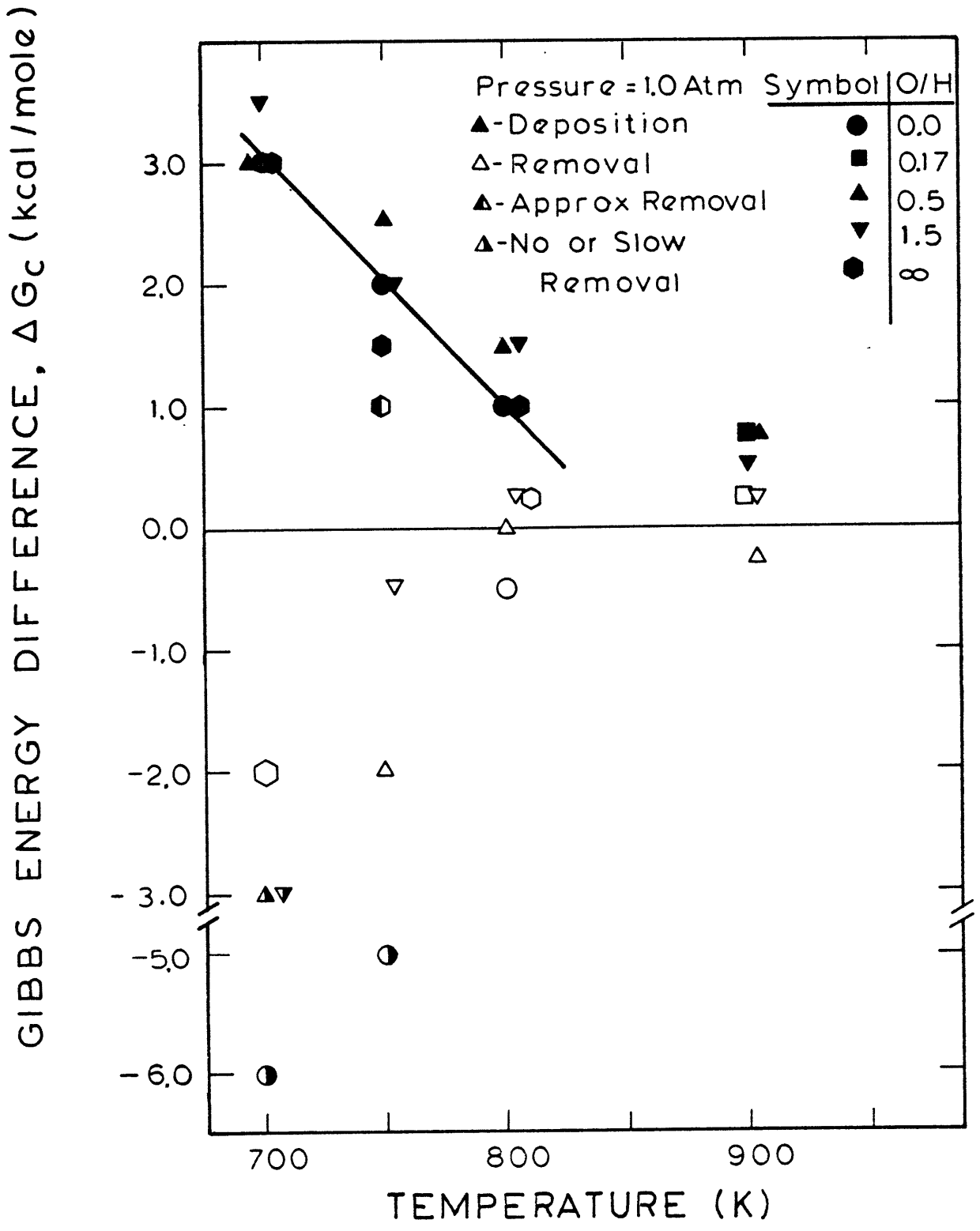

Figure 4-39 Carbon Deposition and Removal Boundary for Various O/H Ratio over Nickel

high water concentration predicted by the graphite-gas equilibrium at both 700 and 750K is also not obtainable over either a nickel or cobalt catalyst. This is important when considering the optimization of the Bosch process (See Section 5.0). As important is the understanding of the observed phenomena through the development of a viable mechanism which can account for the variation from the graphite equilibrium. Both Schenck (1927), and Browning and Emmett (1952) believed they were studying the equilibrium of the reaction

$$CH_4 + nMe \rightleftarrows Me_nC + 2H_2$$

where Me can be either nickel (where n=3) or cobalt where n=2 or 3). However, equilibrium cannot occur if the decomposition occurs to form carbon

$$Me_nC \longrightarrow C + nMe$$

since the solid species must be present. The methane decomposition reaction must also not occur,

$$CH_4 \rightleftarrows C + 2H_2$$

since this would raise the hydrogen partial pressure, and, since the carbide equilibrium occurs at higher methane concentrations, hydrogen would begin to react with, and deplete the available carbide. It should be pointed out that the phase rule only allows carbide and metal, or carbon to be in equilibrium with methane and hydrogen.

From the experimental results, it can be noted that weight increses have been observed which are much greater than could be accounted for by the formation of a carbide. So, if a carbide formed it must have been continuously decomposing if it were to account for the mass increases observed in the experiments.

Carbides have, in fact, been shown to exhibit a metastable behavior. Sec-

tion 2.2.3 dealt with the formation and decomposition of both nickel and cobalt carbide. The important conclusions from that section were as follows. Hofer et al. (1949, 1950) have shown that both nickel and cobalt carbides decompose readily at temperatures of 630K, the time required was less than one hour. Nagakura (1957, 1961) reported that in a temperature programmed study, decomposition did not occur until 704K. He also indicated that the maximum rate of carbide appearance (formation less decomposition) occurred at 623K. For the cobalt system, the decomposition of Co_2C occurred at 723K and at 750K for Co_3C. The maximum rate of formation (formation-decomposition) of both carbides occurred at temperatures between 723 and 773K. It should also be noted that Renshaw et al. (1971) observed Ni_3C at temperatures as high as 823K. In Nagakura's study, only free metal and carbon were observed at temperatures above 773K for Ni and 823K for Co. All of these indicate that the existence of both nickel and cobalt carbide at temperatures between 700 and 800K is highly likely.

The metastable nature of cobalt carbide was used to explain the results of Browning and Emmett's investigation of the equilibrium of the $Co\text{-}Co_2C\text{-}CH_4\text{-}H_2$ system. The discussion presented in Section 2.2.2.3 explained the observed scatter in equilibrium $CH_4\text{-}H_2$ gas compositions between that expected for gas in equilibrium with graphite, and with a metal and carbide phase. This was believed to result from the relative stability of the carbide with respect to carbon. If, in one experiment, more carbide were present, the carbide equilibrium was approached. If carbon was present, the reverse was true.

Browning and Emmett (1952) also studied the equilibrium of nickel carbide with both nickel and gas phase of methane and hydrogen. This was discussed in Section 2.2.2.3. Contrary to their results of the study of cobalt carbide, little scatter was observed in their nickel data. Also, the stability of the

carbide was shown to be greater than that of cobalt carbide. Upon X-ray analysis, confirmation of the hexagonal close-packed structure of Ni_3C was made. These results confirm that measurements of the carbide equilibrium was in fact being made. Upon comparison of this low temperature study with the high temperature results of both Dent (1945) and Rostrup-Nielsen (1972), it is seen that the data fall on a line which results from a plot of ΔG_c vs temperature (Figure 2-13a) Since thermodynamics would predict a straight line for a given process, when ΔH and ΔS are constant, ($\Delta G = \Delta H - T\Delta S$), it is believed that the solid species in equilibrium with the gas phase, at high temperature (above 700K), is the carbide and metal phase.

The results of this thesis which were obtained over nickel and cobalt have several interesting similarities. First, the point at which carbon deposition ceases deviates more from graphite at lower temperatures. This would be expected if the carbon deposition boundary corresponded, not with the graphite-gas equilibrium, but with an equilibrium with a different solid phase, such as a carbide (see Section 2.2.2). Most important, is the agreement between the experimental results over nickel and the nickel-nickel carbide-methane-hydrogen equilibrium line of Figure 2-13a as shown in Figure 4-40. Secondly, although for the experiments over cobalt at temperatures of 800 and 900K carbon deposition and removal were observed close to the point where the rate of weight change equaled zero, for most of the other cases this was not so. There either existed a region of no weight change or, as for the temperature of 700K, no carbon removal was observed. This indicates that either the method of weight detection was not sufficiently sensitive, or below the point at which carbon deposition ceased the catalyst was converted to a less active from. In almost all cases carbon removal occurred only if ΔG_c of the gas mixture was less than 0.0 kcal/mole. This would also be true for a system where graphite was present.

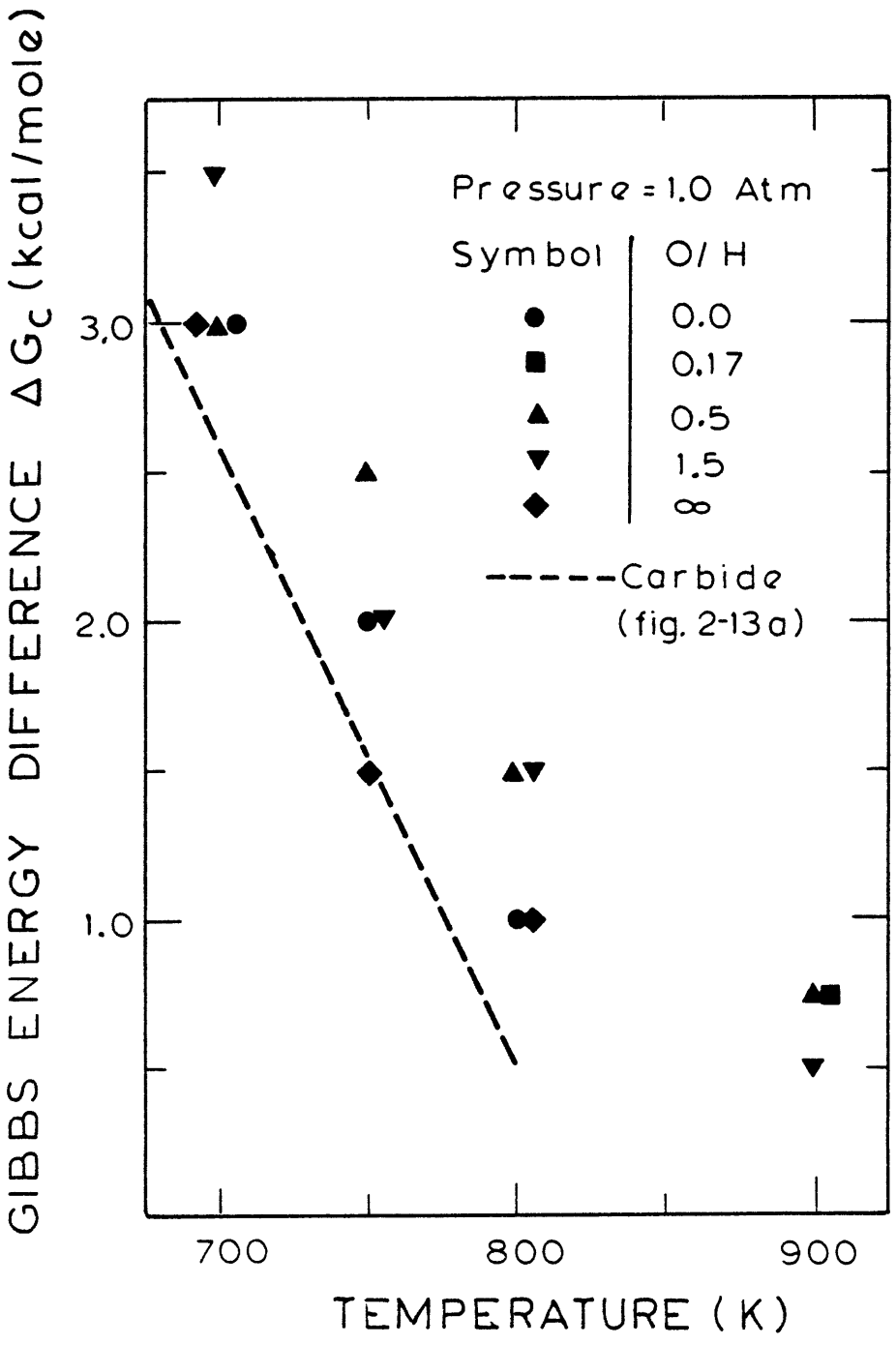

Figure 4-40 Carbon Deposition Boundary and $Ni - Ni_3C - CH_4 - H_2$ Equilibrium

In developing a mechanism for the deposition of carbon there are several reactions which are considered. First, although metastable, the formation of both nickel and cobalt carbides are known to occur. This is represented by the general reaction

$$CH_4 + nMe \rightleftarrows Me_nC + 2H_2$$

The formation of carbide can also occur from the reactions

$$H_2 + CO + nMe \rightleftarrows Me_nC + H_2O$$

and

$$2CO + nMe \rightleftarrows Me_nC + CO_2$$

The carbide has also been shown to decompose to free metal and carbon

$$Me_nC \longrightarrow C + nMe$$

It is being suggested in this thesis that the formation of carbon occurs by this reaction series. Quite specifically, the carbon is formed via an intermediate carbide. The net result, using the methane-hydrogen-carbon reaction as one example, is

$$CH_4 \longrightarrow C + H_2$$

The phase diagram presented in Figure 4-41 shows the positions of the graphite-gas and nickel-nickel carbide-gas equilibrium. The one for cobalt is similar. The lines have been drawn for 700 and 800K. As temperature is increased the graphite and carbide lines are seen to move together. The carbide phase line indicates the points at which the gas phase is in equilibrium with both metal and metal carbide. Above the line, the free metal will react to form carbide,

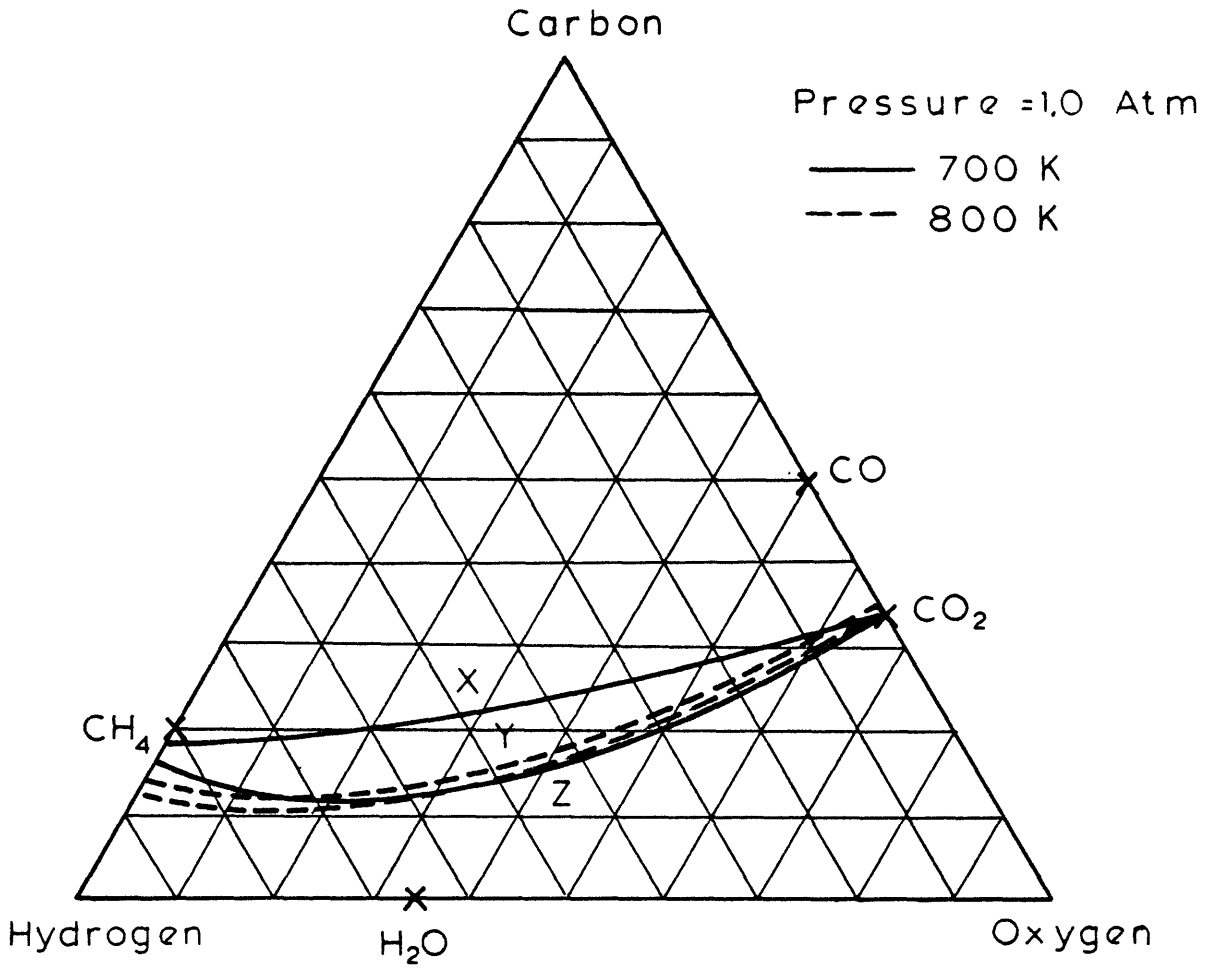

Upper Curve: Metal Carbide - Gas Equilibria
Lower Curve: Graphite - Gas Equilibria

Figure 4-41 Phase Diagram for Nickel Catalyzed Bosch Process

below the line, the carbide will react to form free metal. Thr graphite equilibrium is different since there is only one solid phase which is considered along with the gas phase. Gas mixtures, which are represented above the line, deposit carbon, while ones which are below the line remove carbon.

In the experiments studied in this thesis, carbon deposition was observed in the region of the phase diagram marked "x". This was a given distance from the graphite gas equilibrium. If the upper boundary is in fact a carbide phase line, in the region "x" metal carbide is present. For most of the experiments there existed a region of no weight change. Although carbon removal was not always observed below the graphite phase line (ΔG_c = 0.0 kcal/mole), very rarely was it observed above. In the region "y" and "z", that below the carbide phase line, no carbide would be expected to be present. If carbon formation only occurred through a carbide intermediate, no carbon deposition would be expected in region "y". The reaction

$$Me_nC + 2H_2 \longrightarrow nMe + CH_4$$

is not observed in that region either because the carbide decomposes to carbon quickly, or the amount present is a relatively small fraction of the total mass of metal plus carbon.

Carbon removal was in fact observed under some conditions. This must have occurred via the reaction

$$C + 2H_2 \longrightarrow CH_4$$

which will only occur from reaction gas mixture where ΔG_c is less than 0.0 kcal/mole. For the most part, Figures 4-27 and 4-39 support this thermodynamic agrument.

In this analysis, the carbon deposition could have been considered to re-

sult from a carbon with a different Gibbs energy. The Gibbs energy difference could have been accounted for by structural differences such as those described in the analysis by Rostrup-Nielsen (1972). However, if this were the case carbon removal would have been expected in region "y" just adjacent to the phase line resulting from the hypothesized non-graphitic carbon. Also the agreement (Figure 4-40) between the experimental data over nickel and the nickel carbide equilibrium data presented in Figure 2-13a give strong evidence that the phase boundary results from a carbide.

In summary, carbon deposition occurred via a metal carbide intermediate, upon reaching the metal-metal carbide-gas equilibrium carbon deposition ceased. In the region "y" between the carbide and graphite phase lines, where no carbide was present, no carbon deposition or removal was detected. Below the graphite phase line, carbon removal was observed. The rate, however was slow and became negligible as the temperature of the experiments was lowered.

4.4 Hydrogen Content of Carbons Formed Under Various Conditions

Measurements of the hydrogen content of carbons formed by the reaction of mixtures of hydrogen and carbon monoxide were carried out over nickel and cobalt at 700 and 800K, similar to those by Walker et al. (1957). The samples of carbon were prepared by reaction of the gas mixtures over Ni/Al_2O_3 or Co (1-5μ) powder. Typically 50 or 100 mg of catalyst were employed. The procedure began with the heating, to reaction temperature, of the sample in a stream of hydrogen ($20cm^3/s$). Once at reaction temperature, the catalyst was reduced for an hour. After reduction, either a 5% H_2/CO or 50% H_2/CO gas mixture was passed over the catalyst at a flowrate of $20cm^3/s$. By weighing the catalyst at given intervals, the point at which the catalyst weight had doubled could be determined. At that point, the hydrogen-carbon monoxide mixture was replaced by 20 cm^3/s of helium and the power to the reactor was shut

off. After the reactor had cooled down to room temperature, the catalyst sample was removed, bottled in air, and sent for analysis.

The analysis of the wt.% carbon and hydrogen was measured by Huffman Laboratories. Their analyses are given in Table 4-2. As can be seen, the hydrogen content of the carbon sample is proportional to the hydrogen content in the gas feed, and inversely proportional to temperature. In the same table, the results of a few similar experiments of Walker et al. (1959) have been included for comparison. His complete results are given in Tables 2-3 and 2-4.

As can be seen, the values of the hydrogen contents of carbons which he reported for iron at 800K are similar to the ones which were measured for carbon formed over nickel and cobalt in this thesis (Table 4-2). Overall, the results are similar.

Although one would expect the hydrogen content of the carbon to increase with gas mixtures richer in hydrogen, the explanation for the variation with temperature is not so straight forward. If one can picture the process of surface carbon reacting with adsorbed hydrogen to form a carbon-hydrogen mixture, then this phenomena can be explained on both a thermodynamic and kinetic basis. Since an increase in temperature will cause the surface hydrogen to desorb, a high surface concentration will exist at low temperature. This high surface concentration will result in high hydrogen composition on a kinetic basis. As long as the chemical or physical solubility of hydrogen in carbon has not been reached, the concentration would be limited by some rate process which would be proportional to the available hydrogen.

The C/H ratios are similar to those of Walker et al. (1959). The values Table 4-2 range from 5.74 to 32.3. The lowest value observed by Walker was

Table 4-2

Carbon-Hydrogen Analysis

	700K wt%		atom C/H	atom% H
	C	H		
Co 1-5 m powder				
5%H_2/CO	46.62	0.30	12.95	7.2
50%H_2/CO	4.204	0.61	5.74	14.8
800K				
5%H_2	42.63	0.11	32.30	3.0
50%H_2/CO	49.18	0.15	27.32	3.5
Ni/Al_2O_3 powder				
700K				
5%H_2/CO	59.69	0.46	10.81	8.5
50%H_2/CO	48.51	0.44	9.19	9.8
800K				
5%H_2/CO	54.17	0.30	15.05	6.2
50%H_2/CO	40.35	0.28	12.01	7.7
Walker et al. (1959) Fe				
801K				
5%H_2/CO			19.5	4.9
66%H_2/CO			9.6	9.4

7.3. One question that might be ask would be in regard to the effect upon equilibrium the presence of hydrogen could have. Figures 4-27 and 4-39, show no corelation between ΔG_c and O/H ratio of the gas phase. This seems plausible, since it would not appear that the presence of the small hydrogen atom would change the crystal structure and hence the Gibbs energy of the graphite.

5.0 Application of Results

The major difficulty which Holmes et al. (1970) encountered with the operation of the iron catalyzed Bosch process was with the less than equilibrium water concentrations in the exit of the reactor. This constrained the process to high recycle ratios. Manning (1976) and Sacco (1977) showed how the process could be optimized by operating at 915K. This corresponded to the intersection of the graphite-gas and the iron-iron oxide-gas equilibrium, at an O/H ratio of 0.5. This point represents the temperature at which the maximum water concentration is obtained at an O/H ratio of 0.5.

With the results obtained for cobalt and nickel in this thesis, the equilibrium water concentrations obtainable at a given temperature and O/H of 0.5 can be determined. These concentrations are shown in Figure 5-1 along with those for graphite and iron. As can be seen both the nickel and cobalt show a great improvement over the 16% water obtainable with the iron catalyst, reaching a maximum water concentration of 32% at 800K for cobalt, and 25% at 825K for nickel. The water concentrations in Figure 5-1 were determined with the values of ΔG_c of the carbon deposition boundary of Figures 4-27 and 4-39. The values of ΔG_c between 700 and 800K were obtained by a linear interpolation of the experimental points. Above 800K, ΔG_c was assumed to be constant and equal to that for graphite. For nickel, the values of ΔG_c between 700 and 800K were obtained by a linear interpolation of the experimental points. Since an extrapolation to 825K, from low temperature data, reveals that ΔG_c is equal to 0.5 kcal/mole, and ΔG_c = 0.5 kcal/mole at 900K, it was assumed that between these two temperatures the value was constant. If Figure 5-1 is examined, it may be observed that the maximum water concentration occurs where ΔG_c first begins to deviate from a constant. For cobalt this is 800K, while for nickel this is 825K. Since the increasing deviation

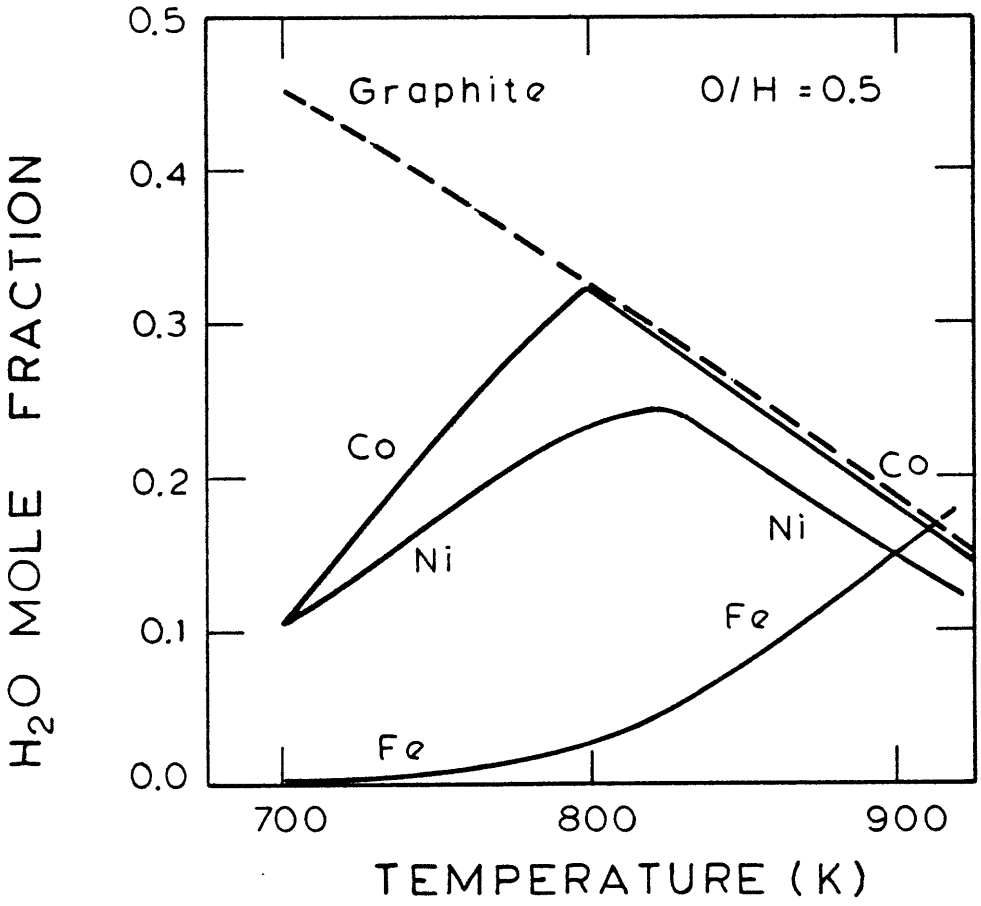

Figure 5-1 Equilibrium Water Concentration of a Bosch Reactor for Graphite Iron, Cobalt and Nickel Systems

from a constant ΔG_c was shown to correspond with the nickel carbide equilibrium, the maximum water concentration occurs at the merger of the carbide equilibrium with the carbon-gas equilibrium, where carbon is assumed to have a Gibbs energy of 0.5 kcal/mole. This is similar to the iron system, in that the maximum water concentration occurred at the intersection of the iron-iron oxide-gas and graphite-gas equilibrium lines.

To consider the effect of water concentration on a Bosch recycle reactor (Figure 5-2), a mass balance must be performed on the system. Consider for every 2 moles of hydrogen and 1 mole of carbon dioxide fed to the reactor, 2 moles of water are produced. The number of moles of gases recycled (H_2, CO, CO_2, CH_4,) are just the total number of moles produced upon reaction of hydrogen and carbon dioxide less the water removed by condensation

$$\frac{2}{x_{H_2O,EQ}} - 2$$

The removal of water by condenstation is considered to be 100% only to simplify the calculations. Taking one mole of carbon dioxide feed to the reactor as a basis for the material balance, the number of moles of gas recycled per mole of carbon dioxide fed is

$$r = 2\left(\frac{1}{x_{H_2O,EQ}} - 1\right)$$

The recycle ratios are plotted in Figure 5-3 for graphite, nickel, cobalt, and iron. As can be seen by comparing Figure 5-1 with 5-3, the minimum recycle ratio corresponds to the maximum water concentration. This is also evident by examination of the equation for the recycle ratio, r. Considering the minimum recycle ratio of 10.6 for the iron system, and 4.3 for the cobalt

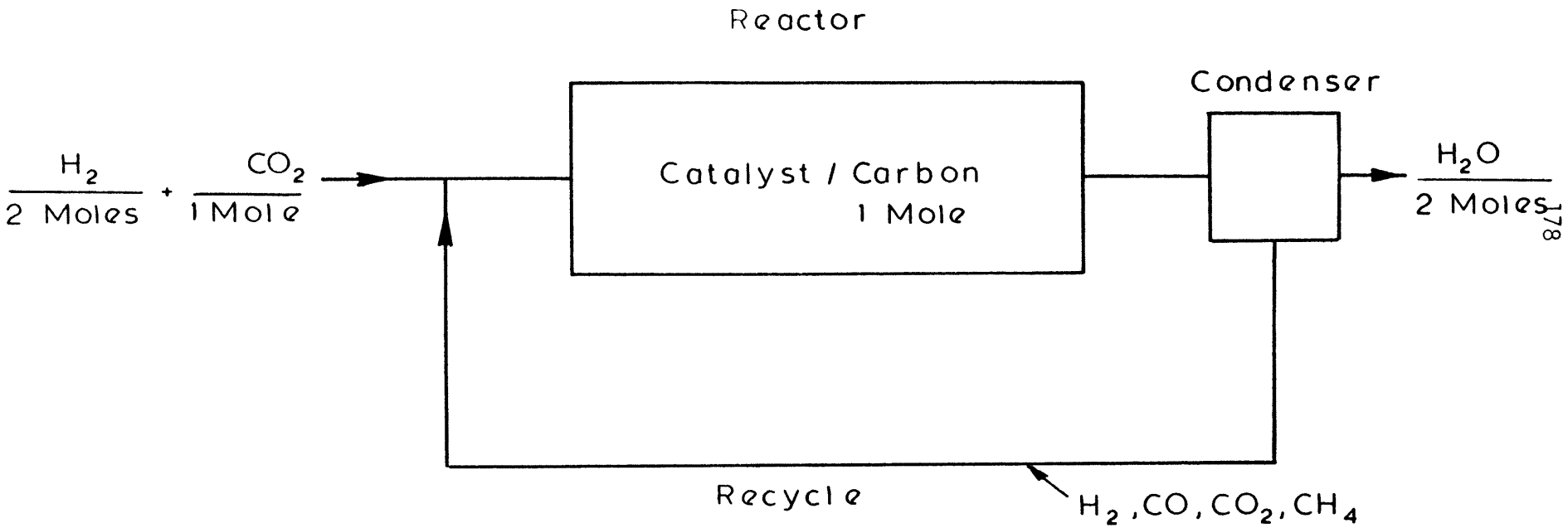

Figure 5-2 Bosch Recycle Reactor

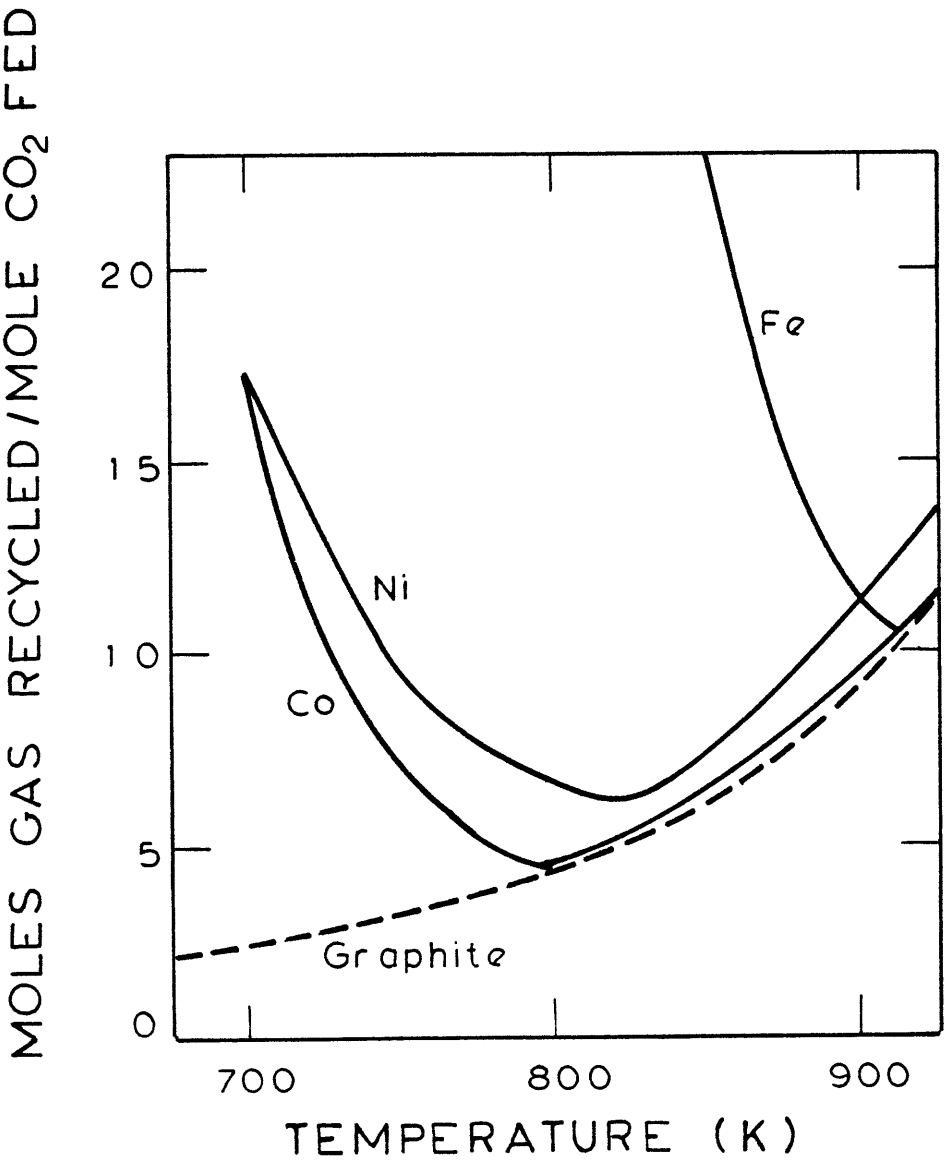

Figure 5-3 Gas Recycle Ratio for a Bosch Recycle Equilibrium Reactor

system, a reduction of 58% can be achieved through the use of a cobalt catalyst.

Manning (1976) suggested that if a prereactor was utilized, a substantial amount of the total available water could be recovered in a single pass. By reacting a 2/1 mixture of hydrogen and carbon dioxide over an iron catalyst above 900K, equilibrium may be obtained in a single pass for the reverse water-gas shift reaction

$$H_2 + CO_2 \rightleftarrows CO + H_2O$$

without the formation of carbon or methane (Kusner, 1962). For a feed of 2 moles of hydrogen and 1 mole of carbon dioxide, the maximum water produced is 1 mole, however equilibrium calculations presented in Figure 5-4 show that this only occurs at very high temperature. Operation of the shift reactor is limited by the melting of the iron, which occurs at 1810K. Thermodynamic calculations reveal that when the shift reactor is operated at 1000 to 1800K, atmospheric pressure, and an O/H ratio of 0.5, iron will remain in its reduced state.

Figure 5-5 shows a shift pre-reactor in series with a Bosch reactor. The moles of gas recycled in the Bosch reactor per mole of carbon dioxide fed to the shift reactor can be calculated assuming both reactors go to equilibrium. For a gas feed of 2 moles of hydrogen and 1 mole of carbon dioxide χ moles of water are recovered in the shift reactor, while the remaining $2-\chi$ moles are recovered from the Bosch reactor. The moles of gas recycled per mole of carbon dioxide feed can be determined to be

$$r = (2-\chi)\left(\frac{1}{\chi_{H_2O,Eq}} - 1\right)$$

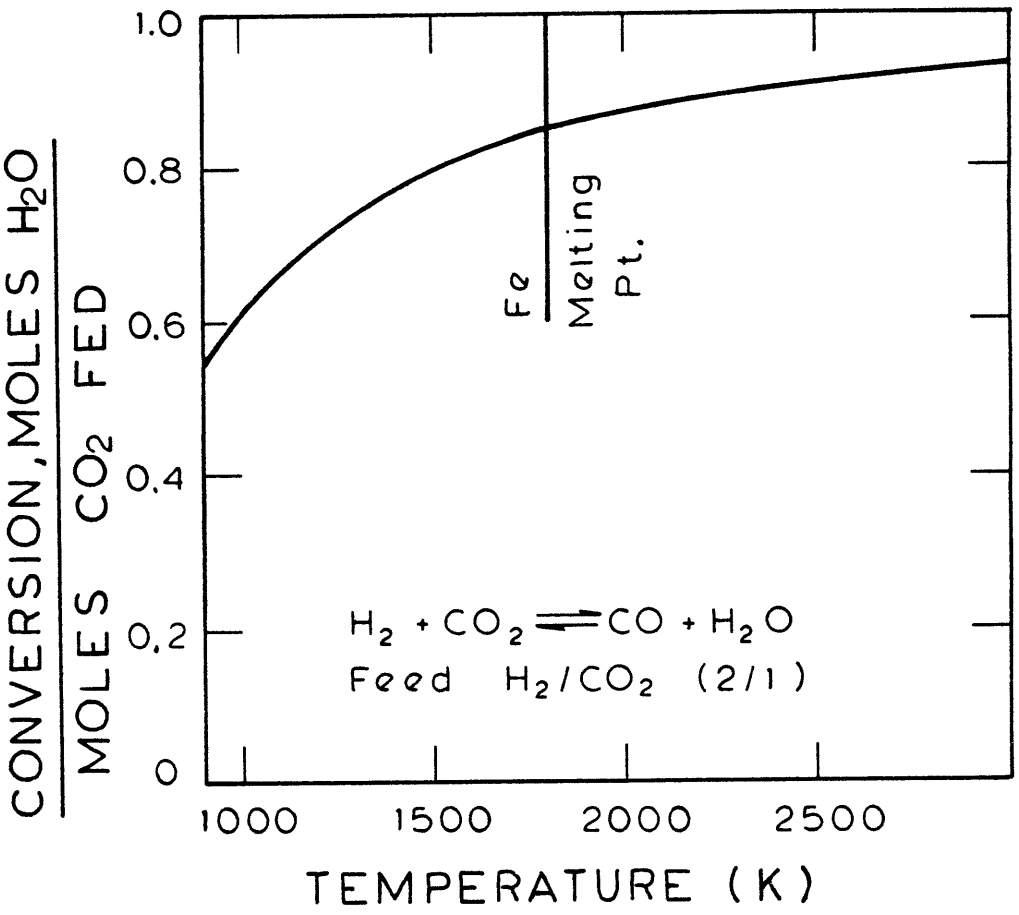

Figure 5-4 Equilbrium Conversion of the Reverse Water - Gas Shift Reaction

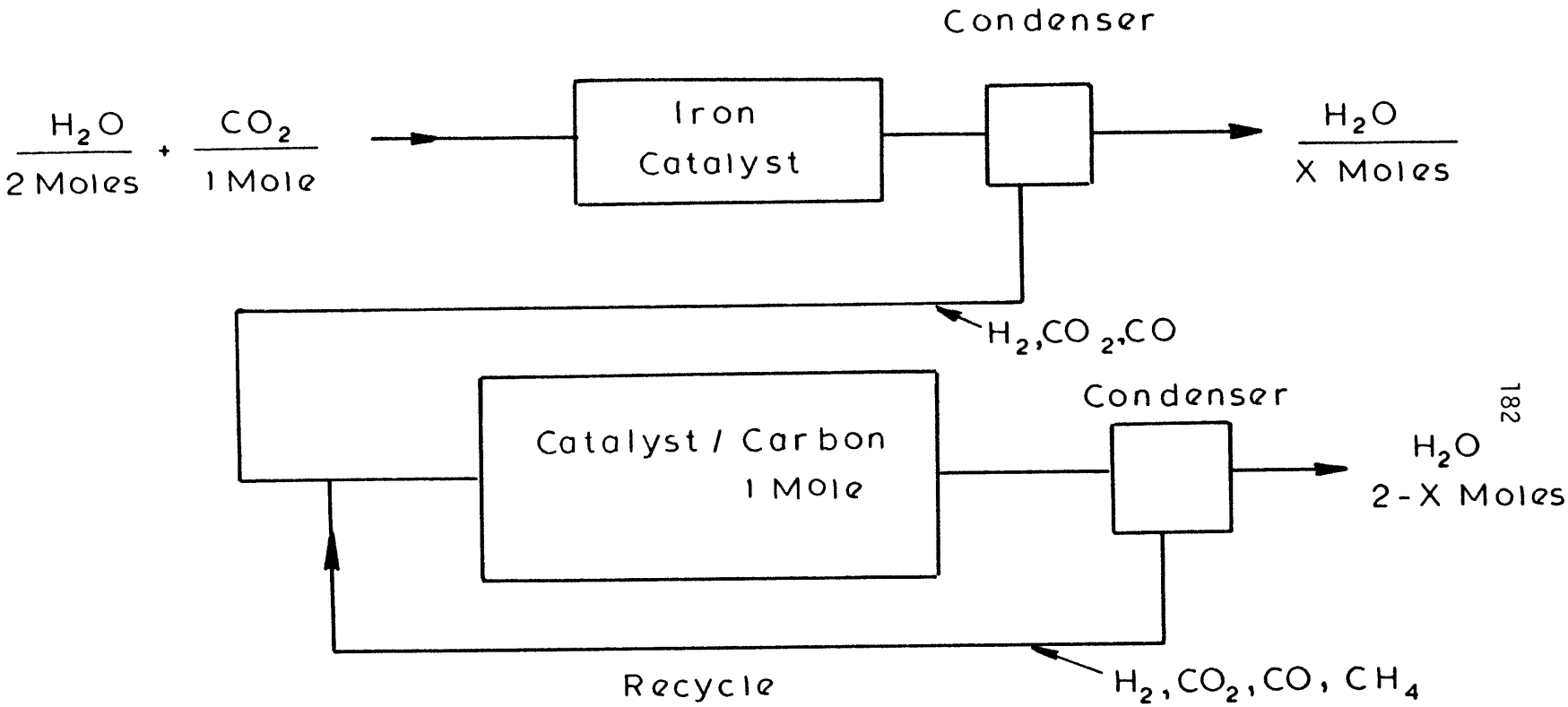

Figure 5-5 Reverse Water-Gas Shift Pre-Reactor / Bosch Reactor

This is the same as that for the Bosch reactor alone, except that the multiplier 2 has been replaced by 2-X to account for the removal of water in the shift reactor. Since the conversion in the shift reactor, X, can vary between 0 and 1, the reduction the recycle ratio can be reduced by a maximum of one half. If a temperature of the shift reactor below the melting point is chosen for operation, say 1200K, X would equal 0.71. So the ratio of the recycle ratio for the Bosch reactor with and without a pre-reactor would be equal to 0.65. This represents quite a large reduction in the recycle ratio. Although a large reduction in recycle ratio can be achieved through the use of a pre-reactor, an additional heat exchanger, for the condensation and removal of the water from the product stream, is necessary.

6.0 Conclusions

The principal conclusions of this thesis are two-fold, the first deals with the application of the results to the Bosch process and the advantages of a nickel or a cobalt catalyst over an iron one. In section 5.0, it was shown that the minimum recycle ratio could be obtained using a cobalt catalyst at 800K. The recycle ratio was equal to 4.3. Although not as efficient as cobalt, by using a nickel catalyst at 825K, a recycle ratio of 6.0 could be obtained. The optimum condition of iron yielded a recycle ratio of 10.5 at 915K. The advantages of cobalt and nickel over iron are quite evident.

The second conclusion deals with the solid species which should be considered when determining the carbon deposition boundary. At temperatures of 800 and 900K, the graphite-gas equilibrium was approached over a cobalt catalyst. This was shown for various O/H ratios. At 700 and 750K carbon deposition stopped at a Gibbs energy of carbon of 3.0 and 1.5 respectively. Carbon removal did not begin until gas compositions for which ΔG_c was less than 0.0 were passed over the catalyst. For the nickel system the same trends were observed.

The metastable nature of both nickel and cobalt carbide was substantiated by Hofer et al.(1949, 1950), Nakagura (1957, 1961) and Renshaw (1971). The carbon deposition boundary over nickel, measured in this thesis, is in good agreement with the equilibrium experiments of the Ni-Ni_3C-CH_4-H_2 system (Figure 4-40). These factors support the hypothesis that the carbon deposition boundary in the nickel system is quite definitely determined by the nickel-nickel carbide-gas equilibrium. Although not conclusive, it is quite probable that the cobalt-cobalt carbide-gas equilibrium corresponds with the carbon deposition boundary in that system.

7.0 Recommendations

From the equilibrium results obtained, and the application of them in Section 5.0, it is recommended that both nickel and cobalt catalysts be studied in prototype reactors such as those described by Holmes et al. (1970). The temperatures of the studies should be carried out around 800 and 825K for cobalt and nickel, respectively. The most suitable form of catalyst is most probably a fine wire mass. Also, through the use of a pre-reactor, the recycle ratio of the Bosch reactor may be decreased by at least 35%.

8.0 Appendix

8.1 Calculation of Equilibrium Gas Compositions

The calculation of equilibrium gas compositions for a given temperature pressure, O/H ratio, and ΔG_c was necessary for the experimental determination of the carbon deposition boundaries. To begin the computations, any three independent reactions are chosen. Three such reactions and their equilibrium constants are

$$H_2 + CO_2 \rightleftarrows CO + H_2O \ (1), \quad K_{P_1} = \frac{P_{CO}\, P_{H_2O}}{P_{H_2}\, P_{CO_2}}$$

$$3H_2 + CO \rightleftarrows H_2O + CH_2 \ (2), \quad K_{P_2} = \frac{P_{H_2O}\, P_{CH4}}{P_{H_2}^3\, P_{CO}}$$

$$CH_4 \rightleftarrows 2H_2 + C \ (3), \quad K_{P_3} = \frac{P_{H_2}^2}{P_{CH_4}}$$

Thermodynamic data (Stull and Prophet, 1971) allow the determination of the three equilibrium constants. Thermodynamic data for carbon are given for the form β-graphite. In actuality this may not be present in the system. By allowing K_{P_3} to vary as

$$K_{P_3} = K_{P_3}\Big|_{\text{GRAPHITE}} \exp(-\Delta G_c/RT)$$

computations for different forms of carbon may be made. ΔG_c is the difference in Gibbs energy between an observed carbon and β-graphite.

If the temperature and ΔG_c are set, the three equilibrium constants may be determined. By then setting the pressure and O/H ratio, two equations may

be derived. For the pressure,

$$P_{total} = P_{H_2} + P_{CO} + P_{H_2}^2/K_{P_3} + K_{P_2}\ K_{P_3}\ P_{CO}^2/K_{P_1} + K_{P_2}\ K_{P_3}\ P_{H_2}\ P_{CO}$$

A second equation may be obtained by fixing the O/H ratio. The O/H ratio is equal to,

$$O/H = \frac{P_{H_2O} + P_{CO} + 2P_{CO_2}}{2P_{H_2} + 2P_{H_2O} + 4P_{CH_4}}$$

Again by rearranging the equilibrium constants and substituting,

$$O/H = \frac{K_{P_2}\ K_{P_3}\ P_{H_2}\ P_{CO} + P_{CO} + 2\ K_{P_2}\ K_{P_3}\ P_{CO}^2/K_{P_1}}{2P_{H_2} + 2K_{P_2}\ K_{P_3}\ P_{H_2}\ P_{CO} + 4\ P_{H_2}^2/K_{P_3}}$$

Now the computation is in terms of two equations and two unknowns. This set may be solved using the Newton-Raphson solution technique for two simultaneous equations which is outlined in the Chemical Engineers Handbook (Perry and Chilton, 1973).

8.2 Nomenclature

C_{wt}	carbide weight per cent
ΔC	concentration difference, g/cm^3
d	diameter
d	distance between diffracting planes in X-ray analysis
D	diffusion coefficient, cm^2/s
G	Gibbs energy
ΔG_c	Gibbs energy difference between observed reaction and one involving graphite
h	thickness
ΔH	enthalpy difference
ΔH_f	enthalpy of formation
ΔH_{SOLN}	enthalpy of solution
K_P	equilibrium constant
L_c	crystal dimension perpendicular to the basal plane
M	molecular weight
P	pressure
r	radius
r	recycle ratio
R	ratio of hollow inner core radii to filament radii
R_D	rate of diffusion
R_M	mass rate of filament growth
ΔS	entropy difference
t	time
T	temperature
χ	fraction conversion

$\chi_{H_2O, EQ}$	equilibrium water mole fraction
α	crystalline form
β	crystalline form
γ	surface tension
μ	Gibbs energy
ρ	density g/cm^3

8.3 Literature References

Baird, T., J.R. Fryer and B. Grant, "Carbon Formation on Iron and Nickel Foils by Hydrocarbon Pyrolysis-Reactions at 700°C," Carbon, 12, 591 (1974)

Baker, R.T.K., M.A. Barber, P.S. Harris, F.S. Feates and R.V. Waite, "Nucleation and Growth of Carbon Deposits from the Nickel Catalyzed Decomposition of Acetylene," J. Catalysis, 26, 51 (1972)

Baker, R.T.K., G.R. Gadsby and S. Terry, "Fromation of Carbon Filaments from Catalysed Decomposition of Hydrocarbons," Carbon, 13, 245 (1975a)

Baker, R.T.K., P.S. Harris, J. Henderson and R.B. Thomas, "Formation of Carbonaceous Depositits from the Reaction of Methane Over Nickel," Carbon, 13, 17 (1975b)

Baker, R.T.K., P.S. Harris, R.B. Thomas and R.J. Waite, "Formation of Filamentous Carbon from Iron, Cobalt and Chromium Catalyzed Decomposition of Acetylene," J. Catalysis, 30, 86 (1973)

Baker, R.T.K. R.J. Waite, "Formation of Carbonaceous Depositions from the Platinum-Iron Catalyzed Decomposition of Acetylene," J. Catalysis, 37, 101 (1975)

Barin, I., O. Knacke "Thermochemical Properties of Inorganic Substances," Spinger-Verlag, New York, (1973)

Boehm, H.P. "Carbon from Carbon Monoxide Disproportionation on Nickel and Iron Catalysts: Morphological Studies and Possible Growth Mechanisms," Carbon, 11, 583 (1973)

Bogatski, D.P. "Diagram of the Ni-O_2 System and the Physico-Chemical Nature of the Solid Phase in this system," Zhur, Obshchei Khim, 21, 9 (1951)

Browning, L.C, T.W. DeWitt and P.H. Emmett, "Equilibria in the Systems Fe_2 C-Fe CH_4-H_2 and Fe_3C-Fe-CH_4-H_2," J. Am. Chem. Soc., 72. 4211 (1950)

Browning, L.C. and P.H. Emmett, "Equilibrium Measurements in the Ni_3C-Ni-CH_4H_2 and Co_2 C-Co-CH_4-H_2 Systems," J. Am. Chem. Soc., 74, 1680 (1952)

Dal Nogare, S. and R.S. Juvet, "Gas-Liquid Chromatography, Theory and Practice," Wiley,New York (1962), pp. 257-264

Dent, J.F., L.A. Moignard, W.H. Blackbraun and D. Herbden, "An Investigation into the Catalytic Synthesis of Methane by Town Gas Manufacturing," 49th Report of the Joint Research Committee of the Gas Research Board and th University of Leeds, GRB20 (1945)

Derbyshire, F.J., A.E.B. Presland and D.L. Trimm, "The Formation of Graphite Films by Precipitation of Carbon from Nickel Foils, Carbon, 10 114 (1972)

Diamond, S. and C. Wert, "The Diffusion of Carbon in Nickel Above and below the Curie Temperature," Trans. Met. Soc. AIME, 239, 705 (1967)

Dunn, W.W., R.B. McLellan and W.A. Oates, "The Solubility of Carbon in Cobalt and Nickel," Trans. Met. Soc. AIME, 242, 2129 (1968)

Evans, E.L., J.M. Thomas, P.A. Thrower and P.L. Walker, "Growth of Filamentary Carbon on Metallic Surfaces During the Pyrolysis of Methane and Acetone," Carbon, 11, 441 (1973)

Hofer, L.J.E., E.M. Cohn and W.C. Peebles, "Isothermal Decomposition of the Carbide in A Carburized Cobalt Fischer-Tropsch Catalyst," J. Phys. Col. Chem. 53, 661 (1949)

Hofer, L.J.E., E.M. Cohn and W.C. Peebles "Isothermal Decomposition of Nickel Carbide," J. Phys. Col. Chem., 54, 1161 (1950)

Holmes, R.F., E.E.K Keller and C.D. King "A Carbon Dioxide Reduction Unit Using Bosch Reaction and Expendable Catalyst Cartridges," ASA CR-1682, (November 1970)

Kubaschewski, O., Metallurigical Thermochemistry, Pergamon Press, New York, (1967)

Kusner, R.E., "Kinetics of the Iron Catalyzed Reverse Water-Gas Shift Reaction," PhD Thesis, Case Institute of Technoloby, Ohio (1962)

Manning, M.P., "An Investigation of the Bosch Process," Massachusetts Institute of Technology, ScD (1976)

Matheson Gas Products, Gloucester, Massachusetts, private communication, (1979)

Muan, Al and E.F. Osborn, "Phase Equilibria Among Oxides in Steel Making," Addison-Wesly Publishing Co., Reading, Massachusetts (1965)

Nagakura, S., "Study of Metallic Carbides by Electron Diffraction Part I. Formation and Decomposition of Nickel Carbide, "J. Phys. Soc. Jap., 12, No. 5, 482 (1957)

Nagakura, S., "Study of Metallic Carbides by Electron Diffraction Part IV. Cobalt Carbides," J. Phys. Soc. Jap, 16, No.6, 1213 (1961)

Oberlin, A., M. Endo and T. Koyama, "Filamentous Growth of Carbon Through Benzene Decomposition," J. Crys. Growth, 32 335 (1976)

Perry, R.H. and C.H. Chilton, "Chemical Engineers' Handbook," McGraw-Hill, New York (1973)

Purcell, J.E. and L.S. Ettre, "Analysis of Hydrogen with Thermal Conductivity Detecters," J. Gas Chromatog., 3, 69 (1965)

Renaud, M. And L. Bonnetain,"Determination of the Excess Energy of Carbon Formation in the Decomposition of Carbon Monoxide and Methane,"J. Catalysis, 33, 160 (1974)

Renshaw, G.D., C. Roscoe and P.L. Walker, "Disproportionation of CO II. Over Cobalt and Nickel Single Crystals,"J. Catalysis, 22, 394 (1971)

Rohsenow, W.M. and H. Choi, "Heat, Mass, and Momentum Transfer",Prentice-Hall, Englewood Cliffs, New Jersey (1961)

Rostrup-Nielsen, J.R.,"Equilibria of Decomposition Reactions of Carbon Monoxide and Methane over Nickel Catalysts,"J. Catalysis, 27, 343 (1972)

Sacco, A.,"An Investigation of the Reactions of Carbon Dioxide, Carbon Monoxide, Methane, Hydrogen, and Water Over Iron, Iron Carbides, and Iron Oxide,"PhD Thesis, Massachusetts Institute of Technology (1977)

Schenk, R.,"Gleichgewichtsuntersuchungen uber die Reduktions-Oxydations-ind Kohlungsvorgange beim Eisen II.,"Z. Anorg. Chem., 164, 313 (1927)

Selman, G.L., P.J. Ellison and A.S. Darling, "Carbon in Platinum and Palfadium: Solubility Determinations and Diffusion at High Temperatures," Plat. Metals Rev. 14, 14 (1970)

Shovensin, A.V., A.N. Minkevitch and B.V. Shcherbedinskii, "Diffusion of Carbon into Cobalt and Nickel,"Izvestiya Vysshikh Uchebn. Zavedenii, Chernia Met., No. 1, 95 (1965)

Stull, D.R. and H. Prophet, "JANAF Thermochemical Tables,"2nd ed., National Bureau of Standards, Washington (1971)

Stull, D.R., E.F. Westrum and G.C. Sinke,"The Chemical Thermodynamics of Organic Compounds, " p. 334, Wiley, New York, (1969)

Walker, P.L., J.F. Rakszawski, and G.R. Imperial, "Carbon Formation from Carbon Monoxide-Hydrogen Mixtures Over Iron Catalysts I. Properties of Carbon Formed," J. Phys. Chem., 73, 133 (1959)